Aggregation of IgG mAb Biotherapeutics: Sources, Methods of Characterization, and Biological Implications

By

Srivalli N. Telikepalli

Submitted to the graduate degree program in Pharmaceutical Chemistry and the Graduate Faculty of the University of Kansas in partial fulfillment of the requirements for the degree of Doctor of Philosophy.

_____

Chairperson: David B. Volkin, Ph.D

_____

C. Russell Middaugh, Ph.D

_____

Teruna J. Siahaan, Ph.D

_____

Thomas J. Tolbert, Ph.D

_____

Eric J. Deeds, Ph.D

Date Defended: October 15, 2014

The Dissertation Committee for Srivalli Nagaleela Telikepalli

certifies that this is the approved version of the following dissertation:

Aggregation of IgG mAb Biotherapeutics: Sources, Methods of Characterization, and Biological Implications

_____

Chairperson: David B. Volkin, Ph.D

Date approved: October 15, 2014

ABSTRACT

One of the predominant concerns with protein therapeutics is their tendency to aggregate at various stages of protein production, purification, filling, transportation, and administration. This occurrence has biological significance; while there is no definite, general cause and effect relationship for all protein drugs, many studies suggest that protein aggregates in certain biotherapeutics can decrease efficacy or cause untoward immune responses in human patients. Current research suggests that certain types of protein aggregates may be more immunogenic than others.

In this Ph.D. thesis research work, three different IgG monoclonal antibodies (2 IgG1 mAbs, one in solution and one in lyophilized form and one IgG2 mAb in solution) were stressed by a variety of different conditions and the resulting aggregates and particles were characterized using a broad array of methods. Some of the characteristics examined included aggregate/ particle size, count, and morphology, as well as the covalent cross-linking and structural integrity of the protein within the aggregates. In all cases, accelerated stability studies, similar to those performed in the biopharmaceutical industry, were utilized to generate aggregates. In the first study, an IgG1 mAb in solution was subjected to freeze-thaw, shaking, stirring, and heat stress in the presence and absence of NaCl. Depending on the solution and stress conditions, very different types of aggregates and particles formed. In the second study, an IgG1 mAb in lyophilized form was shaken to mimic worst-case shipping condition, which led to extensive cake breakage and upon reconstitution, displayed increased turbidity and subvisible particles compared to the unstressed sample. This study highlights potential stability concerns regarding lyophilized protein undergoing various shipping processes. In the third study, the impact of

protein particle size on inducing an early and late phase immune response in an *in-vitro* assay using human peripheral blood mononuclear cells (PBMC) was investigated. Stir-induced IgG2 mAb aggregates were size-enriched using fluorescence activated cell sorting (FACS) and tested for their ability to induce PBMC cytokine responses, at two phases of the immune response. The size-enriched particles were simultaneously characterized to determine traits, other than size, that may be responsible for the *in-vitro* assay responses. Amorphous subvisible particles 5-10 μm in size, containing protein with partially altered secondary structure and elevated surface hydrophobicity (compared to controls), and containing elemental fluorine, displayed relatively elevated cytokine release profiles compared to other size ranges.

Studies carried out as part of this Ph.D. thesis highlight the importance of 1) comprehensively characterizing protein aggregates and particles to better understand their formation, 2) the need for closer evaluation of the effects of shaking stress on lyophilized protein formulations during shipping, and 3) studying the potential biological implications of a subset of protein particles in an *in vitro* system, along with developing a better understanding these aggregate's physicochemical properties, should provide improved insights into why some protein aggregates elicit higher immune responses than others *in vivo*.

DEDICATED TO:

My family,

especially my parents,

Hanumaiah and Arunasri Telikepalli,

and my brother,

Satyanarayana Telikepalli

ACKNOWLEDGEMENTS

The work presented in this thesis could not have been possible without the valuable contributions from scientists at the University of Kansas, Janssen, Human Genome Sciences (currently GlaxoSmithKline), and Amgen under the supervision of my advisor Dr. David Volkin.

I would first like to thank my advisor, Dr. David Volkin for his invaluable advice, guidance, and support in all of my work throughout my five years at KU. He has helped me become a better scientist. I appreciate all of the time and effort that he put into my projects. He is a terrific scientist and I've learned so much from him. I would like to thank Dr. Russ Middaugh for imparting his scientific knowledge to students and always encouraging us to think outside the box. I would like to thank him for his valuable input and suggestions for the projects. I want to express my deepest gratitude to Dr. Sangeeta Joshi. She has seen me in both my ups and downs as a graduate student and has always encouraged me. She has been a great source of both scientific and personal advice and I sincerely appreciate her friendship.

I want to thank assistance, both monetary and in material form, from Janssen, Human Genome Sciences (HGS), and Amgen. From HGS, I would like to specifically thank Drs. Angela Blake-Haskins, Melissa Perkins, Kristin O'Berry, and Kevin O'Brien. They have given very helpful input and evoked important discussions for our group meetings and for our paper. In our collaboration with Amgen, I want to express my sincere gratitude to Dr. Marisa Joubert and Dr. Linda Narhi. It was an absolute pleasure working with both of them. They both have been so patient and accommodating despite the tight deadlines. I sincerely appreciate all of the time and hard work they put in and for all of their valuable ideas and suggestions that have allowed me to work on such an interesting topic. Despite being on maternity leave, Marisa

worked so hard and spent so much time on this project! I truly appreciate all of her hard work! In addition to Marisa and Linda, I want to thank Dr. Vibha Jawa for providing us with valuable input for our publication. I want to thank Meghana Deshpande and Dr. Nancy Jiao for helping us with our experiments. I would like to thank Drs. John Ferbas and Keith Kelley for their valuable information regarding the FACS instrumentation. In addition to all of our collaborations with companies, I'd like to thank NIH Biotechnology Training Grant (5-T32-GM008359) and Kansas Bioscience Authority for funding and making the work presented in this thesis possible.

I want to thank all of my committee members such as Drs. Teruna Siahaan, Thomas Tolbert, Eric Deeds, Jennifer Laurence, Mario Rivera, and Sue Lunte. Their comments and valuable suggestions at the quarterly meetings and on my thesis have greatly helped me in developing a successful thesis project. In addition, I'd like to thank the co-authors on the papers such as Dr. Ozan Kumru, Dr. Jae Hyun Kim, and Cavan Kalonia for helpful discussions and for their assistance on the projects. In addition, I'd like to thank all of the other current and past members of the Macromolecule and Vaccine Stabilization Center. They have all become my very good friends, and it has been a wonderful experience working with every one of them. Thanks to all of you for making these past five years very memorable for me. Dr. Prem Thapa, Heather Shinogle, and Dr. David Moore from the KU Microscopy Lab have been so friendly, dedicated, patient, and helpful in numerous experiments. I appreciate all of their valuable time and help they provided me. The faculty in the Department of Pharmaceutical Chemistry has offered excellent classes at KU, which have thoroughly helped me in my graduate school research. I know the knowledge I've gained from this program will also help me immensely in my career as well. Thanks to all of the faculty members in the Department of Pharmaceutical Chemistry!

Last but definitely not least, I want to thank everyone in my family. I have recently gained a few wonderful additions to my family. I want to thank my mother and father-in law, brothers-in-law, sister-in-law, and niece; they all have been extremely supportive and encouraging. I want to thank my husband, Vidyashankara Iyer, whom I met in this lab 5 years ago, for his love, encouragement, support, and patience. He listened to all of my stories of triumphs and failures without complaint. My grandparents, aunts, uncles, and cousins, have always supported me and encouraged me. I value their love, support, and good wishes as I defend my thesis. I want to thank my brother, Satyanarayana Telikepalli. He has always been one of my strongest supporters and has always encouraged me. The strongest support system that I've ever had was from my parents. I could not have done any of this without their love, patience, and encouragement. They have instilled in me the value of hard-work and importance of education. My family is the most important aspect of my life and I couldn't have done any of this without them. Love you all, and thank you all for always being there for me!

TABLE OF CONTENTS

CHAPTER 1: INTRODUCTION

1.1 OVERVIEW

Aggregation of protein biopharmaceuticals can reduce the efficacy of the drug as well as increase concerns about its immunogenicity upon administration to patients. The work presented in this thesis will be focused on a specific class of proteins called antibodies, or immunoglobulins, which have been gaining a lot of interest in the past two decades as the fastest growing category of protein drugs in clinical development. In this review, monoclonal antibodies (mAbs) are of particular interest. These antibodies, produced by identical B plasma immune cells cloned from a single parent cell, are monospecific and usually bind to one epitope on one antigen.

The prevalence of mAbs is also noticeable in the commercial drug markets. As of 2010, 7% of the global therapeutic market was composed of mAbs (9 blockbusters making more than $1 billion in sales). As of June 2011, there were 28 approved mAbs in the EU or US with 1064 industry sponsored clinical trials, costing hundreds of millions of dollars.[1] Between 2010 to 2015, it is predicted that all medicines will have a growth rate of 3-6% compound annual growth rate. MAbs alone show a 9.2% compound annual growth rate during this same period.[1] So even though these biologics make up a small portion of total pharmaceutical sales, they will be representing much of the growth during these years.[1] This dramatic rise in their production has made them very important molecules for study.

Immunoglobulins are produced by B lymphocytes and function to identify and tag foreign antigens for attack by other parts of the immune system or directly neutralize its target by recognizing a unique part of the antigen, called the paratope. The region of the antibody that recognizes the paratope is called the epitope. Antibody preparations are often employed as research reagents as well as for diagnosis, monitoring, and treatment of various diseases such as

cancer, autoimmune, and other inflammatory diseases. Their high specificity and selectivity also allow them to be used in conjunction with radioisotopes, cytotoxic agents, or biologic response modifiers that can directly target diseased cells without effecting normal cells, thus causing fewer side effects to patients.

1.1.1 Structure of Antibodies

Immunoglobulins are glycoproteins that are Y (or an array of Y) shaped structures with two identical heavy chains and two identical light chains (see Figure 1) connected by disulfide bonds. In the case of IgG molecules, each heavy chain is approximately 50 kDa and each light chain 25 kDa. There are five types of heavy chains (and five types of immunoglobulins), which define the antibody class, or isotype. They are denoted as α, found in IgA; δ, found in IgD; ε, found in IgE; γ, found in IgG; and μ, found in IgM. The α and γ contain about 450 amino acids while the μ and ε contain about 550 amino acids.[2] The light chain is either of the λ or κ type, which is about 211 to 217 amino acids long, respectively.[3] Each chain is composed of domains 70-110 amino acids long.[3] As shown in Figure 1, the light chain is composed of a variable (V_L) and constant domain (C_L). The heavy chain consists of a variable domain (V_H) followed by a constant domain (C_H1), a hinge region, and two more (C_H2, C_H3; for isotype γ, α, δ) or three more (C_H2, C_H3, C_H4; for μ and ε) constant domains depending on the isotype. The constant region is the same for all antibodies of the same isotype and species, but different in antibodies of different isotypes and from different sources. The variable region is different in each B cell producing it, but is the same for antibodies produced by a single B cell or a B cell clone. All domains consist of beta barrel or immunoglobulin fold structures that are stabilized by disulfide bond and hydrophobic interactions. These individual domains interact with one another and fold into three equal-sized

oblong spherical shapes linked by a flexible hinge region. The hinge region allows flexibility for bivalent antigen binding and allows activation of effector functions.

Antibodies can be divided into Fab (Fragment antigen binding) and Fc (Fragment crystallization) regions and have very different functions. The Fab region, consisting of one constant and one variable domain from the heavy and light chain of the antibody, binds to the antigen. At the amino terminal end of the Fab is the antigen-binding site composed of the complementary binding regions (CDRs) and the framework (not shown in Figure) region. CDRs are composed of a total of 6 beta loops (3 in the heavy chain and 3 in the light chain), with the framework region forming beta sheets in between each CDR. The Fc portion of the antibody modulates immune cell activity and comprises two heavy chains, with either two or three domains depending on the class of the antibody. Each domain is composed of between 7 (for the constant domains) and 9 (for the variable domains) beta strands. [3]

Our focus for this thesis is on IgG molecules. IgGs are further divided into the following subclasses: IgG1, IgG2, IgG3, and IgG4 consisting of γ1, γ2, γ3, γ4 heavy chains, respectively. The differences among these subclasses are mostly due to the length of the hinge region and number and location of interchain disulfide bonds. In addition to the interchain disulfide bonds, IgGs have intrachain disulfide bonds, residing in each domain of the heavy and light chains (indicated by the red –S-S- within each domain). There is one oligosaccharide chain in IgGs and this N-linked sugar chain resides on the C_H2 domain at Asn 297. This oligosaccharide is very important for binding of the C1q component of the complement cascade and can effect antibody conformation.

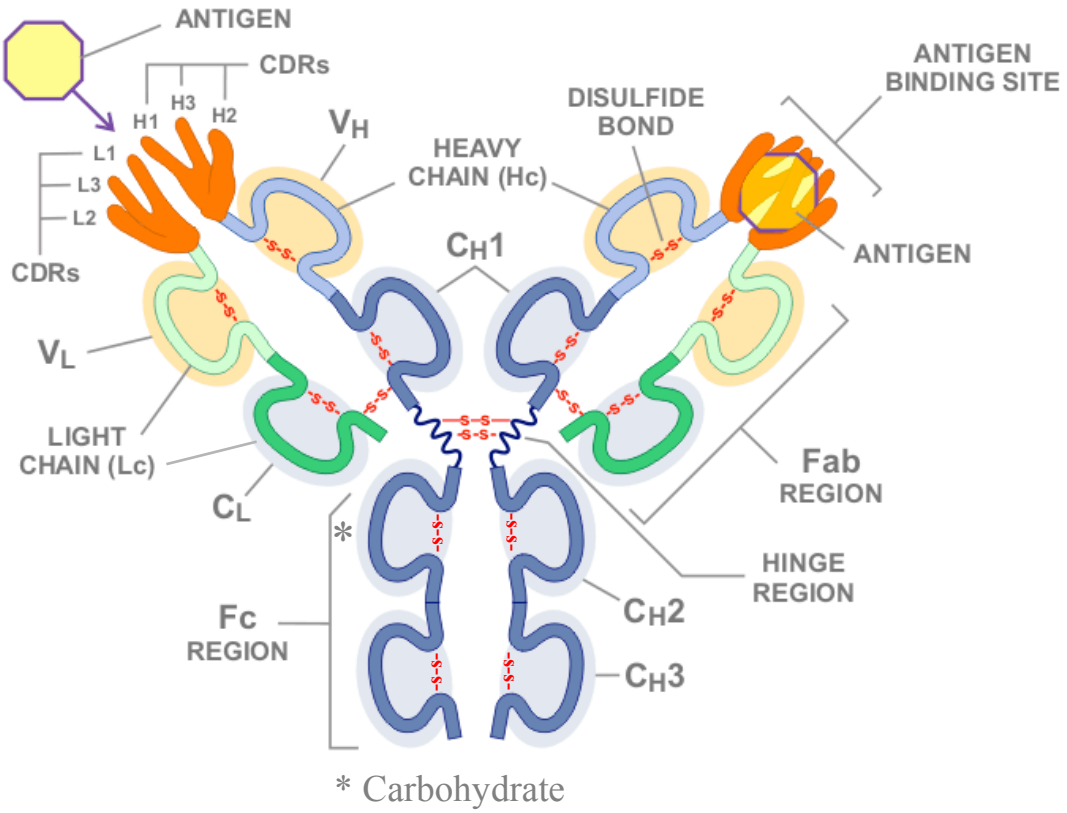

Figure 1. Representative structure of an IgG antibody.[4] (Ref: adapted from http://www.novimmune.com/science/antibodies.html with permission)

1.1.2 Modes of Action of Monoclonal Antibody Therapies

Antibody therapeutics have many modes of action, which make them very effective biological agents. They can either directly or indirectly inhibit disease progression. Directly, they can block the function of targeting signal molecules, neutralize toxins, inhibit the function of growth factor receptors, or hinder the function of adhesion molecules.[5,6] Depending on the disease, they are capable of changing the rate at which cell surface receptors are internalized or cleaved.[5,6] Antibodies can also inhibit cell cycle progression or DNA repair, induce regression of angiogenesis, and stimulate apoptosis and many targeting functions.[5,6] Indirectly, they can inhibit disease progression with the help of the immune system by recruiting cells with cytotoxic potential, such as monocytes, macrophages, or natural killer cells, in an antibody-dependent cell

mediated cytotoxicity (ADCC) process.[6,7] The Fc region on the antibody binds to Fc receptors on the cells while the Fab region of the antibody binds to the cell surface receptors of the target cell. This action can elicit lysis or phagocytosis of the target cell by cytotoxic cells. A complement dependent cytotoxicity (CDC) process can also occur when the mAb binds to the target cell surface and fixes complement, resulting in activation of a complement cascade and generation of a membrane attack complex that leads to cell lysis.[5]

1.1.3 Stability of mAbs

The structural integrity and stability of mAbs, similar to protein molecules in general, is governed by covalent bonds as well as by non-covalent electrostatic, weakly polar, and hydrophobic interactions. Covalent bonding (present in peptide bonds, disulfide-crosslinking, N and O-glycosylation) in combination with various non-covalent interactions maintain the protein in the folded state, in its native three dimensional conformation. Electrostatic interactions (dipole-dipole, charge-dipole, and charge-charge interactions), present in H-bonding and salt-bridges, along with stacking interactions of aromatic side chains also contribute to stability of the molecule. The largest contributors to stabilization of the protein in its native, folded conformation, however, are hydrophobic interactions (where surface exposure of nonpolar regions is minimized) and H bonding.[8,9] At the same time, there is only a narrow window of stability between the folded and unfolded forms of a protein, and the non-covalent interactions governing the folded conformation of the protein can be easily perturbed and cause the protein to lose its native conformation. Finally, these different covalent and non-covalent interactions help to retain both the physical and chemical stability of mAbs. Chemical stability involves processes where covalent bonds within the amino acid residues or the peptide backbone are altered and the chemical composition is changed. Physical stability does not necessarily involve breaking or

forming of any covalent bonds but alters the physical state of the molecule through disruption of non-covalent interactions leading to structural alterations, and under certain conditions, irreversible formation of aggregates.[10]

1.1.3.a. Chemical and physical stability from a pharmaceutical perspective

There are ample references that discuss chemical stability of protein-based drugs in detail. Chemical processes include events such as oxidation[11], deamidation[12], isomerization[13], beta-elimination[14], disulfide scrambling[15,16], and peptide fragmentation[17], where key amino acid residues are involved in each of these processes.[2,9] Physical instabilities can manifest themselves through denaturation, aggregation, precipitation, and surface adsorption.[2,9,18]

1.1.3.b. Colloidal vs. Conformational Stability of mAbs

Both colloidal and conformational stabilities of mAbs can contribute to the overall aggregation pathway depending on the specific protein, formulation, and environmental stress.[19,20] Colloidal stability arises from a balance of attractive and repulsive forces between protein molecules as they approach one another. In general, a solution containing particles is colloidally stable if there is repulsion between the particles but is unstable and readily agglomerates if there is little or no repulsion between the particles.[20] Colloidal stability of proteins can be modulated by changing surface charge either by mutating solvent-exposed amino acid residues (introducing charged residues to increase repulsive interactions) or by altering the solution environment to decrease attractive intermolecular interactions between protein molecules. Changing solution pH and/or ionic strength can thus greatly impact the colloidal stability of proteins.

Conformational stability arises through modulating the amount of unfolded or partially unfolded aggregation-prone protein molecules in solution. It is maintained by keeping the protein in its folded, native state. Adding nonspecific stabilizing compounds such as sucrose to a protein solution, which preferentially excludes from protein surfaces, is one method of increasing the conformational stability of a protein. Mutating amino acid residues within the interior of the protein to enhance packing, altering solution conditions to favor the folded state (near-neutral pH), or adding specific ligands that bind to a specific binding pocket within the native state of the protein molecule can all increase the conformational stability of protein molecules.

Solution conditions can potentially determine which of these two stability parameters is more dominant. Depending on the situation, either conformational changes or colloidal changes can be the rate-limiting step.[19-22] Colloidal and conformational stability effects on protein aggregation have been studied in detail using a variety of IgG1 mAbs. [21,22] Sahin et al. modulated the surface charges of an IgG1 mAb by increasing the pH and observed more attractive interactions and concurrently a change from small oligomer formation to high molecular weight aggregates and precipitates.[21] Brummit et al. hypothesized that in the presence of attractive colloidal interactions, amyloid and insoluble aggregates will be observed, but under conditions where repulsive interactions are dominant, amorphous aggregates may be observed in some cases.[22] In terms of effects on conformational stability, the extent of structural alterations has also been shown to be strongly correlated with the level of aggregate formed, at least in some cases.[23]

1.2. MECHANISMS OF PROTEIN AGGREGATION AND PARTICLE FORMATION

Generally, protein aggregation can proceed by several pathways as described in Figure 2. According to Roberts et al, protein aggregation generally involves the following processes: (1) protein structural alterations leading to formation of non-native, aggregation prone structures (conformational stability effects);[24] 2) reversible self-association of the protein mediated by possible charge-charge interactions among others (colloidal stability effects);[24] and 3) conformational rearrangement of the oligomers to make the aggregates irreversible. These irreversible aggregates can continue to grow through different methods of aggregation addition to form 4) soluble aggregates; 5) soluble, high-molecular weight aggregates; 6) large insoluble aggregates.[25]

Other mechanisms include homogeneous and heterogeneous nucleation dependent aggregation in which impurities induce protein unfolding and aggregation.[26] Additionally, it has also been proposed that reversible association of the native monomer, surface induced events, or chemically-modified products may also play a role in aggregate formation. [27] It is difficult to discern which mechanism is dominant because often all of these mechanisms are operating to different extents at the same time.

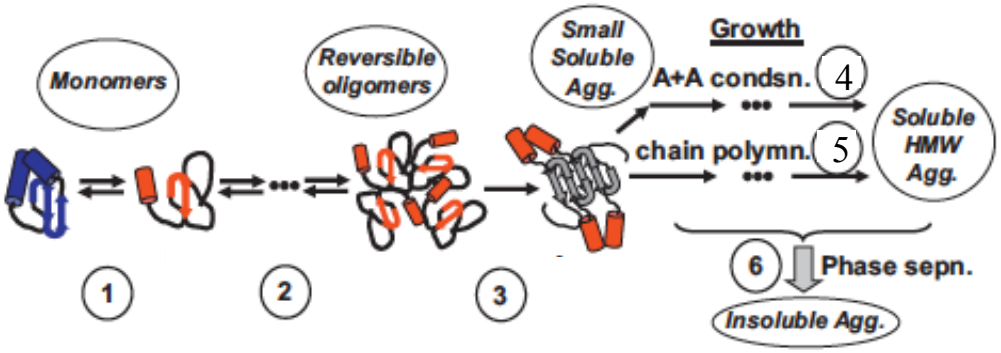

Figure 2. Representation of a few important steps in non-native protein aggregation (Ref: Obtained with permission from Roberts et al.[25]

1.3 IMMUNOGENICITY OF THERAPEUTIC PROTEINS

There have been many instances in which protein aggregates and particles in therapeutic drugs were suspected of causing immunogenic responses in patients[28-30]: (1) patients injected with an altered formulation of erythropoetin developed pure red cell aplasia; [31-33] (2) injection of aggregated Factor VIII to hemophiliac patients worsened the symptoms of hemophilia; [33] (3) patients who were given hGH with 50-70% aggregates developed anti-hGh antibody, but such a response was dramatically reduced after they were given a formulation with fewer aggregates; [33] and (4) and 80-100% patients developed binding and neutralizing antibodies when IL-2 was administered subcutaneously over a period of time. When IVIG (intravenous immunoglobulin) was administered, the presence of a large amount of aggregates triggered anaphylaxis due to fixation and activation of the complement cascade. Fortunately, engineered human and humanized monoclonal antibodies have shown much lower anti-drug immune responses in humans than these earlier-developed biotherapeutics, but the concern to make safer protein therapeutics can never be diminished.[34]

1.3.1. Factors leading to immunogenicity

While the presence of protein aggregates and particles can potentially impact the immunogenicity of biotherapeutics, other factors related to the drug formulation, process development, and patient related factors can also greatly impact the immune responses. Drug related factors such as non-human sequences, novel epitopes generated by amino acid substitution for enhanced stability, or changes in glycosylation patterns can expose cryptic B cell and T cell epitopes in a protein causing it to appear foreign to the immune system. Alterations in

structure causing a protein species to show repetitive arrays may lead to efficient crosslinking of B cell receptors leading to B cell activation and consequently to breaking of immune tolerance to self-protein.[35]

Process related factors such as container types, the presence of metal, silicone oil, or tungsten derived from various operations can be culprits as well. Certain excipients used in formulating protein drugs have been shown to increase patient immune responses. One example is with Eprex, which is a version of EPO that is formulated with tween 80 instead of human serum albumin. This was thought to be one of the factors responsible for the development of antibodies against this protein.[36]

Patient related aspects such as genetic factors, age, disease, immune status, and concomitant treatment need to be considered as well. The route, frequency, and dose of administration can also impact the extent of an immune response. All of these factors can complicate our understanding of the immunogenic potential of a therapeutic protein drug.[30]

1.3.2 Some proposed biological mechanisms that may result in immunogenicity

The production of binding or neutralizing anti-drug antibodies (ADAs) are thought to be the source of the observed immune responses to therapeutic proteins. [37] The effects of these ADAs may range from being harmless to their being potentially fatal to patients. Specifically, repeated administration of some drugs can induce the formation of these ADAs, but clinical prediction of ADA formation is very difficult.

ADA formation is thought to arise from 2 pathways: through a classical pathway or by breaking of immune tolerance.[38-40] The presence of foreign epitopes triggers a classical immune

response. The foreign antigen is internalized, processed, and presented by antigen presenting cells (APC) through the major histocompatibility complex II (MHC II) to T cells. CD4+ T cell becomes activated upon recognition of this MHC II-peptide complex. This primed T cell recognizes and activates B cells by secreting certain cytokines causing them to proliferate and produce antibodies.[40] Foreign antigens generally trigger a classical immune response that is dependent on T-cell activation described in detail elsewhere.[41] When the antigen contains repetitive epitopes, the response can proceed through a T cell independent manner through Toll-like receptors on the B cell or by antigen cross-linking of the BCR; these processes can also stimulate antibody secretion from B cells.[42] Many recombinant protein drugs available in the market, however, are not foreign but homologous to endogeneous human protein. So a classical immune response is not the expected pathway for immunogenicity; instead breaking of B cell tolerance is more likely the source of any immunogenicity. The body has complex regulating mechanisms for suppressing and inactivating self- reactive B and T cells called central and peripheral tolerance. These self-reactive cells can sometimes evade this central tolerance in the primary lymphoid organs or peripheral tolerance in the peripheral organs. When the cells evade these control mechanisms and B cell tolerance is broken, antibody production against these protein drugs and subsequent immune reactions ensues.[38,40]

1.4 MAB PARTICLE FORMATION

Protein aggregation is ubiquitous in pharmaceutical settings and can occur during many stages of protein drug production, long-term storage and shipping, and even during administration to the patient.[43] As discussed above, the formation of aggregates and particles may lead to an immune response [44-46], and a decrease in the efficacy of the drug due to cross reactivity of antibodies that can neutralize endogeneous proteins, or anaphylactic shock.[45,47-50]

Therefore understanding the parameters causing aggregation and particle formation is essential to develop strategies to minimize its occurrence. Recently there has been an increase in interest in the 0.1-10 μm sized protein aggregates, often referred to as protein particles, specifically due to their potential increased immunogenic responses.[51,52] Throughout this chapter, the term "aggregation" will be used generally when referring to the formation of all types and sizes of aggregates. However, when aggregates larger than 100 nm are specifically being discussed, they will be referred to as "protein particles." The focus of this manuscript is on formation of these protein particles.

Temperature[53-58], freeze-thaw[54,58-61], mechanical stresses[55,62-70], and light[71,72] all have contributed to various instances of mAb particle formation. Each of these environmental stresses are typically encountered at various stages of drug development so their impact on particle formation is important to understand. Increased particle formation has even occurred at various points during lyophilization, which is performed to increase the storage stability of the protein.[73-77] The potential mechanisms of how these stresses cause particle formation is discussed briefly in the next few paragraph.

Heating a protein solution can either partially unfold or more extensively unfold the protein. This can expose interior hydrophobic regions to varying extents, which may serve as hotspots for nucleation and more extensive aggregation. Additionally, elevated temperatures can provide sufficient kinetic energy to the protein molecules in the solution to speed up chemical reactions such as deamidation or oxidation, both of which can lead to increased aggregation. [2,78] Cold denaturation is also possible since the strongly temperature-dependent hydrophobic interactions, known for keeping the protein in the native conformation, may become weaker at lower temperatures. Many studies have shown that IgGs exposed to heating, formed primarily

large micron sized particles, consisting of non-native covalent cross-links, with large perturbations in secondary structure and high ANS binding. [23,54,58]

Freezing is another stress a protein drug can encounter. During this process, protein can adsorb to ice/liquid interfaces and unfold. Cryoconcentration of buffer components and protein can lead to local concentration differences, or pH changes, since some buffers tend to crystallize. These pH or concentration changes in some instances can favor aggregation.

Mechanical stresses, such as agitation and stirring, introduce shear effects, or may cause a protein to adsorb to container-liquid or air-water interface leading to partial unfolding. The partially unfolded molecules can be transported throughout the bulk solution, triggering increased aggregation events. Additionally, these agitation stresses, can cause local thermal effects or cavitation, creating a favorable environment for the formation of hydroxyl and hydrogen radicals capable of oxidation reactions. [79-83,23]

A very common environmental stress that a protein drug may encounter is light. Tryptophan, tyrosine, phenylalanine, and cysteine residues can undergo photooxidation reactions, which can lead to changes in primary, secondary, and tertiary structures.[84]

Lyophilization of a protein solution is one approach commonly employed to stabilize proteins that are not sufficiently stable in liquid formulations, but the various stages of the lyophilization process such as freezing, primary and secondary drying, and reconstitution may all structurally damage proteins.[85-89] Freezing causes similar effects to those described above. [85,88,89] Primary drying removes the frozen bulk water and concentrates the protein and stabilizers, permitting the possibility of unfavorable interactions to occur.[86,90] During the secondary drying step, non-frozen water bound to the protein or excipients is removed, increasing the possibility of

protein instability. The stability of a lyophilized protein may be affected by the reconstitution addition rate and diluent composition.[76,91] Diluents added too rapidly may not give the dried protein enough time to rehydrate and properly assume its native conformation. If added too slowly, however, this may allow an increased amount of time for particles to form. [76,92] Particle formation can be affected by choosing diluents with various whetting capabilities (i.e., surfactants) or with differing ionic strengths. Aggregation of mAbs in the lyophilized state upon reconstitution has been correlated with non-native intermolecular disulfide bond formation[93] and an increase in the levels of subvisible particles.[94] A freeze-dried cake's moisture content and cake structure are also considerations since they too can affect the extent to which a protein may aggregate in the solid state. [73-76,90,95,96] Some lyophilized protein preparations with high moisture content have shown increased chemical degradation due to the increased ability of water to participate in physical and chemical degradation processes.[97] However, this is not a general rule and there are exceptions that have been reported.[95,98] It has also been shown that cake collapse can be an important factor in determining protein stability in the solid state.[73-75]

Formulation composition parameters such as concentration, pH, and ionic strength can also influence the aggregation of protein pharmaceuticals. Often high protein concentrations are required for best efficacy or for improved patient friendly dosage forms (e,g., self-administration by subcutaneous injection). High protein concentrations can make self-association interactions more favorable[79,99,100,101] but at the same time, can make conformational unfolding less favorable.[79,102] Such formulations cannot be directly analyzed by many analytical techniques without dilution, which can cause weak reversible interactions to dissociate resulting in changes in the aggregate population distribution.[79,103,104] The pH of the formulation can not only affect protein surface electrostatic interactions, but acidic pH can cause hydrolysis reactions in the

protein while basic conditions can promote deamidation and oxidation reactions.[20,79] Increasing the ionic strength of a solution may increase or decrease protein colloidal stability depending on the protein, the type and amount of salt and the formulation pH.[105,80] The addition of a small amount of salt (<0.15 M) can neutralize protein surface charge and decrease electrostatic interactions due to increased charge screening.[20,106] Generally, these electrostatic interactions are usually essential for maintaining a native, folded protein conformation, and its absence can destabilize protein solutions and induce aggregation. If these interactions favor non-native state of a protein, reducing them by the addition of salt can hinder aggregation.[105] An appropriate distribution of anisotropic charge or the peptide bond itself, because of its dipole nature, can cause protein-protein interactions to become attractive and aggregation to occur.[20] At high salt concentrations and depending on the salt type, there may be preferential binding of ions to the protein, which can destabilize the native conformation and increase solubility[20] (i.e., chaotropic effect). Divalent cationic salt ions could also bind to surface amino acid side chains or cross-link residues to provide increased conformational stabilization yet potentially increase aggregation.[105]

Protein therapeutics come into contact with many different solid-liquid and air-liquid interfaces throughout production. There have been many instances where syringe surfaces[107-110], containers[111,112], or stoppers[112] have led to particle formation. When mAb solutions were agitated in the presence of siliconized syringe walls with air bubbles, subvisible particles were observed consisting of silicone oil droplets and aggregated proteins. The combination of effects from the stress and interaction with the silicone-oil water interface and air-water interface led to the observed particles.[109]

Even stainless steel particles that sometimes are shed during some types of filling processes, can serve as heterogeneous nuclei for microparticle formation.[113,114] Heterogeneous

particles have also arisen from interaction with tungsten[115] or silicon oil[107], used in the production of prefilled syringes. In one study, vials, which were filled with an IgG formulation using a piston pump, showed an increase in subvisible particle formation (1.5-3μm) consisting of protein with no structural changes. It was hypothesized that nanoparticles that were being shed from the pump were heterogeneous nucleation sites for formation of protein microparticles.[114] A similar study was performed to further look at the effect of filling pumps to cause particulation. It was found that the rotary piston pump formed many more IgG microparticles upon filling of a mAb solution than a rolling diaphragm pump, peristaltic pump, and time-pressure filler pumps.[113] Tungsten, which may be present in prefilled syringes, seemed to induce large particles but this was highly dependent on solution pH, probably due to electrostatic interactions between protein and tungsten molecules.[115]

1.5 MAB PARTICLE CHARACTERIZATION

A better understanding of protein aggregation can only be gained by developing robust analytical techniques for monitoring its occurrence and the nature of the aggregates. Protein aggregates can be classified into multiple categories by 1) size, 2) reversibility, 3) conformation, 4) covalent modification, and 5) morphology.[116] Various techniques used to look at these aggregate characteristics will be briefly described. However, the user of any technique must always be aware of the potential pitfalls of each and every technique since not every method is useful for all types of protein particle samples.[27,110,117] Techniques for sizing and counting of aggregates will be briefly discussed followed by discussion of commonly used protein particle characterization techniques.

1.5.1 Particle Sizing and Counting

Depending on environmental conditions, aggregates can form in various size ranges: soluble (<100 nm), submicrometer (100-1000 nm), subvisible (1-100 μm), and visible (>100 μm).[116] There is no single technique available that can be used to characterize this broad size range of aggregates. Therefore a variety of analytical techniques must be used.[110] Some of the most common analytical techniques used to size and count aggregates and particles are discussed below but an in-depth discussion of these techniques and their potential advantages and disadvantages are discussed elsewhere in the literature. [68,118,119] As mentioned earlier, protein particles between 0.1-10 μm in size have been receiving a lot more scrutiny over the past few years due to the hypothesis that they have an increased potential to cause untoward immunogenic responses.[52] Therefore, in this chapter we will focus on this size range, but briefly summarize the techniques for quantification of small soluble aggregates.

1.5.1.1 Soluble Aggregates (<100 nm)

Information about small, soluble protein aggregates, while not the focus of this review, can be obtained from a variety of techniques. Most commonly used techniques are size exclusion chromatography (SEC), dynamic light scattering (DLS), analytical ultracentrifugation (AUC), and asymmetrical field flow fractionation (AFFF). Additionally, SEC can be coupled to a multi-angle light scattering detector (MALS) to gain information on the absolute molecular weight of the aggregates. [120,121]

1.5.1.2 Submicron (100-1000 nm)

Techniques like dynamic light scattering (DLS), Nanosight Particle Tracking Analysis (NTA), and Resonant Mass Measurement (RMM) cover this size range. DLS is a light scattering technique, which provides molecular weight information about aggregates in solution. DLS is a

quick, often high throughput technique that determines the size of aggregates based on measurements of time-dependent fluctuations in scattered light intensity, which arise from random motions of molecules in solution. From this information and by knowledge of the viscosity and temperature of the solution, a diffusion coefficient can be determined, which can then be used to calculate the hydrodynamic radius by the use of the Stokes Einstein equation. The samples, however, need to be homogenous with low polydispersity since size determination can be biased towards large particles even if only a few large particles are present.

NTA is a complementary technique to DLS used to monitor protein particle size, but has the advantage of being able to count particles as well. [122] It consists is an optical microscope linked to a light scattering detector, which allows visualization of the actual Brownian motion of nanometer-sized particles. Unlike DLS, NTA has the capacity to track and monitor the diffusional movements of individual particles and calculate their size using a modified Stokes-Einstein Equation,[122] while DLS calculates the "average" diffusional coefficient from the entire ensemble of particles within the solution, NTA calculates size from individual particles. This greatly diminishes the bias towards the contribution of larger particles, associated with many light scattering techniques. Therefore NTA can better analyze polydisperse samples than DLS.

The Resonant Mass Measurement (RMM) technique measures the size of particles between approximately 400 nm to 2 μm and has the ability to differentiate protein particles from silicone oil droplets. [123-125] The sensor consists of a suspended beam that resonates at a specific frequency. When a protein particle passes through the microchannel resonator, the frequency changes. The change in frequency is measured and is used to calculate the buoyant mass of the particle. By knowing the density of the fluid and approximating the density of the particle, the

dry mass of the particle and its corresponding diameter (assuming an equivalent spherical approximation) can be calculated.

Turbidity and nephelometry can be used to measure the light transmitted through the sample solution or light scattered by the sample solution relative to formazin standards, respectively. These techniques are not limited to any one size range of aggregates and thus can be used as an overall assessment of aggregation. Nephelometry measures the amount of light scattered, typically at 850 or 860 nm and at a scattering angle of 90°. For turbidimetry, the transmitted light is measured using a UV/Visible spectrophotometer at a wavelength between 320 to 800 nm (where proteins do not absorb light). The measurement is simple to perform and nondestructive, yet it doesn't provide quantitative information about the size, shape, or types of aggregates, so it more useful for comparative purposes. Additionally, high turbidity can also arise from larger size aggregates or from the opalescence of high protein concentration solutions, which does not always indicate that there is a large amount of aggregates or particles present in the sample.[119]

1.5.1.3 Micron (Subvisible)

A combination of techniques such as Optical Microscopy, Coulter Counters, Light Obscuration, Flow-Imaging (MFI and Flowcam), and Fluorescent Activated Cell Sorter (FACS) can be used to count, size and characterize subvisible particles in the range of 1-100 μm.

Optical microscopy is a compendial method that requires samples to be filtered onto a membrane and visually analyzed. This technique, however, requires a large sample volume. The filtration step can potentially alter protein aggregates. In addition, protein particles may be difficult to visualize without additional staining steps. This requires manual evaluation of the

filtered particles, which can be very time-consuming. Because of this, it is seldomly used on its own as a characterization tool, but is used in conjunction with other characterization techniques.

Flow Imaging Microscopy (Flowcam) and Microflow-Imaging (MFI) are similar techniques. In both methods, particles pass through a flow cell past a high-powered charge-coupled device (CCD) camera where high resolution images of the particles are captured and stored into databases. The particle images are analyzed by specialized software to provide information about size, count, and various morphological parameters, such as aspect ratio or transparency of the particles. Unfortunately, protein particles can adhere to the glass surface of the flow cells, and can often be very difficult to remove thus requiring careful sample preparation and cleaning procedures. These techniques allow the user to perform operations that were too complex previously such as examining how the morphology of the protein particles varies with formulation, solution, and stress conditions. Additionally, these morphological parameters allow easy differentiation of protein from non-proteinaceous particles, such as air bubbles or silicone-oil droplets [126]. Unlike it's light obscuration counterpart, these two orthogonal techniques are more likely to detect translucent protein particles.[126]

Light obscuration is a compendial technique that measures the amount of light blocked by a particle as it passes through a laser beam. This blocked light intensity is proportional to the cross-sectional area of an equivalently sized sphere, which can then be used to calculate the size of a particle. While this technique is easy to perform, it cannot differentiate between bubbles, oil droplets, or dust particles. In addition, it often under counts transparent protein particles since they do not block light to the same extent as the polystyrene beads used to calibrate the instrument. Finally, light obscuration methods often require high sample volumes, although lower volume compendial methods for biotechnology products have recently become

available.[119]

Coulter Counters, or electrical sensing zone methods, rely on the change in electrical resistance of a particle as it passes through an electrical sensing zone to calculate particle size (based on equivalent spherical diameter). However, the solution generally needs to be highly conductive to measure electric current and the technique can often underestimate the smaller sizes. These conductive solutions can pose some problems for protein solutions that are highly sensitive to ionic strength. This technique can cover a broad size range, from 0.5 μm to 1000 μm, if multiple apertures and different conductive solutions are used. While this technique does not provide morphological information, it does not have some of the limitations that other optical detectors face regarding issues concerning refractive index, shape, and compactness. [119]

A Fluorescent Activated Cell Sorter (FACS) is a flow cytometry instrument with sorting capabilities. It can be used to sort fluorescently labeled particles or can be used without fluorescence labeling to detect, quantitate, and collect micron sized particles by measuring light scattering. FACS can monitor individual particles and gives very reliable size distribution data. The advantage of this technique is that particles of interest can be detected and captured for further analysis. Unfortunately, this technique dilutes particles significantly during analysis making the sample recovery difficult during routine use.

1.5.1.4 Visible (> 100 μm)

Larger particles can be detected visually without any instrument, although well-defined viewing parameters are essential to obtain reproducible results. The United States Pharmacopeia (USP) requires parenteral preparations to be "essentially free from visible particles," while the European Pharmacopoeia (Ph.Eur.), states injections have to be "practically free from particles."

The Ph. Eur. chapter provides specific methods for visual assessment of particles, under defined background and lighting conditions.[30] Even though extensive training is required to perform this operation, the results are still based on viewer's judgment. Some manual visual inspection procedure use a scale provided in the Deutscher Arzneimittel Codex that describes the presence of visible particles from a scale of 0 (no particles) to 10 (particles visible immediately in large amounts) within 5 s.[119]

1.5.2 Protein Particle Characterization

Aggregates not only vary by size and counts, but also by their morphology and composition including conformation and covalent modifications of protein within the particles.[79,116] The conformation of the protein can be described by its secondary and tertiary structures and by its surface hydrophobicity, and can range from being native, partially unfolded, or extensively unfolded. Aggregates can also have various covalent linkages, some resulting from disulfide cross-linking, which are reducible, and other crosslinks that are not be reducible. Additionally, amino acid residues can be modified by chemical reactions which lead to formation of thioether and dityrosine covalent bonds, oxidation of methionines or cysteines, or deamidation reactions, etc.[116] The morphology of protein molecules within particles and aggregates can be studied by a variety of techniques and can range from amorphous to fibrillar in structure. Characterizing aggregates with respect to these traits is potentially just as important as being able to size and count them. Protein particles containing many of these physicochemical aspects have been implicated in different immunogenic responses.[35,127,128]

1.5.2.1 Conformational Alterations

Biophysical techniques such as Circular Dichroism (CD), Fourier Transform Infrared Spectroscopy (FTIR), Raman Spectroscopy, and Fluorescence Spectroscopy can be used to study conformational changes in proteins leading to aggregation. These techniques will be briefly discussed, but detailed information can be obtained from other sources.[129,130]

CD is a measure of the unequal absorption of right and left-handed circularly polarized light. Near-UV CD is used to monitor wavelengths between 250-350 nm and can give information regarding the tertiary structure characteristics of a protein by monitoring certain amino acid residues. Far-UV CD can be used to study changes in secondary structure of the protein, by examining wavelengths between 170-250 nm to monitor the protein polypeptide backbone conformation, such as alpha helices, beta sheets, or random coil. However, larger protein particles or turbid solutions can give inconsistent results from absorption flattening and differential scattering effects, but recent developments are being made to look at the structure of protein within immobilized particles using a rotating cylindrical sample cell and ultrathin path length cells.[119,131]

Fourier Transform Infrared Spectroscopy (FTIR) analysis can provide an estimate of the amount of various secondary structure components in a protein solution by looking at the vibration characteristics of the bonds in the protein backbone, especially in the Amide I region between 1600-1700cm^{-1}. [79,132-134] The use of FTIR Microscopy allows increased sensitivity and makes it possible to determine the composition of protein molecules within a single protein particle [126]. The advantage of FTIR analysis of proteins is that it can be performed in optically clear and turbid solutions or with solid samples. Unfortunately, the sensitivity is fairly low and a relatively large amount of aggregate needs to be present to detect changes in the protein higher order structure. Raman spectroscopy gives similar and complementary information as FTIR,

based on inelastic Raman scattering. Proteinaceous and nonproteinaceous particles can also be analyzed by Raman spectroscopy. Similar to FTIR microscopy, it also requires a lot of aggregated sample to detect structural changes.[135]

Fluorescence spectroscopy relies on monitoring the emission of photons from certain high energy states to certain low energy states. It can be used to study changes in tertiary structure of proteins by monitoring changes in environment around aromatic amino acid residues, primarily Trp, but minimally near Tyr residues. This approach, which monitors the environment around aromatic residues is called intrinsic fluorescence spectroscopy. In extrinsic fluorescence spectroscopy, fluorescent dyes such as 1,8 anilinonapthalene sulfonic acid, thioflavin T, sypro orange, nile red, or congo red, whose florescence properties change upon exposure to more apolar environments, are used to monitor changes in surface hydrophobicities or levels of aggregates in protein samples.[136,137] The dyes, however, can also interfere with the aggregates present in solution and may either cause more aggregation or disrupt the aggregates present by their own binding to regions on the protein. Perhaps the best method using fluorescence with individual protein particles employs FACS equipped with fluorescent detectors (described above). Mach et al have used this technique with a monoclonal antibody and showed that is simple to differentiate proteinaceous particles after staining them with a fluorescent hydrophobic dye.[138]

1.5.2.2 Covalent Modifications

SDS-PAGE is the simplest and fastest technique used to look for the presence of reducible or non-reducible covalent linkages (i.e., disulfide bonds) in protein samples. The technique uses an electric field to separate molecules based primarily on their molecular weight

by unfolding and coating protein molecules with a highly negatively charged detergent. However, the sample preparation itself (adding sodium-dodecyl sulfate solution and extensive heating) may modify the aggregates and cause non-covalent aggregates to dissociate, leading to inaccurate quantitation of the resulting bands. A similar technique can be performed using a capillary based system (CE-SDS) to determine the amount of covalent, disulfide linkages in aggregates. [139] It has been performed with several mAbs and used for detection of aggregates.[140,141]

Peptide mapping can also be used to determine if any chemical modifications occurred on the primary sequence of a mAb. First, the protein is treated enzymatically to produce peptide fragments which are then separated, monitored and identified using a combination of UPLC techniques in conjunction with UV and mass spectrometry. Using this method, a mAb, subjected to extended storage, was analyzed for the extent of deamidation and methionine oxidation.[142] In another study, a mAb was subjected to mechanical, chemical, and thermal stress treatment and then analyzed for chemical modifications.[78] It was shown that different types of aggregates contained varying levels of different types of chemical modifications.[78]

1.5.2.3 Morphology and Composition

The simplest way of obtaining morphological information is by using MFI, described above. The technique provides digital images of protein particles and calculates a variety of morphological parameters (area, intensity, equivalent circular diameter, perimeter, circularity, maximum ferret diameter, aspect ratio, and edge particles) of particles in solution. This technique is fast and requires minimal sample preparation. For additional images, one can rely on an FTIR microscope, which often is accompanied with an optical microscope (described above).

The highest resolution images, however, and the greatest morphological information can be gained from Atomic Force Microscopy (AFM), Scanning Electron Microscopy (SEM), or Transmission Electron Microscopy (SEM).[143] AFM can be used to obtain the surface topology of protein aggregates by using a small cantilever that moves directly over the surface of the sample with automatic height adjustments. The utility of the method is illustrated by a recent study with stressed mAbs.[144] SEM can be used to visualize aggregates from a few nanometers to several microns in size by striking the sample with a beam of electrons, which scan the surface, giving information about the composition and topology of the sample. Sample preparation for SEM often requires coating the surface of aggregates with a conductive material, which may destroy or modify the aggregates. Transmission Electron Microscopy[145] can also be a viable technique for visualizing aggregates down to nanometers in size. Unlike SEM, the electron beam directly interacts and passes through the sample to form an image. While sample preparation generally requires staining with uranyl acetate, samples can also be analyzed with minimal sample preparation, using a Cryo-electronic Microscopy (Cryo-EM).[146] This technique also provides morphological information of the sample, but unlike SEM or TEM, the sample can be visualized in its native state. [147] Composition of protein aggregates can be obtained by performing Energy-dispersive X-ray spectroscopy (usually in conjunction with SEM or TEM) to obtain elemental information of protein within aggregates or particles. [126,148] The signal is obtained when a beam of electrons interacts with the sample. The beam of electrons can collide and eject electrons of different elements located in distinct energy levels to create a "hole". When another electron, from a higher energy state, occupies the empty electron "hole," the difference in energy to fill the position is released as an x-ray signal, measured by an energy-dispersive spectrometer. These x-ray signals emitted are characteristic of certain elements which can then be easily determined.[149]

It is extremely valuable to understand the uses and drawbacks for each of these techniques when interpreting data. Additionally, it is very important to always mention the method used in conjunction with the results since each technique is performed by relying on different scientific principles. Assumptions about shape, refractive index, and density of protein particles are made and using polystyrene standards for various measurement techniques, although convenient, may not accurately reflect the comparative properties of protein particles. Currently there are no standards available that adequately mimic protein particles in terms of these parameters, even though extensive work is underway to develop them.

1.6 MAB PARTICLE PREVENTION

While there are many ways in which mAbs can aggregate and form particles, there are also many approaches that have been developed to minimize and ultimately prevent particle formation. The first step is often to predict the aggregation potential of a protein based on computer modeling, by finding aggregation "hotspots" and minimizing them by modification of amino acid sequences.[30] However, this can be problematic as it may introduce a foreign epitope or cause the protein to alter its biological activity.

The most common excipients used to stabilize protein molecules are amino acid derivatives, sugars, osmolytes, or salts.[106] Some amino acids, such as proline or arginine, are often added to decrease aggregation, probably due to their contribution to inter-molecular self-association due to hydrophobic stacking or by preferential exclusion mechanism.[106] Osmolytes stabilize protein structure by preferential hydration mechanism and solvophobic effects.[106] Salts can increase or decrease stability of the protein through nonspecific interactions and these effects

can vary depending on their concentration. For long term storage, anti-microbials may be added to the formulation to extend their lifetime but studies have shown that the presence of these can lead, in some cases, to partial unfolding of a protein and consequent aggregation.[150]

In the early stages of drug development, it is necessary to determine a protein's aggregation behavior as it is subjected to freeze-thaw, agitation, heat, or mechanical stresses. Conditions similar to this will often be encountered during the production and handling of a protein drug. For these kinds of conditions, various additives can be included in the formulation to prevent aggregation. These stabilizers generally function by minimizing conformational changes of the native protein to suppress aggregation. For possible shaking stress that may occur during shipping or during freeze-thaw, non-ionic surfactants are often added to compete with the protein for air-water interfaces and to decrease the protein's surface adsorption on these interfaces. Surfactants minimize ice-protein interactions by reducing surface adsorption, but if they are contaminated with peroxides or exposed to a sufficient amount of light, they can degrade and cause oxidation reactions. In such cases, methionine or tryptophan is often included in the formulations to prevent or reduce oxidation reactions due to polysorbate degradation. Surfactants could also cover exposed hydrophobic sites of the protein itself and thus prevent aggregation.[67] Polysorbates have been used in many mAb formulations such as Rituxan, Remicade, ReoPro and Humira.[151] In both freezing and shaking stresses, surface adsorption to various interfaces is one major source of aggregation. Therefore minimizing the surface area of the interface can decrease aggregation. During freeze-thawing, it is common to employ a slow freezing rate since this will generate larger crystals, with a lower surface area. Additionally, increasing the protein concentration can be beneficial, especially for preventing freezing and

shaking-related aggregates, since higher protein concentration would lead to a smaller fraction of protein being adsorbed at the interface than if the formulation was more dilute.

Prevention against thermal stress can also be accomplished by addition of sugars (e.g., sucrose, trehalose) since they stabilize the protein by preferential exclusion. Sugars also can have more affinity for the native state than for the non-native state. Arginine can also be included to increase the solubility of aggregation-prone molecules. It is in fact known to suppress heat-induced aggregation of mAbs.[106]

1.7. ATTRIBUTES OF AGGREGATES THAT MAY BE LINKED TO INCREASED IMMUNE RESPONSE

Some aggregate characteristics may impact immune responses more than others. Specifically increased uptake of particles by antigen presenting cells (APCs) or extended exposure of them to T cells could play a role in the immune response,[152-155] especially since the first step in inducing an immunogenic response is by APCs. In fact, protein aggregates activate APCs and can be easily phagocytized[155]. However, while APC uptake is a requirement for immunogenicity, it does warrant it, but is good for predictive purposes. APC binding and uptake of the antigen can be modulated by altering size, surface molecule organization, hydrophobicity/hydrophilicity, shape, surface charge, and conformation.[156,157] Additionally, it appears that the type of aggregate itself may be an important factor as well.

The size of antigens is thought to play one of the largest roles in their immunogenicity. Soluble aggregates do not seem to cause significant immune responses.[158] Even though there is no clear conclusion concerning what size of particles seem to be optimal for phagocytosis[157], it is

known that APCs have evolved to process antigens that were similar in size to viruses (20-100 nm) and bacteria (a few micrometers).[157,159] It is also believed that subvisible (micron) sized particles can act as adjuvants and enhance T cell responses by attracting dendritic cells, which uptake aggregates. [42,160-163] Due to their larger size, microparticles can also present multiple copies of antigens on their surface, facilitating B cell activation.[163] However, interpretation of some of this data needs to be taken with caution as many studies looking at the impact of size were performed using different types of beads to carry the antigen and were not pure protein particles. Therefore, how accurately these results correlate with actual protein particles remains to be seen.

The structure of aggregates themselves is very important as well. Native-like aggregates appear to be more capable of producing ADAs that could cross-react with the native monomer. [42,164] Additionally, molecular weight, mass, and solubility of the aggregates can play a role in the immunogenicity of a biotherapeutic. Protein self-assembly into virus like particles display repeating, equally spaced epitopes, which mimic those present in viruses or bacteria. The immune system has evolved to target these repetitive patterns and mount a strong immune response.[30,157,165] Other pathogen-associated molecular patterns such as the exposure of hydrophobic portions of biological molecule have become evolutionary danger signals to the immune system to recruit cells for repair, destruction, or increased immunity.[156] In some studies, microspheres with hydrophobic surfaces were more readily phagocytized than those with hydrophilic surfaces.[159,166,167]

Particle shape and geometry may influence attachment and internalization and impact the overall rate of phagocytosis by macrophages.[168,169] Tabata et al showed that phagocytosis of oblate ellipsoids is better than phagocytosis of prolate ellipsoids or spheres, but attachment of

prolate ellipsoids is better than that of oblate ellipsoids of certain volumes.[166] Those with the longest dimensions close to 2-3 microns have the highest attachment.[166] They described their findings by mentioning that phagocytosis is an energy intensive process requiring actin reorganization. The oblate ellipsoid, which requires the least actin remodeling by the cytoskeleton, will be internalized faster. In addition to influencing binding and uptake, aggregate morphology may influence how it becomes accessible for peptide processing.[128]

Surface charge is another factor that may influence APC uptake. Cationic microparticles can be taken up, often non-specifically, by macrophages and dendritic cells (DC), [167,170,171] although, this is not always the case.[170] The cell surface *in vivo* is usually negatively charged due to the presence of sulfated proteoglycans. Thus, ionic attraction between cationic microparticles and the negatively charged surface often can lead to binding and internalization. [159]

The type of aggregate may be an important immunogenic factor. Specifically oxidized samples have often showed higher immune response in many studies. This could be because a large amount of reactive oxidized species in biological pathways may be considered as danger signal by the immune system.[172] Oxidized mAbs in one case showed a relatively high immune response [173], whereas, in another study, two oxidized IgG2 mAbs did not.[174] As discussed above, it has been shown that high immunogenic responses were apparent from protein samples consisting of a large number of subvisible particles, various levels of native conformation, and those oxidized either by metal-catalyzed[42,164,175,176] or hydrogen peroxide.[175] Therefore the type of chemical modifications and the extent of structural alterations in proteins within aggregates/particles can determine immunogenic potential in conjunction with aggregate size and

number. Surface charge and morphology of protein particles has also been shown to play a role in some cases.

1.8 CHAPTER REVIEWS

1.8.1 Structural Characterization of IgG1 mAb Aggregates and Particles Generated Under Various Stress Conditions (Chapter 2)

Chapter 2 presents a case study looking at protein particle formation of an IgG1 mAb using different analytical techniques to study the effect of four different stresses (freeze-thaw, shaking, stirring, and heating) and the effect of salt on the size, number, and nature of aggregates/particles. Initially, aggregates and particles were sized and counted by SEC, NTA, MFI, turbidity, and visual assessments. Particle morphology was examined by MFI and TEM. The protein within the particles that formed under the same four stresses, but in the presence of 150 mM NaCl, was analyzed for covalent crosslinking (by SDS-PAGE), secondary structure content (FTIR in solution/FTIR Microscopy), and surface hydrophobicity (extrinsic fluorescence using 1,8 ANS). Radar plots, generated from MFI data, were also utilized as a data visualization tool to study the effects of the stress and salt on particle size distribution and morphology of subvisible particles.

The possible causes for aggregation and particle formation under each stress condition is discussed and compared with other similar studies using monoclonal antibodies. These comparisons showed that aggregate and particle formation varies with the protein, type of stress, and solution conditions. Freeze-thaw was the mildest condition. Only in the presence of NaCl, some subvisible particles containing protein with native secondary structure and low surface hydrophobicity were formed. Shaking generated predominantly transparent and amorphous

micron-sized particles, a combination of fiber-like and spherical-like nanometer sized particles. These particles contained protein that had largely native like secondary structure and low surface hydrophobicity with very little covalent crosslinking. Both stirring and heating in the presence of salt were harsher conditions. Stirring generated a large quantity of submicron, micron, and visible particles. In the absence of NaCl, more spherical nanometer particles were observed compared to the other NaCl-stressed samples. Insoluble protein, isolated after centrifugation, was more highly covalently linked and displayed greater surface hydrophobicity than the protein in the soluble fraction. The subvisible particles contained protein with some decrease in native like secondary structure. Heating of an IgG1 sample in the absence of NaCl was generally a mild stress and did not form a large number of soluble aggregates or nanometer and micron-sized particles. Heating in the presence of NaCl, however, generated particles of all sizes in great abundance. Nanometer particles were fibrillar in morphology. The insoluble aggregates, separated by centrifugation, contained a higher level of covalently linked aggregates than the protein in the supernatant but both demonstrated high levels of ANS binding. Subvisible particles contained protein with non-native like secondary structure. The heat stressed samples had very highly non-native-like secondary structure. The combination of structural changes from the heating stress (conformation effects) and decreased shielding of repulsive charges (colloidal effects) by the NaCl led to the large amounts of aggregate and particle formation.

Our work follows some general trends but some exceptions are also noted. All stresses showed increased aggregation in the presence of NaCl but in different size ranges. This observation highlights the fact that protein aggregate formation cannot always be detected by one technique and a range of analytical tools need to be used for full characterization.

1.8.2. Characterization of the Physical Stability of a Lyophilized IgG1 mAb after Accelerated Shipping-like Stress (Chapter 3)

The impact of mechanical stress on the stability of lyophilized protein therapeutics has not previously been studied in detail. This chapter focuses on understanding if shaking stress, mimicking the transportation and shipping conditions that a lyophilized protein may encounter, can decrease the physical stability of the protein upon reconstitution. We implemented a stress shipping test based on guidelines from ASTM International Standard Test Methods for Vibration Testing of Shipping Containers [177]. Our initial studies showed that the physical stability of both a liquid and lyophilized formulation of an IgG1 mAb during shaking was similar, contrary to our notion that the lyophilized sample should be more stable. The lyophilized sample displayed physical instability upon reconstitution upon shaking stress. This was an interesting result and was further investigated.

An array of analytical techniques were utilized to size and count protein aggregates and particles forming over a broad size range using SEC, DLS, NTA, RMM, MFI, and solution turbidity. The morphology and composition of these particles were further examined using radar chart analysis of MFI data, SDS-PAGE and FTIR Microscopy. Interestingly, shaking stress only led to increases in turbidity and subvisible particle counts (as assessed by MFI). In conjunction with analyzing the effect of mechanical stress on the physical stability of this mAb, we also analyzed the effect of moisture content, reconstitution medium type and addition rate, storage duration, storage temperature, and cake structure on the physical stability of this mAb. In all cases, shake-stressing of the lyophilized mAb, followed by reconstitution, led to increases in turbidity and subvisible particle formation. Minimal changes in conformation or covalent linking of protein within the particles was detected by FTIR analysis or SDS-PAGE upon stress

and reconstitution. The effect of moisture content and reconstitution addition rate were minimal on the stressed mAb. However, the reconstitution of the shake-stressed sample took longer than the unstressed lyophilized sample. Reconstitution medium was an important factor impacting the physical stability of this protein upon stress. The potential causes of increased subvisible particle counts and the effect of reconstitution medium upon shaking stress are discussed. Significant differences in physical stability were not observed when the effect of extent of shaking on subsequent storage stability of the lyophilized IgG mAb was analyzed. Solution turbidity and subvisible particle concentration increased with increasing storage duration and with increasing temperature of storage. The cake integrity, resulting from the shake stress, did impact the extent of degradation. As the mechanical stress applied to the lyophilized cake was increased (with more cake collapse), subsequent storage stability decreased.

This case study highlights that post-lyophilization mechanical stress, which may be encountered by the lyophilized protein during shipping and transportation, can result in physical instability of the lyophilized protein. This study highlights the importance of monitoring shake sensitivity of lyophilized protein cakes as part of formulation development strategies. Future work requiring more lyophilized proteins to be characterized in this manner is suggested.

1.8.3. Physical characterization and *in vitro* biological impact of highly aggregated antibodies separated into size enriched populations by FACS (Chapter 4)

The goal of this chapter is to study the impact of protein aggregate size on the *in vitro* early and late phase immune response using stir stressed IgG2 mAb particles (mAb2) and an *In Vitro* Comparative Immunogenicity Assessment Assay (IVCIA), which was developed by our scientific collaborators at Amgen.

To study the impact of protein particle size in the IVCIA assay, a mAb2 solution was stirred to generate protein particles of varying sizes. The protein particles were first separated into various size populations using either (1) low speed centrifugation to enrich for nanometer vs. micron sized particles, or (2) the Fluorescence Activated Cell Sorter (FACS) to separate and collect enriched fractions of different micron-sized protein particles. The enriched fractions were assessed for their immunogenic potential in the IVCIA but due to the dilute nature of FACS sorted particles, the sample prepared immediately before FACS separation was biophysically characterized. We were able, however, to examine particle morphology and composition of the FACS isolated particles by a combination of MFI, TEM and SEM-EDX.

In an initial set of experiments, we showed that micron sized protein particles, compared to nanometer-sized particles, displayed the highest cytokine signature readout in the IVCIA assay. The FACS separation did not dramatically alter the properties of the stir stressed sample and the enrichment was high even after the necessary two freeze thaws. The sample just prior to FACS separation contained particles that were amorphous containing some alteration in overall secondary structure with increased surface hydrophobicity. Interestingly, particles generated by stirring contained fluorine as measured by SEM-EDX; the element was not present in the buffer, control mAb2 or heated mAb2. Its impact in our assay needs to be assessed in the future. Limitations and advantages of using FACS for sorting subvisible particles are discussed. We also highlighted that both protein mass and number of particles are important factors for consideration in monitoring their ability to generate cytokine responses in this assay. Even though the PBMC response was low due to the dilute nature of the particles, it appeared that in this assay, with this mAb, 5-10 μm sized protein particles displayed relatively elevated levels of cytokine responses compared to the other sized protein particles tested.

1.8.4. Summary, conclusions, and future directions (Chapter 5)

Chapter 5 summarizes the observations and understanding gained from studying three different monoclonal antibodies. In the first study, presented in Chapter 2, the effects of different stresses on the aggregation behavior of a mAb were characterized by a host of different techniques. Different stresses led to formation of aggregates with very different characteristics. It is suggested that it is not enough to just count and size aggregates and particles but it is necessary to thoroughly characterize them as well. The second study, presented in Chapter 3, looked at the physical stability of a lyophilized mAb undergoing agitation stress, which mimics the stress encountered by the protein during transportation and shipping. The objective here was to bring attention to the fact that mechanical stress that a lyophilized protein may encounter during transportation may lead to increased particle formation. Since this kind of work has not been done before, a detailed mechanism is lacking. Strategies are described on how to better understand this occurrence. In the final study, presented in Chapter 4, a new application for FACS is described and the potential of an in-vitro assay, based on human immune cells, was presented. The advantages and limitations of FACS and the capacity of the cell-based assay to rank relative immunogenic potential of various stressed samples are discussed. While future work is suggested to get a clearer understanding of this very complex topic, some insight into the impact of protein particle size in this *in vitro* cell-based immunogenicity model system is obtained.

1.9 REFERENCES

1. Elvin JG, Couston RG, van der Walle CF 2013. Therapeutic antibodies: market considerations, disease targets and bioprocessing. Int J Pharm 440(1):83-98.
2. Wang W, Singh S, Zeng DL, King K, Nema S 2007. Antibody structure, instability, and formulation. J Pharm Sci 96(1):1-26.
3. Kindt TJ, Goldsby RA, Osborne BA, Kuby J. 2007. Immunology. 6 ed., New York, NY: W.H. Freeman and Company.
4. Accessed on October 5, 2014, at: http://www.novimmune.com/science/antibodies.html. Novimmune. Antibodies: On the front line of human immune defense.
5. Golay J, Introna M 2012. Mechanism of action of therapeutic monoclonal antibodies: promises and pitfalls of in vitro and in vivo assays. Arch Biochem Biophys 526(2):146-153.
6. Shuptrine CW, Surana R, Weiner LM 2012. Monoclonal antibodies for the treatment of cancer. Seminars in cancer biology 22(1):3-13.
7. Chung S, Lin YL, Reed C, Ng C, Cheng ZJ, Malavasi F, Yang J, Quarmby V, Song A 2014. Characterization of in vitro antibody-dependent cell-mediated cytotoxicity activity of therapeutic antibodies - impact of effector cells. Journal of immunological methods 407:63-75.
8. Pace CN, Shirley BA, McNutt M, Gajiwala K 1996. Forces contributing to the conformational stability of proteins. FASEB journal : official publication of the Federation of American Societies for Experimental Biology 10(1):75-83.
9. Krishnamurthy R, Manning MC 2002. The stability factor: importance in formulation development. Curr Pharm Biotechnol 3(4):361-371.
10. Manning MC, Chou DK, Murphy BM, Payne RW, Katayama DS 2010. Stability of protein pharmaceuticals: an update. Pharm Res 27(4):544-575.
11. Stroop SD, Conca DM, Lundgard RP, Renz ME, Peabody LM, Leigh SD 2011. Photosensitizers form in histidine buffer and mediate the photodegradation of a monoclonal antibody. J Pharm Sci 100(12):5142-5155.
12. Volkin DB, Mach H, Middaugh CR 1995. Degradative covalent reactions important to protein stability. Methods in molecular biology 40:35-63.
13. Yi L, Beckley N, Gikanga B, Zhang J, Wang YJ, Chih HW, Sharma VK 2013. Isomerization of Asp-Asp motif in model peptides and a monoclonal antibody Fab fragment. J Pharm Sci 102(3):947-959.
14. Volkin DB, Mach H, Middaugh CR 1997. Degradative covalent reactions important to protein stability. Molecular biotechnology 8(2):105-122.
15. Liu H, May K 2012. Disulfide bond structures of IgG molecules: structural variations, chemical modifications and possible impacts to stability and biological function. MAbs 4(1):17-23.
16. Wang X, Kumar S, Singh SK 2011. Disulfide scrambling in IgG2 monoclonal antibodies: insights from molecular dynamics simulations. Pharm Res 28(12):3128-3144.
17. Pipes GD, Campbell P, Bondarenko PV, Kerwin BA, Treuheit MJ, Gadgil HS 2010. Middle-down fragmentation for the identification and quantitation of site-specific methionine oxidation in an IgG1 molecule. J Pharm Sci 99(11):4469-4476.
18. Manning MC, Patel K, Borchardt RT 1989. Stability of protein pharmaceuticals. Pharm Res 6(11):903-918.

19. Chi EY, Krishnan S, Kendrick BS, Chang BS, Carpenter JF, Randolph TW 2003. Roles of conformational stability and colloidal stability in the aggregation of recombinant human granulocyte colony-stimulating factor. Protein Sci 12(5):903-913.
20. Chi EY, Krishnan S, Randolph TW, Carpenter JF 2003. Physical stability of proteins in aqueous solution: mechanism and driving forces in nonnative protein aggregation. Pharm Res 20(9):1325-1336.
21. Sahin E, Grillo AO, Perkins MD, Roberts CJ 2010. Comparative effects of pH and ionic strength on protein-protein interactions, unfolding, and aggregation for IgG1 antibodies. J Pharm Sci 99(12):4830-4848.
22. Brummitt RK, Nesta DP, Chang L, Chase SF, Laue TM, Roberts CJ 2011. Nonnative aggregation of an IgG1 antibody in acidic conditions: part 1. Unfolding, colloidal interactions, and formation of high-molecular-weight aggregates. J Pharm Sci 100(6):2087-2103.
23. Joubert MK, Luo Q, Nashed-Samuel Y, Wypych J, Narhi LO 2011. Classification and characterization of therapeutic antibody aggregates. J Biol Chem 286(28):25118-25133.
24. Saito S, Hasegawa J, Kobayashi N, Tomitsuka T, Uchiyama S, Fukui K 2013. Effects of ionic strength and sugars on the aggregation propensity of monoclonal antibodies: influence of colloidal and conformational stabilities. Pharm Res 30(5):1263-1280.
25. Roberts CJ, Das TK, Sahin E 2011. Predicting solution aggregation rates for therapeutic proteins: approaches and challenges. Int J Pharm 418(2):318-333.
26. Wang W, Roberts CJ 2013. Non-arrhenius protein aggregation. Aaps J 15(3):840-851.
27. Philo JS, Arakawa T 2009. Mechanisms of protein aggregation. Curr Pharm Biotechnol 10(4):348-351.
28. Baker MP, Reynolds HM, Lumicisi B, Bryson CJ 2010. Immunogenicity of protein therapeutics: The key causes, consequences and challenges. Self/nonself 1(4):314-322.
29. Wang W, Singh SK, Li N, Toler MR, King KR, Nema S 2012. Immunogenicity of protein aggregates--concerns and realities. Int J Pharm 431(1-2):1-11.
30. Wang W, Roberts CJ editors. 2010. Aggregation of Therapeutic Proteins. ed., Hoboken, NJ: John Wiley & Sons. p 486.
31. Bunn HF 2002. Drug-induced autoimmune red-cell aplasia. N Engl J Med 346(7):522-523.
32. Casadevall N, Nataf J, Viron B, Kolta A, Kiladjian JJ, Martin-Dupont P, Michaud P, Papo T, Ugo V, Teyssandier I, Varet B, Mayeux P 2002. Pure red-cell aplasia and antierythropoietin antibodies in patients treated with recombinant erythropoietin. N Engl J Med 346(7):469-475.
33. Lehrman SR 2008. Protein Aggregation: Relevance to Pharmaceutical Development and Disease Pathology. AAPS Newsmagazine:18-24.
34. Harding FA, Stickler MM, Razo J, DuBridge RB 2010. The immunogenicity of humanized and fully human antibodies: residual immunogenicity resides in the CDR regions. MAbs 2(3):256-265.
35. Filipe V, Jiskoot W, Basmeleh AH, Halim A, Schellekens H 2012. Immunogenicity of different stressed IgG monoclonal antibody formulations in immune tolerant transgenic mice. MAbs 4(6).
36. Hermeling S, Schellekens H, Crommelin DJ, Jiskoot W 2003. Micelle-associated protein in epoetin formulations: aA risk factor for immunogenicity? Pharm Res 20(12):1903-1907.
37. Schellekens H 2002. Immunogenicity of therapeutic proteins: clinical implications and future prospects. Clinical therapeutics 24(11):1720-1740; discussion 1719.

38. Schellekens H 2005. Factors influencing the immunogenicity of therapeutic proteins. Nephrol Dial Transplant 20 Suppl 6:vi3-9.
39. Hermeling S, Crommelin DJ, Schellekens H, Jiskoot W 2004. Structure-immunogenicity relationships of therapeutic proteins. Pharmaceutical research 21(6):897-903.
40. Ratanji KD, Derrick JP, Dearman RJ, Kimber I 2014. Immunogenicity of therapeutic proteins: influence of aggregation. Journal of immunotoxicology 11(2):99-109.
41. Jawa V, Cousens LP, Awwad M, Wakshull E, Kropshofer H, De Groot AS 2013. T-cell dependent immunogenicity of protein therapeutics: Preclinical assessment and mitigation. Clinical immunology 149(3):534-555.
42. Fradkin AH, Carpenter JF, Randolph TW 2009. Immunogenicity of aggregates of recombinant human growth hormone in mouse models. J Pharm Sci 98(9):3247-3264.
43. Cromwell ME, Hilario E, Jacobson F 2006. Protein aggregation and bioprocessing. Aaps J 8(3):E572-579.
44. Hermeling S, Crommelin DJ, Schellekens H, Jiskoot W 2004. Structure-immunogenicity relationships of therapeutic proteins. Pharm Res 21(6):897-903.
45. Rosenberg AS 2006. Effects of protein aggregates: an immunologic perspective. Aaps J 8(3):E501-507.
46. Schellekens H 2002. Bioequivalence and the immunogenicity of biopharmaceuticals. Nat Rev Drug Discov 1(6):457-462.
47. Schellekens H 2003. Immunogenicity of therapeutic proteins. Nephrol Dial Transplant 18(7):1257-1259.
48. Bee JS, Chiu D, Sawicki S, Stevenson JL, Chatterjee K, Freund E, Carpenter JF, Randolph TW 2009. Monoclonal antibody interactions with micro- and nanoparticles: adsorption, aggregation, and accelerated stress studies. J Pharm Sci 98(9):3218-3238.
49. Dintzis RZ, Okajima M, Middleton MH, Greene G, Dintzis HM 1989. The immunogenicity of soluble haptenated polymers is determined by molecular mass and hapten valence. J Immunol 143(4):1239-1244.
50. Bachmann MF, Zinkernagel RM 1997. Neutralizing antiviral B cell responses. Annu Rev Immunol 15:235-270.
51. Singh SK, Afonina N, Awwad M, Bechtold-Peters K, Blue JT, Chou D, Cromwell M, Krause HJ, Mahler HC, Meyer BK, Narhi L, Nesta DP, Spitznagel T 2010. An industry perspective on the monitoring of subvisible particles as a quality attribute for protein therapeutics. J Pharm Sci 99(8):3302-3321.
52. Carpenter JF, Randolph TW, Jiskoot W, Crommelin DJ, Middaugh CR, Winter G, Fan YX, Kirshner S, Verthelyi D, Kozlowski S, Clouse KA, Swann PG, Rosenberg A, Cherney B 2009. Overlooking subvisible particles in therapeutic protein products: gaps that may compromise product quality. J Pharm Sci 98(4):1201-1205.
53. Andersen CB, Manno M, Rischel C, Thorolfsson M, Martorana V 2009. Aggregation of a multidomain protein: A coagulation mechanism governs aggregation of a model IgG1 antibody under weak thermal stress. Protein Science 19:279-290.
54. Hawe A, Kasper JC, Friess W, Jiskoot W 2009. Structural properties of monoclonal antibody aggregates induced by freeze-thawing and thermal stress. Eur J Pharm Sci 38(2):79-87.
55. Joubert MK, Luo Q, Nashed-Samuel Y, Wypych J, Narhi LO 2011. Classification and characterization of therapeutic antibody aggregates. J Biol Chem.
56. Menzen T, Friess W 2014. Temperature-ramped studies on the aggregation, unfolding, and interaction of a therapeutic monoclonal antibody. J Pharm Sci 103(2):445-455.

57. Sahin E, Weiss WFt, Kroetsch AM, King KR, Kessler RK, Das TK, Roberts CJ 2012. Aggregation and pH-temperature phase behavior for aggregates of an IgG2 antibody. J Pharm Sci 101(5):1678-1687.
58. Zhang A, Singh SK, Shirts MR, Kumar S, Fernandez EJ 2012. Distinct aggregation mechanisms of monoclonal antibody under thermal and freeze-thaw stresses revealed by hydrogen exchange. Pharm Res 29(1):236-250.
59. Barnard JG, Singh S, Randolph TW, Carpenter JF 2011. Subvisible particle counting provides a sensitive method of detecting and quantifying aggregation of monoclonal antibody caused by freeze-thawing: insights into the roles of particles in the protein aggregation pathway. J Pharm Sci 100(2):492-503.
60. Cordes AA, Carpenter JF, Randolph TW 2012. Accelerated stability studies of abatacept formulations: comparison of freeze-thawing- and agitation-induced stresses. J Pharm Sci 101(7):2307-2315.
61. Radmanovic N, Serno T, Joerg S, Germershaus O 2013. Understanding the freezing of biopharmaceuticals: first-principle modeling of the process and evaluation of its effect on product quality. J Pharm Sci 102(8):2495-2507.
62. Eppler A, Weigandt M, Hanefeld A, Bunjes H 2010. Relevant shaking stress conditions for antibody preformulation development. Eur J Pharm Biopharm 74(2):139-147.
63. Fesinmeyer RM, Hogan S, Saluja A, Brych SR, Kras E, Narhi LO, Brems DN, Gokarn YR 2009. Effect of ions on agitation- and temperature-induced aggregation reactions of antibodies. Pharm Res 26(4):903-913.
64. Huh JH, White AJ, Brych SR, Franey H, Matsumura M 2013. The Identification of Free Cysteine Residues Within Antibodies
and a Potential Role for Free Cysteine Residues in Covalent
Aggregation Because of Agitation Stress. J Pharm Sci 102(6):1701-1711.
65. Ishikawa T, Kobayashi N, Osawa C, Sawa E, Wakamatsu K 2010. Prevention of stirring-induced microparticle formation in monoclonal antibody solutions. Biological & pharmaceutical bulletin 33(6):1043-1046.
66. Jayaraman M, Buck PM, Ignatius AA, King KR, Wang W 2014. Agitation-induced aggregation and subvisible particulate formation in model proteins. Eur J Pharm Biopharm 87(2):299-309.
67. Kiese S, Papppenberger A, Friess W, Mahler HC 2008. Shaken, not stirred: mechanical stress testing of an IgG1 antibody. J Pharm Sci 97(10):4347-4366.
68. Mahler HC, Muller R, Friess W, Delille A, Matheus S 2005. Induction and analysis of aggregates in a liquid IgG1-antibody formulation. Eur J Pharm Biopharm 59(3):407-417.
69. Simler BR, Hui G, Dahl JE, Perez-Ramirez B 2012. Mechanistic complexity of subvisible particle formation: links to protein aggregation are highly specific. J Pharm Sci 101(11):4140-4154.
70. Thomas CR, Geer D 2011. Effects of shear on proteins in solution. Biotechnology letters 33(3):443-456.
71. Qi P, Volkin DB, Zhao H, Nedved ML, Hughes R, Bass R, Yi SC, Panek ME, Wang D, Dalmonte P, Bond MD 2009. Characterization of the photodegradation of a human IgG1 monoclonal antibody formulated as a high-concentration liquid dosage form. J Pharm Sci 98(9):3117-3130.
72. Mason BD, Schoneich C, Kerwin BA 2012. Effect of pH and light on aggregation and conformation of an IgG1 mAb. Molecular pharmaceutics 9(4):774-790.

73. Schersch K, Betz O, Garidel P, Muehlau S, Bassarab S, Winter G 2010. Systematic investigation of the effect of lyophilizate collapse on pharmaceutically relevant proteins I: stability after freeze-drying. J Pharm Sci 99(5):2256-2278.
74. Schersch K, Betz O, Garidel P, Muehlau S, Bassarab S, Winter G 2012. Systematic investigation of the effect of lyophilizate collapse on pharmaceutically relevant proteins, part 2: stability during storage at elevated temperatures. J Pharm Sci 101(7):2288-2306.
75. Schersch K, Betz O, Garidel P, Muehlau S, Bassarab S, Winter G 2013. Systematic investigation of the effect of lyophilizate collapse on pharmaceutically relevant proteins III: collapse during storage at elevated temperatures. Eur J Pharm Biopharm 85(2):240-252.
76. Wang W 2000. Lyophilization and development of solid protein pharmaceuticals. Int J Pharm 203(1-2):1-60.
77. Murphy BM, Zhang N, Payne RW, Davis GC, Abdul-Fattah AM, Matsuura JE, Herman AC, Manning MC 2012. Structure, Stability, and Mobility of a Lyophilized IgG1 Monoclonal Antibody as Determined Using Second-Derivative Infrared Spectroscopy. J Pharm Sci 101(1):81-91.
78. Luo Q, Joubert MK, Stevenson R, Ketchem RR, Narhi LO, Wypych J 2011. Chemical modifications in therapeutic protein aggregates generated under different stress conditions. J Biol Chem 286(28):25134-25144.
79. Mahler HC, Friess W, Grauschopf U, Kiese S 2009. Protein aggregation: pathways, induction factors and analysis. J Pharm Sci 98(9):2909-2934.
80. Wang W, Nema S, Teagarden D 2010. Protein aggregation--pathways and influencing factors. Int J Pharm 390(2):89-99.
81. Hawe A, Wiggenhorn M, van de Weert M, Garbe JH, Mahler HC, Jiskoot W 2012. Forced degradation of therapeutic proteins. J Pharm Sci 101(3):895-913.
82. Maa YF, Hsu CC 1997. Protein denaturation by combined effect of shear and air-liquid interface. Biotechnol Bioeng 54(6):503-512.
83. Thomas CR, Dunnill P 1979. Action of shear on enzymes: studies with catalase and urease. Biotechnol Bioeng 21(12):2279-2302.
84. Kerwin BA, Remmele RL, Jr. 2007. Protect from light: photodegradation and protein biologics. J Pharm Sci 96(6):1468-1479.
85. Mahler HC, Friess W, Grauschopf U, Kiese S 2009. Protein aggregation: pathways, induction factors and analysis. J Pharm Sci 98(9):2909-2934.
86. Heljo VP, Harju H, Hatanpaa T, Yohannes G, Juppo AM 2013. The effect of freeze-drying parameters and formulation composition on IgG stability during drying. Eur J Pharm Biopharm 85(3):752-755.
87. Abdul-Fattah AM, Dellerman KM, Bogner RH, Pikal MJ 2007. The effect of annealing on the stability of amorphous solids: chemical stability of freeze-dried moxalactam. J Pharm Sci 96(5):1237-1250.
88. Awotwe-Otoo D, Agarabi C, Read EK, Lute S, Brorson KA, Khan MA, Shah RB 2013. Impact of controlled ice nucleation on process performance and quality attributes of a lyophilized monoclonal antibody. Int J Pharm 450(1-2):70-78.
89. Bhatnagar BS, Bogner RH, Pikal MJ 2007. Protein stability during freezing: separation of stresses and mechanisms of protein stabilization. Pharm Dev Technol 12(5):505-523.
90. Carpenter JF, Pikal MJ, Chang BS, Randolph TW 1997. Rational design of stable lyophilized protein formulations: some practical advice. Pharm Res 14(8):969-975.

91. Cao W, Krishnan S, Ricci MS, Shih LY, Liu D, Gu JH, Jameel F 2013. Rational design of lyophilized high concentration protein formulations-mitigating the challenge of slow reconstitution with multidisciplinary strategies. Eur J Pharm Biopharm 85(2):287-293.
92. Shire SJ, Gombotz W, Bechtold-Peters K, Andya JD editors. 2010. Current Trends in Monoclonal Antibody Development and Manufacturing. ed., New York: Springer. p 350.
93. Andya JD, Hsu CC, Shire SJ 2003. Mechanisms of aggregate formation and carbohydrate excipient stabilization of lyophilized humanized monoclonal antibody formulations. AAPS pharmSci 5(2):E10.
94. Davis JM, Zhang N, Payne RW, Murphy BM, Abdul-Fattah AM, Matsuura JE, Herman AC, Manning MC 2013. Stability of lyophilized sucrose formulations of an IgG1: subvisible particle formation. Pharm Dev Technol 18(4):883-896.
95. Breen ED, Curley JG, Overcashier DE, Hsu CC, Shire SJ 2001. Effect of moisture on the stability of a lyophilized humanized monoclonal antibody formulation. Pharm Res 18(9):1345-1353.
96. Carpenter JF, Chang BS, Garzon-Rodriguez W, Randolph TW 2002. Rational design of stable lyophilized protein formulations: theory and practice. Pharmaceutical biotechnology 13:109-133.
97. Towns JK 1995. Moisture content in proteins: its effects and measurement. J Chromatogr A 705(1):115-127.
98. Costantino HR, Langer R, Klibanov AM 1995. Aggregation of a lyophilized pharmaceutical protein, recombinant human albumin: effect of moisture and stabilization by excipients. Bio/technology 13(5):493-496.
99. Yadav S, Liu J, Shire SJ, Kalonia DS 2010. Specific interactions in high concentration antibody solutions resulting in high viscosity. J Pharm Sci 99(3):1152-1168.
100. Saluja A, Kalonia DS 2008. Nature and consequences of protein-protein interactions in high protein concentration solutions. Int J Pharm 358(1-2):1-15.
101. Roefs SP, De Kruif KG 1994. A model for the denaturation and aggregation of beta-lactoglobulin. Eur J Biochem 226(3):883-889.
102. Minton AP 2005. Influence of macromolecular crowding upon the stability and state of association of proteins: predictions and observations. J Pharm Sci 94(8):1668-1675.
103. Liu J, Andya JD, Shire SJ 2006. A critical review of analytical ultracentrifugation and field flow fractionation methods for measuring protein aggregation. Aaps J 8(3):E580-589.
104. Shire SJ, Shahrokh Z, Liu J 2004. Challenges in the development of high protein concentration formulations. J Pharm Sci 93(6):1390-1402.
105. Wang W, Roberts CJ 2010. Aggregation of Therapeutic Proteins.
106. Hamada H, Arakawa T, Shiraki K 2009. Effect of additives on protein aggregation. Curr Pharm Biotechnol 10(4):400-407.
107. Thirumangalathu R, Krishnan S, Ricci MS, Brems DN, Randolph TW, Carpenter JF 2009. Silicone oil- and agitation-induced aggregation of a monoclonal antibody in aqueous solution. J Pharm Sci 98(9):3167-3181.
108. Majumdar S, Ford BM, Mar KD, Sullivan VJ, Ulrich RG, D'Souza A J 2011. Evaluation of the effect of syringe surfaces on protein formulations. J Pharm Sci 100(7):2563-2573.
109. Gerhardt A, McGraw NR, Schwartz DK, Bee JS, Carpenter JF, Randolph TW 2014. Protein aggregation and particle formation in prefilled glass syringes. J Pharm Sci 103(6):1601-1612.

110. Demeule B, Messick S, Shire SJ, Liu J 2010. Characterization of particles in protein solutions: reaching the limits of current technologies. Aaps J 12(4):708-715.
111. Vazquez-Rey M, Lang DA 2011. Aggregates in monoclonal antibody manufacturing processes. Biotechnol Bioeng 108(7):1494-1508.
112. 2014. Guidance for Industry: Immunogenicity Assessment for Therapeutic Protein Products. In Services UDoHaH, Administration FaD, (CDER) CfDEaR, (CBER) CfBEaR, editors., ed., Silver Spring, MD.
113. Nayak A, Colandene J, Bradford V, Perkins M 2011. Characterization of subvisible particle formation during the filling pump operation of a monoclonal antibody solution. J Pharm Sci.
114. Tyagi AK, Randolph TW, Dong A, Maloney KM, Hitscherich C, Jr., Carpenter JF 2009. IgG particle formation during filling pump operation: a case study of heterogeneous nucleation on stainless steel nanoparticles. J Pharm Sci 98(1):94-104.
115. Jiang Y, Nashed-Samuel Y, Li C, Liu W, Pollastrini J, Mallard D, Wen ZQ, Fujimori K, Pallitto M, Donahue L, Chu G, Torraca G, Vance A, Mire-Sluis T, Freund E, Davis J, Narhi L 2009. Tungsten-induced protein aggregation: solution behavior. J Pharm Sci 98(12):4695-4710.
116. Narhi LO, Schmit J, Bechtold-Peters K, Sharma D 2012. Classification of protein aggregates. J Pharm Sci 101(2):493-498.
117. Philo JS 2009. A critical review of methods for size characterization of non-particulate protein aggregates. Curr Pharm Biotechnol 10(4):359-372.
118. Wang T, Joshi SB, Kumru OS, Telikepalli S, Middaugh CR, Volkin DB 2013. Case Studies Applying Biophysical Techniques to Better Characterize Protein Aggregates and Particulates of Varying Size.205-243.
119. Zolls S, Tantipolphan R, Wiggenhorn M, Winter G, Jiskoot W, Friess W, Hawe A 2012. Particles in therapeutic protein formulations, Part 1: overview of analytical methods. J Pharm Sci 101(3):914-935.
120. Ahrer K, Buchacher A, Iberer G, Josic D, Jungbauer A 2003. Analysis of aggregates of human immunoglobulin G using size-exclusion chromatography, static and dynamic light scattering. J Chromatogr A 1009(1-2):89-96.
121. Ye H 2006. Simultaneous determination of protein aggregation, degradation, and absolute molecular weight by size exclusion chromatography-multiangle laser light scattering. Anal Biochem 356(1):76-85.
122. Filipe V, Hawe A, Jiskoot W 2010. Critical evaluation of Nanoparticle Tracking Analysis (NTA) by NanoSight for the measurement of nanoparticles and protein aggregates. Pharm Res 27(5):796-810.
123. Burg TP, Godin M, Knudsen SM, Shen W, Carlson G, Foster JS, Babcock K, Manalis SR 2007. Weighing of biomolecules, single cells and single nanoparticles in fluid. Nature 446(7139):1066-1069.
124. Das TK 2012. Protein particulate detection issues in biotherapeutics development--current status. AAPS PharmSciTech 13(2):732-746.
125. Weinbuch D, Zolls S, Wiggenhorn M, Friess W, Winter G, Jiskoot W, Hawe A 2013. Micro-flow imaging and resonant mass measurement (archimedes) - complementary methods to quantitatively differentiate protein particles and silicone oil droplets. J Pharm Sci 102(7):2152-2165.

126. Wuchner K, Buchler J, Spycher R, Dalmonte P, Volkin DB 2010. Development of a microflow digital imaging assay to characterize protein particulates during storage of a high concentration IgG1 monoclonal antibody formulation. J Pharm Sci 99(8):3343-3361.
127. Joubert MK, Hokom M, Eakin C, Zhou L, Deshpande M, Baker MP, Goletz TJ, Kerwin BA, Chirmule N, Narhi LO, Jawa V 2012. Highly aggregated antibody therapeutics can enhance the in vitro innate and late-stage T-cell immune responses. J Biol Chem 287(30):25266-25279.
128. Rombach-Riegraf V, Karle AC, Wolf B, Sorde L, Koepke S, Gottlieb S, Krieg J, Djidja MC, Baban A, Spindeldreher S, Koulov AV, Kiessling A 2014. Aggregation of human recombinant monoclonal antibodies influences the capacity of dendritic cells to stimulate adaptive T-cell responses in vitro. PloS one 9(1):e86322.
129. van Holde KE, Johnson WC, Ho PS. 2006. Principles of Physical Biochemistry. Second ed., Upper Saddle River, NJ: Pearson Prentice Hall. p 710.
130. Jiskoot W, Crommelin D editors. 2005. Methods for Structural Analysis of Protein Pharmaceuticals. ed., Arlington, VA: American Association of Pharmaceutical Scientists. p 677.
131. Ganesan A, Price NC, Kelly SM, Petry I, Moore BD, Halling PJ 2006. Circular dichroism studies of subtilisin Carlsberg immobilised on micron sized silica particles. Biochim Biophys Acta 1764(6):1119-1125.
132. Schule S, Friess W, Bechtold-Peters K, Garidel P 2007. Conformational analysis of protein secondary structure during spray-drying of antibody/mannitol formulations. Eur J Pharm Biopharm 65(1):1-9.
133. Matheus S, Mahler HC, Friess W 2006. A critical evaluation of Tm(FTIR) measurements of high-concentration IgG1 antibody formulations as a formulation development tool. Pharm Res 23(7):1617-1627.
134. Vermeer AW, Bremer MG, Norde W 1998. Structural changes of IgG induced by heat treatment and by adsorption onto a hydrophobic Teflon surface studied by circular dichroism spectroscopy. Biochim Biophys Acta 1425(1):1-12.
135. Lankers M, Munhall J, Valet O 2008. Differentiation between foreign particulate matter and silicone oil induced protein aggregation in drug solutions by automated raman spectroscopy. Microscopy and Microanalysis 14:1612-1613.
136. Hawe A, Sutter M, Jiskoot W 2008. Extrinsic fluorescent dyes as tools for protein characterization. Pharm Res 25(7):1487-1499.
137. He F, Phan DH, Hogan S, Bailey R, Becker GW, Narhi LO, Razinkov VI 2010. Detection of IgG aggregation by a high throughput method based on extrinsic fluorescence. J Pharm Sci 99(6):2598-2608.
138. Mach H, Bhambhani A, Meyer BK, Burek S, Davis H, Blue JT, Evans RK 2011. The use of flow cytometry for the detection of subvisible particles in therapeutic protein formulations. J Pharm Sci 100(5):1671-1678.
139. Flatman S, Alam I, Gerard J, Mussa N 2007. Process analytics for purification of monoclonal antibodies. J Chromatogr B Analyt Technol Biomed Life Sci 848(1):79-87.
140. Lee HG 2000. High-performance sodium dodecyl-sulfate-capillary gel electrophoresis of antibodies and antibody fragments. J Immunol Meth 234:71-81.
141. Hunt G, Nashabeh W 1999. Capillary electrophoresis sodium dodecyl sulfate nongel sieving analysis of a therapeutic recombinant monoclonal antibody: a biotechnology perspective. Anal Chem 71:2390-2397.
142. Xie H, Gilar M, Gebler JC. 2009. Analysis of deamidation and oxidation in monoclonal antibody using peptide mapping with UPLC/MS. ed., Milford, MA: Waters Corporation.

143. Ohno O, Cooke TD 1978. Electron microscopic morphology of immunoglobulin aggregates and their interactions in rheumatoid articular collagenous tissues. Arthritis Rheum 21(5):516-527.
144. Lee H, Kirchmeier M, Mach H 2011. Monoclonal antibody aggregation intermediates visualized by atomic force microscopy. J Pharm Sci 100(2):416-423.
145. Sung JJ, Pardeshi NN, Mulder AM, Mulligan SK, Quispe J, On K, Carragher B, Potter CS, Carpenter JF, Schneemann A 2014. Transmission Electron Microscopy as an orthogonal method to characterize protein aggregates. J Pharm Sci.
146. Podell DN, Packman CH, Maniloff J, Abraham GN 1987. Characterization of monoclonal IgG cryoglobulins: fine-structural and morphological analysis. Blood 69(2):677-681.
147. Parmenter CD, Cane MC, Zhang R, Stoilova-McPhie S 2008. Cryo-electron microscopy of coagulation Factor VIII bound to lipid nanotubes. Biochem Biophys Res Commun 366(2):288-293.
148. Li G, Torraca G, Jing W, Wen Z-q 2009. Applications of FTIR in identification of foreign materials for biopharmaceutical clinical manufacturing. Vibrational Spectroscopy 50(1):152-159.
149. Goldstein J, Echlin P, Joy DC, Lifshin E, Lyman CE. Scanning Electron Microscopy and X- Ray Microanalysis. 3 ed.: Springer. p 690.
150. Hutchings RL, Singh SM, Cabello-Villegas J, Mallela KM 2013. Effect of antimicrobial preservatives on partial protein unfolding and aggregation. J Pharm Sci 102(2):365-376.
151. Maggio ET 2010. Use of excipients to control aggregation in peptide and protein formulation. J Excipients and Food Chem 1(2):40-49.
152. Stockinger B 1992. Capacity of antigen uptake by B cells, fibroblasts or macrophages determines efficiency of presentation of a soluble self antigen (C5) to T lymphocytes. European journal of immunology 22(5):1271-1278.
153. Gengoux C, Leclerc C 1995. In vivo induction of CD4+ T cell responses by antigens covalently linked to synthetic microspheres does not require adjuvant. International immunology 7(1):45-53.
154. Chirino AJ, Ary ML, Marshall SA 2004. Minimizing the immunogenicity of protein therapeutics. Drug discovery today 9(2):82-90.
155. Scott DW, De Groot AS 2010. Can we prevent immunogenicity of human protein drugs? Ann Rheum Dis 69:i72-76.
156. Seong SY, Matzinger P 2004. Hydrophobicity: an ancient damage-associated molecular pattern that initiates innate immune responses. Nature reviews Immunology 4(6):469-478.
157. Bachmann MF, Jennings GT 2010. Vaccine delivery: a matter of size, geometry, kinetics and molecular patterns. Nature reviews Immunology 10(11):787-796.
158. Gamble CN 1966. The role of soluble aggregates in the primary immune response of mice to human gamma globulin. International archives of allergy and applied immunology 30(5):446-455.
159. Xiang SD, Scholzen A, Minigo G, David C, Apostolopoulos V, Mottram PL, Plebanski M 2006. Pathogen recognition and development of particulate vaccines: does size matter? Methods 40(1):1-9.
160. O'Hagan DT, Rahman D, McGee JP, Jeffery H, Davies MC, Williams P, Davis SS, Challacombe SJ 1991. Biodegradable microparticles as controlled release antigen delivery systems. Immunology 73(2):239-242.

161. Yamamoto N, Fukai F, Ohshima H, Terada H, Makino K 2002. Dependence of the phagocytic uptake of polystyrene microspheres by differentiated HL60 upon the size and surface properties of the microspheres. Colloids and Surfaces B: Biointerfaces 25(2):157-162.
162. Storni T, Ruedl C, Renner WA, Bachmann MF 2003. Innate immunity together with duration of antigen persistence regulate effector T cell induction. J Immunol 171(2):795-801.
163. O'Hagan DT, Singh M, Ulmer JB 2006. Microparticle-based technologies for vaccines. Methods 40(1):10-19.
164. Hermeling S, Schellekens H, Maas C, Gebbink MF, Crommelin DJ, Jiskoot W 2006. Antibody response to aggregated human interferon alpha2b in wild-type and transgenic immune tolerant mice depends on type and level of aggregation. J Pharm Sci 95(5):1084-1096.
165. Dintzis HM, Dintzis RZ, Vogelstein B 1976. Molecular determinants of immunogenicity: the immunon model of immune response. Proceedings of the National Academy of Sciences of the United States of America 73(10):3671-3675.
166. Tabata Y, Ikada Y 1988. Effect of the size and surface charge of polymer microspheres on their phagocytosis by macrophage. Biomaterials 9(4):356-362.
167. Foged C, Brodin B, Frokjaer S, Sundblad A 2005. Particle size and surface charge affect particle uptake by human dendritic cells in an in vitro model. Int J Pharm 298(2):315-322.
168. Champion JA, Katare YK, Mitragotri S 2007. Particle shape: a new design parameter for micro- and nanoscale drug delivery carriers. Journal of controlled release : official journal of the Controlled Release Society 121(1-2):3-9.
169. Sharma G, Valenta DT, Altman Y, Harvey S, Xie H, Mitragotri S, Smith JW 2010. Polymer particle shape independently influences binding and internalization by macrophages. Journal of controlled release : official journal of the Controlled Release Society 147(3):408-412.
170. Thiele L, Rothen-Rutishauser B, Jilek S, Wunderli-Allenspach H, Merkle HP, Walter E 2001. Evaluation of particle uptake in human blood monocyte-derived cells in vitro. Does phagocytosis activity of dendritic cells measure up with macrophages? Journal of controlled release : official journal of the Controlled Release Society 76(1-2):59-71.
171. Thiele L, Merkle HP, Walter E 2003. Phagocytosis and phagosomal fate of surface-modified microparticles in dendritic cells and macrophages. Pharm Res 20(2):221-228.
172. Gallucci S, Matzinger P 2001. Danger signals: SOS to the immune system. Current opinion in immunology 13(1):114-119.
173. Filipe V, Jiskoot W, Basmeleh AH, Halim A, Schellekens H, Brinks V 2012. Immunogenicity of different stressed IgG monoclonal antibody formulations in immune tolerant transgenic mice. MAbs 4(6):740-752.
174. Bi V, Jawa V, Joubert MK, Kaliyaperumal A, Eakin C, Richmond K, Pan O, Sun J, Hokom M, Goletz TJ, Wypych J, Zhou L, Kerwin BA, Narhi LO, Arora T 2013. Development of a human antibody tolerant mouse model to assess the immunogenicity risk due to aggregated biotherapeutics. J Pharm Sci 102(10):3545-3555.
175. van Beers MM, Sauerborn M, Gilli F, Brinks V, Schellekens H, Jiskoot W 2011. Oxidized and aggregated recombinant human interferon beta is immunogenic in human interferon beta transgenic mice. Pharm Res 28(10):2393-2402.
176. Hermeling S, Aranha L, Damen JM, Slijper M, Schellekens H, Crommelin DJ, Jiskoot W 2005. Structural characterization and immunogenicity in wild-type and immune tolerant mice of degraded recombinant human interferon alpha2b. Pharm Res 22(12):1997-2006.
177. International A. 2008. ASTM Standards. Standard Test Methods for Vibration Testing of Shipping Containers D 999-08, ed., West Conshohocken, PA: ASTM International. p 1-5.

CHAPTER 2: Structural Characterization of IgG1 mAb Aggregates and Particles Generated under Various Stress Conditions

2.1 INTRODUCTION

A current concern with the use of monoclonal antibody-based therapeutics is their tendency to aggregate and form particles during long-term storage and/or during accidental exposure to environmental stresses. The formation of aggregates and particles may lead to an increase in immune response [1-3] or a decrease in efficacy of the drug.[2,4] Protein aggregation can occur during many stages of production (purification, formulation, and filling), or during long-term storage, shipping, and even administration to the patient.[5] Therefore it is important to better understand the reasons for aggregation and particle formation due to different stresses and formulation conditions in order to develop strategies to minimize its occurrence.

Aggregation and particle formation in therapeutic protein formulations can be caused by a variety of environmental stresses or by formulation conditions such as concentration,[6-8] solution pH,[6,9,10] and the presence or absence of certain excipients.[6,7,9] Freezing can not only lead to changes in the formulation pH[6,11,12] and concentration of proteins and excipients,[6] but also to the formation of ice/water interfaces[6,13-15] where protein adsorption can induce partial protein unfolding and subsequent aggregation.[6,9,15-17] Proteins subjected to heating undergo conformational changes that can lead to the formation of aggregates and particles.[9,18] Mechanical stresses may cause shear or interfacial effects in which the protein adsorbs to the air-water interface, leading to structural alterations which can initiate aggregation as well.[9,16,19,20] Stirring and shaking are both mechanical stresses that can also cause cavitation, local thermal effects, bubble entrapment, and transportation of the aggregated protein from the air-water or air-container interface into the bulk solution.[6,21-23]

One major challenge in studying protein aggregation experimentally is that a wide variety of analytical techniques are required to characterize the formation of protein aggregates and particles over a broad size range (from few nanometer to hundreds of microns).[24] In addition, it is also important to have complimentary, orthogonal techniques for analyzing aggregates of similar size ranges since results can differ based on the principles and setup of each technique.[6] In this work, we follow the previously proposed definitions of protein aggregates, across the size ranges of few nanometers to 100s of microns.[25] In this case study, size exclusion chromatography (SEC) is used to analyze smaller aggregates in the size range of tens of nanometers. Although it is a powerful analytical tool for monitoring small nanometer-sized soluble aggregates, upon injection of sample into the column, aggregates can potentially dissociate upon mixing with mobile phase or adhere to the column thereby requiring careful method development and use of orthogonal techniques.[26] For sizing submicron particles (0.1 to 1 μm), Nanosight Tracking Analysis (NTA) is used while for micron (1-100 μm) size particles, Microflow-Imaging technique (MFI) is employed. NTA tracks and sizes individual particles (unlike its DLS counterpart), but has limited sensitivity in detecting low numbers of submicron particles. In addition to sizing and counting particles like light obscuration, MFI also has digital imaging capabilities that can provide morphological information allowing differentiation between silicone and protein particles. To detect visible particles larger than 100 μm, visual assessments are employed. Turbidity is also used as a general method to monitor the formation of aggregates and particles in solution across the various size ranges. Although visual inspection is a commonly used technique, even under pre-defined conditions and with extensive analyst training, results may vary between different analysts. Turbidity provides semi-quantitative information for comparisons of the overall aggregation state of a sample, but it does not provide

information regarding the size or number of particles. Detailed discussions of the strengths and limitations of these analytical techniques are described more thoroughly elsewhere.[27,28]

Recently, there has been an increased emphasis on characterizing the morphology and composition of particles in addition to counting and sizing them.[27] As a starting point for this work, MFI analysis, in addition to sizing and counting of subvisible particles, is used for morphological analysis by utilizing parameters such as aspect ratio and intensity of the digital images.[29,30] For visualization of small, nanometer-sized aggregates, transmission electron microscopy (TEM) is used.[31] SDS-PAGE is used to determine the extent of covalent, disulfide linkages present in aggregates.[32] Extrinsic fluorescence spectroscopy with 8-anilino-1-naphthalene sulfonate (ANS) probe provides information concerning the surface hydrophobicity of aggregates.[33;34,35] FTIR provides insights into the secondary structure of native protein and aggregates in solution,[6,36-38] with the use of a FTIR microscope allowing for selection of individual protein particles for secondary structure analysis.[29]

This paper is a "protein particle formation" case study by utilizing a variety of analytical techniques to examine the effect of four different environmental stresses (freeze-thaw, shaking, stirring, and heating) and formulation composition (salt concentration) on the number, size range morphology, and compositional nature of the IgG1 aggregates/particles formed from stressing the mAb solutions. Additionally, a new data visualization method consisting of radar plot analysis[39] was used to better evaluate the effects of environmental stress and salt concentration on particle size distributions as well as changes in certain morphological parameters measured by MFI. The trends observed in terms of types and amounts of particles formed under the different stress conditions are discussed, along with some comparisons to previous studies with different monoclonal antibodies.

2.2 EXPERIMENTAL SECTION

2.2.1 Materials

Purified monoclonal human IgG1 (mAb) was obtained from Janssen Biotech (Radnor, PA) at 40 mg/mL. The reagents and stir bars required for sample preparation were purchased from Sigma Aldrich (St. Louis, MO), and Fisher Scientific (Pittsburgh, PA). The 3 mL vials and rubber stoppers used to generate protein aggregates were purchased from West Pharmaceuticals (Lionville, PA). For counting and sizing of aggregates (using SEC, NTA, MFI, turbidity, visual assessments), the mAb was diluted to 1 mg/mL using 10 mM sodium acetate buffer, pH 5 ± 150 mM NaCl.[22] This condition was also used for morphological analysis of particles by MFI. For structural and morphological analysis of the aggregates (using TEM, MFI, SDS-PAGE, FTIR-Microscopy, ANS-Fluorescence), the mAb was diluted to 1 mg/ml in 10 mM sodium acetate buffer, pH 5 containing 150 mM NaCl.

2.2.2 Methods

2.2.2.1 Generation of Aggregates

The 40 mg/mL IgG1 mAb solution was diluted to 1 mg/mL in 10 mM sodium acetate buffer, pH 5 ± 150 mM NaCl and then subjected to a variety of accelerated stress conditions. These conditions were selected to match pH solution conditions used previously with a different set of IgG mAbs[22,40] In each case, the buffer controls were stressed similarly to the protein samples and analyzed using various sizing, counting, and characterization techniques. Since the buffer controls showed very low particle counts, the data were not included in the figures. For freeze-thaw stress, the mAb was frozen and thawed one to three times (indicated as cycles) at -

80°C and room temperature, respectively (labeled FT-C1 and FT-C3). For shaking stress, the mAb was agitated at 300 rpm (using an IKA AS260.1 shaking platform) for 1-3 days (labeled shake-D1 and shake-D3). For stirring stress, the mAb was stirred at an intermediate speed (setting 5) on a stirring plate (ThermoSci Pierce Reacti-Therm III #18823 Heating/Stirring Module) using Flea Micro Teflon coated magnets (Fisher Scientific) for 1-3 days (labeled stir-D1 and stir-D3). For thermal stress, the mAb was incubated at 60^{o}C in an incubator (Revco Ultima II) for 1-3 days (labeled heat-D1 and heat-D3).

2.2.2.2 Size-Exclusion Chromatography

A Shimadzu Prominence HPLC system equipped with a diode-array detector was employed with a Tosoh Bioscience TSK-Gel Bioassist G3SW$_{XL}$ (7.8 mm x 30.0 cm) PEEK column and a corresponding PEEK Guard column (TSK Guard Column SW$_{XL,}$ 6.0 mm x 4.0 cm) that were preconditioned with BSA as described previously.[26] Molecular weight standards (Biorad Laboratories; Hercules, CA) were run to test for efficiency of separation and resolution. Both the column and guard column were equilibrated at 30^{o}C for 1 hour using the mobile phase comprised of 0.2 M sodium phosphate, pH 6.8 at a flow rate of 0.7 ml/min. Aggregated samples were centrifuged at 16,000g (851 rotor on an IEC Micromax 3593) for 5 min and 10 µL of supernatant was injected for analysis and monitored simultaneously at 214 and 280 nm for each 30 min sample run.[26] Multimers, dimers, monomer, and fragment peaks were quantified using the LC Solutions data analysis software provided with the instrument as described elsewhere.[26]

2.2.2.3 Nanoparticle Tracking Analysis (NTA)

Submicron (nanometer) sized particles were measured using a Nanosight LM-14 (Nanosight, Amesbury, UK) with a high resolution EMCCD camera. Stressed mAb solutions

were centrifuged at 16,000g for 5 min and 300 uL of the supernatants were injected into the sample holder. The stirred (with and without NaCl) and heat stressed (with NaCl only) samples were diluted by a factor of 100 prior to analysis. Three 30 s movies were taken at ambient temperature for each sample at a viscosity of 0.95 cP. Data analysis was completed using NTA 2.3 software (Nanosight) with the required camera level and gain adjustments. Dilution factors were accounted for in the data analysis.

2.2.2.4 Micro-Flow Digital Imaging

Subvisible (micron sized) protein particles were analyzed and imaged using a MFI DPA 4200 (Protein Simple, Santa Clara, CA). Prior to each analysis, the instrument was primed with purified water to obtain a particle-free baseline. Samples were gently swirled and 1 mL of each sample was removed using a low protein-binding pipette tip and loaded into a sample holder. Some of the samples (stir-D1 and D3 with and without NaCl; shake-D3 with NaCl; and heat-D3 with NaCl) were diluted by a factor of 100 prior to being passed through the instrument at a flow rate of 0.1m/min. The data were obtained as described previously by Kumru et al.[41]

2.2.2.5 Data Visualization with Radar Plots

To generate MFI particle size distribution radar plots, subvisible particle concentrations and sizes for both unstressed and stressed samples were obtained from MFI's MVAS 1.3 software. Similarly, MFI particle morphology radar charts were created using the average mean intensity and aspect ratio values for each sample. All samples were run independently three times (n=3). The data were pre-processed in Excel and two radar plots (one showing average values and one showing variability in the runs) were generated using the MiddaughSuite software created in our lab.[42] The two radar charts were superimposed using Adobe Photoshop CS6. See

Kalonia et al. 2013 and Kim et al. 2012 for a more detailed description of this data visualization methodology as applied to protein aggregation and conformational stability data, respectively.[39,42]

2.2.2.6 SDS-PAGE

Samples were centrifuged at 16,000g for 5 min to separate the soluble fraction (supernatant) from the insoluble fraction (pellet). Both fractions were dissolved in NuPAGE LDS sample buffer (Life Technologies, Carlsbad, CA) with and without 50 mM DTT (BioRad) and incubated at 80^{O}C for 90 s. Approximately 10 μg of each sample was separated on a 3-8% Tris-Acetate gel using Tris-Acetate running buffer (Life Technologies) for 65 min at 150V. A Hi-Mark unstained molecular weight ladder was used as a reference (Life Technologies). The starting protein concentration for the supernatant of one sample (stir-D3) was low so a maximum of 20 μL was loaded. Protein bands were visualized by staining with Bio-Safe Coomassie blue (BioRad).

2.2.2.7 Turbidity

A HACH 2100 AN turbidimeter was used to monitor the turbidity of each of the samples. Prior to running the aggregated samples, NTU calibration standards were used to generate a standard curve.

2.2.2.8 Transmission Electron Microscopy (TEM)

Carbon-coated grids were dipped into methylene chloride for 10 s to remove the top carbon layer and were dried for a few minutes. The images were obtained by uranyl acetate staining and by following the procedure by Kumru et al.[41]

2.2.2.9 Free Thiol Quantitation

Samples were centrifuged at 16,000g for 5 min to separate the soluble (supernatant) and the insoluble (pellet) fractions. The pellet was dissolved in 6M guanidine hydrochloride (Fisher Scientific). The amount of free thiol in the samples as well as in the appropriate controls was measured using the protocol described in the Measure-iT Thiol Assay Kit (Molecular Probes) with a SpectraMax MS plate reader (Molecular Devices; Sunnyvale, CA).

2.2.2.10 Extrinsic Fluorescence Spectroscopy

Samples were centrifuged at 16,000g for 5 min to separate the soluble and insoluble fractions. The pellet was resuspended in 10 mM sodium acetate, 150mM NaCl, pH 5. The protein concentration of each of these supernatant and pellet components was measured using a Nanodrop spectrometer (Thermo Scientific) with light scattering correction. The samples were diluted to 0.1 mg/mL in 10 mM sodium acetate, 150 mM NaCl, pH 5. 8-Anilinonaphthalene-1-sulfonate (ANS; Sigma-Aldrich, St. Louis, MO) was added and the ANS fluorescence of the samples were recorded according to Kumru et al.[41] The signal from the buffer with equivalent amount of ANS was subtracted from all measurements.

2.2.2.11 Fourier Transform Infrared Microscopy

Five μm gold filters (Pall Corporation) were used for analyzing the aggregated samples. Filters were equilibrated by washing with 0.1 M NaOH. The samples were then filtered, washed with ultrapure water, and dried overnight. A Bruker Hyperion FTIR Microscope with a 15X objective was used to image individual particles. Two-hundred-fifty-six scans were recorded from 600-4000 cm^{-1} with a viewing area of about 100 μm x 100 μm. To observe the maximum

change in secondary structure due to heating, a 1 mg/mL sample in acetate buffer (10 mM sodium acetate, 150 mM NaCl, pH 5) was heated for 20 min at 80°C. This heated sample (labeled heated control) was also filtered onto the 5 μm gold filter and dried overnight. OPUS (V6.5) software was used for baseline and atmospheric correction. The second derivative spectra were obtained using a nine-point Savitzky-Golay smoothing function.

2.2.2.12 Fourier Transform Infrared Spectroscopy

The unstressed mAb at 1 and 10 mg/mL in 10 mM sodium acetate, 150 mM NaCl, pH 5 were analyzed with a Bruker Tensor 27 FTIR Spectrometer and a Bio-ATR cell. Two-hundred-fifty-six scans were recorded from 600-4000 cm^{-1} at a resolution of 4 cm^{-1}. To observe changes in secondary structure as a function of temperature, unstressed sample at 10 mg/mL was heated from 10 to 87.5°C at 4 cm^{-1} resolution and 120 s equilibration time with 2.5°C increments for 256 scans.

2.3 RESULTS

2.3.1 Counting and Sizing of Aggregates and Particles Formed under Accelerated Stress Conditions

2.3.1.1 SEC (soluble aggregates, <100 nm)

To determine the amount of smaller (soluble) nanometer aggregates, the stressed IgG1 mAb samples were centrifuged and the resulting supernatants were analyzed by SEC. The amount of protein material that did not elute from the SEC (referred to as insoluble aggregates) was indirectly determined by monitoring the decrease in the total area of the chromatogram

peaks between unstressed (D0) and the stressed samples. The earliest eluted peak was labeled as multimer, the second peak as dimer, the third and largest peak as monomer, and the final peak as fragment based on the estimated molecular weights. In the absence of salt, heat stressed samples produced more fragments, dimers, and insoluble aggregates compared to the unstressed sample (Fig. 2.1A, 2.1I). Stirring formed more multimers and insoluble aggregates (Fig. 2.1G), while freeze-thaw formed a very small amount of multimers and dimers (Fig. 2.1A), compared to the unstressed sample. Shaking (Fig. 2.1E) did not show an increase in any species relative to the unstressed sample. In the presence of 0.15M NaCl, protein was further destabilized and generally resulted in the formation of more aggregates. Heat-stressed mAb in the presence of NaCl (Fig. 2.1J) showed more insoluble aggregates, a larger decrease in monomer, and an increase in multimer compared to its NaCl-free counterpart, which showed some fragment formation and lower levels of impurity (Fig. 2.1I). Stirring the mAb solution in the presence of salt resulted in a large increase in insoluble aggregate and a concurrent decrease in monomer content (Fig. 2.1G vs.2.1 H). Freeze-thaw and shaking did not show changes in any species, but in the presence of NaCl, a slight increase in insoluble aggregate was observed (Fig 2.1D, 2.1F).

2.3.1.2 Nanoparticle Tracking Analysis (NTA) (50-1000 nm particles)

NTA was used to assess the concentration and size distribution of nanometer sized particles (also referred to as submicron particles) formed in stressed and unstressed samples. Stirring of the mAb solution in the absence of NaCl (Fig. 2.2A and 2.2C) generated the largest number of nanometer sized particles (between ~150-250 nm). In contrast, in the presence of salt, heating generated the most nanometer sized particles (Fig. 2.2B and 2.2D). The concentration of nanometer particles present in the unstressed controls was below the instrument's quantitation limit (data not shown).

2.3.1.3 MFI (2-100 μm particles)

Subvisible particle data (concentration and size range of micron size particles) obtained from MFI measurements of stressed and unstressed samples were visualized using radar plots (Fig. 2.3 and Fig. 2.9). This novel data visualization method for MFI data is described in detail elsewhere.[39] As shown in the key to Figure 2.3, the concentric circles represent concentration of particles, with the lowest concentration (10^2) being the innermost circle, and highest concentration ($>10^7$) being the outermost. The 5 corners of the polygon within the circles represent the particle size bins. An increase in size of the polygon towards one corner represents an increase in concentration of particles in that size bin (e.g., stretching of a corner from the innermost concentric circle to the outermost circle in size bin number 3 indicates that there is an increase in the $\geq 10 < 25$ μm particles from 10^2 to $>10^7$ particles/mL).

As shown in Figure 2.3, the size and concentration of subvisible particles formed is highly dependent on the type of stress. In the absence of NaCl, freeze-thaw and heat stressed mAb samples showed the lowest concentration of particles even after 3 cycles/days of stress, while shaking and stirring showed a higher concentration of particles. Stirring produced the most subvisible particles, especially in the 2-25 μm size range. In the presence of NaCl, a higher concentration of particles, especially in the 2-25 μm size range, was observed in all of the stressed mAb samples. The heated mAb showed a large difference in both particle number and size in the presence and absence of salt that increased from day 1 to day 3. A large variability in the larger particles was observed (the lighter shading on the radar plots reflects the standard deviation of the measurements). In general, shaking the mAb solution containing NaCl generated the largest subvisible particles (2-50 μm) (Fig. 2.3). Particle counts of controls were negligible.

2.3.1.4 Turbidity and Visual Assessment

Results of turbidity measurements and visual observations of the stressed mAb solutions are shown in Table 2.1. In samples lacking NaCl, agitation and stirring resulted in the highest number of >100 μm (referred to as visible particles, VP), with stirring producing the greatest turbidity. No major NaCl effect was seen for the freeze-thaw stress. Agitation, stirring, and heating stresses on the mAb formed more VP and higher turbidity in the presence of NaCl than in the absence of it. The highest turbidity levels were measured for stir-D3 samples, followed by stir-D1, and heat-D3. In addition, the presence of NaCl increased the turbidity for the heated (heat-D1 and heat-D3) protein compared to the corresponding heat stressed mAb samples without NaCl. Shaken or stirred mAb samples formed a large number of visible particles regardless of the presence or absence of NaCl.

2.3.2 Structural Characterization of Aggregates and Particles

2.3.2.1 Particle Morphology

As an initial step in characterizing the nature and composition of the particles formed under different stresses, MFI was used to elucidate morphological information (intensity and aspect ratio parameters) of the subvisible particles generated after three days of stress (Fig. 2.3 and Fig. 2.9). Aspect ratio is a ratio of width of the particle relative to the height and intensity is related to the particle absorption characteristics. Data were visualized in the form of a radar plot (Fig. 2.4). Figure 2.4 shows the different stresses applied to mAb solutions with and without NaCl on the x-axis and the MFI morphology parameters, intensity and aspect ratio, on the y-axis. The top and bottom radar charts describe the intensity and aspect ratio, respectively, of the particles as a function of stress and solution condition. As shown in the key to Figure 2.4, the aspect ratio of the micron particles varies from ~0.35 (elongated) to 0.85 (more circular) and the

intensity from about 350 (opaque) to 850 (highly transparent) intensity level units (ILU). It should be emphasized that the concentric circles here do not represent concentration, but rather a change in particle morphology with the outermost circle representing elongated, opaque particles, and the innermost circle representing transparent, circular particles. The corners of the 5-sided polygon represent distinct particle size bins (labeled 1-5 in the figure). The pink-shaded region indicates that an insufficient number of particles were collected in that size range for accurate morphological analysis.

In the absence of NaCl, the shaking of the mAb solution over 3 days resulted in particles that appeared transparent (Fig. 2.4A) and elongated (Fig. 2.4B) over all particle size ranges. In the presence of NaCl under the same stress condition, the particles formed are less transparent (i.e., more opaque) and less elongated (i.e., more circular in shape) over a narrower size range. Stirring-induced mAb particles formed in the presence or absence of NaCl do not show notable differences in intensity or aspect ratio. The concentration of particles in the freeze-thaw and heated samples without NaCl was lower (Fig. 2.3) and an accurate comparison of the morphology change across the size ranges was limited (as shown by the shaded areas in Figure 2.4).

To characterize the morphology of smaller particles, TEM was used to examine the shape of nanometer sized aggregates generated from 3 days of different stresses in the presence of 0.15 M NaCl. Some representative TEM images are shown in Figure 2.5. It can be seen that the type of stress to which the mAb solution was subjected influences the morphology of the aggregates generated. Freeze-thaw and heated aggregates appear very fibrillar, while agitated-induced aggregates appear fibrillar with some spherical aggregates. The stirring-induced aggregates were predominantly spherical in nature in this size range.

2.3.2.2 Non-native disulphide cross-linking

SDS-PAGE was used to study the formation of non-native covalent crosslinking in the stressed mAb. Results for the stirring and heating stressed mAb containing NaCl are shown in Figure 2.6.A and 2.6.B (non-reduced and reduced, respectively). These samples were first centrifuged to separate the supernatant (S) and pellet components (P) prior to electrophoresis. The non-reduced supernatants contained predominantly monomers while the pellets contained high molecular weight species above 500 kDa (i.e., larger than tetramer). Upon reduction of the supernatant and pellet, a complete loss in the high molecular weight material was observed with the light and heavy chains bands of the mAb visible as the primary species. The pellet for stir-D1 and D3, heat-D1 and D3 contained significant amounts of non-native disulfide linked aggregates. The supernatant of heat-D1 protein contained some of these non-native disulfide linked aggregates as well. No disulfide-linked aggregates were detected in freeze-thaw and agitation stressed mAb samples (data not shown). The number of free sulfhydryl groups in the mAb samples was also measured, and virtually no free thiols were present in control or stressed samples (data not shown).

2.3.2.3 Overall secondary structure content

The secondary structure of the aggregated samples was studied using FTIR spectroscopy of control mAb samples and FTIR microscopy of individual particles formed by stress in 10 mM acetate, 150 mM NaCl, pH 5. Representative spectra are shown in Figure 2.7 along with wavelength values from multiple measurements including standard deviations. Two mAb controls were prepared for comparison to the particles formed from stressed samples: an unstressed mAb with native conformation (Figure 2.7A in the form of second derivative FTIR spectra) and particles isolated from an extensively heated mAb sample with some degree of

structural perturbations (Figure 2.7B). Figures 2.7C-2.7F show microscopic images and the corresponding FTIR spectra of isolated amorphous mAb particles generated under different stresses.

In the Amide I region of the second derivative FTIR spectra of the native mAb, two minima at 1637 cm^{-1} and 1690 cm^{-1} were observed (Figure 2.7A). This result is consistent with the predominantly intramolecular beta sheets present in native IgGs. [9,43,44] For the isolated mAb particles from the extensively heat stressed control, severely altered secondary structure displaying extensive loss of intramolecular beta sheet structure (as shown by loss of the two minima seen in the native mAb control, and the appearance of intermolecular beta sheets with minima at 1617 cm^{-1}, and 1693 cm^{-1} (Figure 2.7B)) is seen. For the isolated mAb particles produced by three days of heating at 60^{o}C, the spectra show the sample is more similar to the extensively heated control as evidenced by the presence of the two minima at 1624 cm^{-1} and 1694 cm^{-1}.[45,46] The mAb particles isolated after three freeze-thaw cycles and three days of agitation have FTIR spectra with primarily native-like structure as seen by the second derivative minima at 1634 cm^{-1} and 1691 cm^{-1} and 1635 cm^{-1} and 1692 cm^{-1}, respectively. The stirred aggregates show reproducibly shifted minima in the main second derivative peak to 1631 cm^{-1} indicating some alteration in secondary structure.

2.3.2.4 Surface hydrophobicity

To examine any changes in the exposure of apolar regions in the stressed samples containing NaCl due to structural perturbations or aggregation/self-association, ANS extrinsic fluorescence spectroscopy was used. Stress induced aggregated mAb samples were centrifuged and separated into supernatant and pellet components. They were analyzed along with two controls: the unstressed mAb (D0) and a positive control (Heat-melt). As a positive control to

determine the greatest extent of apolar binding of ANS, the mAb solution was heated from 10 to 87.5°C in the presence of ANS. From the emission spectrum, it was determined that the maximum binding of ANS to the mAb occurred at 72°C suggesting maximal ANS access to apolar sites at high temperature. Representative spectra are shown in Figure 2.8. The control mAb solution (D0) along with supernatants from the FT, shake, and stir-D1 samples (Fig. 2.8A and 2.8B) show very little fluorescence intensity indicating that in these samples, ANS has very little access to the apolar regions of the mAb. In the stir-D1 pellet, slightly higher fluorescence intensity was observed, which suggests some exposure of apolar sites in these aggregates (Fig. 2.8A and 2.8B). The heat-D1 supernatant and pellet show the largest ANS fluorescence intensity increase suggesting the greatest exposure of apolar regions. The heat stressed mAb samples containing NaCl displayed a similar magnitude of fluorescence intensity as the positive control (heat-melt) indicating that this stress condition may also generate samples with extensively apolar exposed regions.

2.4 DISCUSSION

As an initial set of experiments, we first counted and sized protein particles generated under accelerated stress conditions employing an IgG1 mAb solution with and without 0.15 M NaCl. A summary of the counting and sizing results from SEC, NTA, MFI, Turbidity, and Visual Assessments are presented in Table 2.2. Different stresses (in the presence and absence of NaCl) result in the formation of mAb aggregates and particles of varying sizes that cannot be measured by a single analytical method. As shown in Table 2.2, using multiple techniques is therefore very important for analyzing the formation of a broad size range of aggregates. For example, SEC showed that the formation of soluble aggregates was influenced by the presence

of NaCl across the four stresses. NTA results demonstrated that the presence of NaCl affected the extent of nanometer particle formation in the freeze-thaw and heat stressed samples, but not for the agitated and stirred stressed samples. Similarly, MFI detected that NaCl enhanced the formation of micron particles only for the freeze-thaw stressed mAb sample. Finally, turbidity and visual assessments showed changes in particle formation (due to the presence or absence of NaCl) with heat stressed mAb solutions.

Freeze-thaw stress was observed to be the mildest condition in solutions without NaCl since essentially no detectable aggregates or particles were seen (Table 2.2, first row). Upon addition of NaCl (Table 2.2, second row), some insoluble aggregates (detected as a loss of total mass by SEC) and some nanometer and micron particles were detected by NTA and MFI. Shaking the mAb solution with and without NaCl (third and fourth row in Table 2.2) generated a turbid solution with primarily micron (2 to >100 μm) size particles observed by MFI and visual inspection. The shaken solution in presence of NaCl was more turbid with some insoluble aggregates, and a larger number of micron-sized particles 2 to >100 μm. Stirring without NaCl produced a moderately turbid solution consisting of some insoluble aggregates, submicron, micron, as well as a large number of visible entities. Stirring the mAb solutions, in the presence of NaCl, generated the most turbid solutions consisting of a very large amount of insoluble aggregates (20% after day 1 and around 60% after 3 days of stress, as quantified by SEC). The largest differences in aggregate and particle formation were observed due to heating the mAb solution (Table 2.2; rows seven and eight). Heating in the absence of NaCl generated a fairly clear solution consisting of primarily monomers with a very small amount of insoluble aggregates and fragments (SEC), little to no nanometer-sized (NTA), micron (MFI), and visible particles even after three days of stress. In the presence of NaCl, however, a highly turbid

solution formed containing much more insoluble and multimer aggregates as well as a large increase in the number of nanometer, micron, and visible sized particles.

Comparison of these results to other studies shows similar trends in which mAb aggregate and particle formation depends on the type of stress and solution conditions. For an IgG1 mAb with a basic pI range formulated at lower solution pH such as pH 5.0, the addition of NaCl (<0.15 M) may promote protein aggregation and particle formation during environmental stress by a combination of effects resulting from neutralizing protein surface charge and decreasing electrostatic interactions. These effects may promote protein-protein interactions (colloidal stability) or decrease the structural integrity and stability of the protein (conformational stability).[9,47] The last column of Table 2.2 describes the impact of NaCl on various stresses using eight analytical readouts obtained from four instruments. For a given stress, column values can potentially range from 0/8, indicating NaCl had no impact on the aggregation behavior, to 8/8 where NaCl impacted the aggregation behavior of the mAb as measured by all of these analytical methods. Agitation and stirring stresses of the mAb solution were least influenced by the presence of NaCl (1 out of 8). Although the two stresses themselves were damaging to the protein, the addition of NaCl minimally increased mAb instability (as manifested in detectable changes in SEC for percent insoluble aggregate and monomer content for agitation and stirring stresses, respectively). Aggregation of the mAb under freeze-thaw stress was more influenced by the presence of NaCl (3 out of 8). Although freeze-thaw stress does not seem to cause alterations in the conformation of the mAb (see below), increases in percent insoluble and soluble aggregate, as well as nanometer and micron sized particles (by SEC, NTA, and MFI, respectively) were noted due to the presence of NaCl, indicating decreased colloidal stability. Finally, heat stress showed the largest effect of NaCl on mAb instability (6

out of 8). Although heating of the mAb solution in the absence of salt alters the conformational stability of the protein, it does not result in extensive aggregate or particle formation. With the addition of NaCl, however, there is now a large colloidal component to the mAb instability.

Despite the availability of new analytical methods to accurately and precisely count and size protein particles in the submicron and subvisible size range,[27,28,48-51] biophysical characterization of the nature, composition and structural integrity of the protein within these particles remains a major analytical challenge. The focus of this work was to characterize aggregates and particles formed in an IgG1 mAb in the presence of 0.15M NaCl as a function of various stresses (freeze-thaw, shaking, stirring and heating). The primary goal was to characterize the morphology, structural integrity and composition of the IgG1 particles formed in 0.15M NaCl containing solutions by probing the extent of non-native covalent cross-linking, changes in overall protein secondary structure, and alterations in surface hydrophobicity within the particles as formed by each type of stress applied to the mAb solutions. Additionally, we also evaluated the morphology of these particles by TEM and by a newly developed approach from our laboratory to analyze MFI size distribution and morphological data using radar plots.[39] These plots are commonly used to summarize large sets of protein data from multiple biophysical techniques. Radar plots are used to better visualize particle size distribution and morphological parameters of the particles.[39]

The freeze-thaw stress appeared to be mild and essentially did not change the overall higher order structure or covalent crosslinking of the protein within the aggregates. Particles, isolated onto a gold filter, showed no detectable alterations in overall secondary structure relative to the native IgG sample, even after three freeze thaw cycles. The nanometer sized aggregates appeared to have a fibrillar morphology by TEM. The micron sized particles (10-50μm) were

opaque (less transparent) and more elongated. Similarly, freeze-thaw samples showed very low surface hydrophobicity almost equal to that of the native protein. There appeared to be no covalent cross-linking present in the sample and no corresponding higher molecular weight aggregates seen on SDS-PAGE gels (data not shown). Results obtained from similar experiments by Joubert et al.[22] as well as Barnard et al[52] and Zhang et al.[53] with different mAbs were consistent with our observations.

For mAb solutions stressed by shaking, a common stress encountered by many protein drugs during transportation, generated predominantly fibrillar and slightly spherical nanometer particles, while the micron sized particles were more opaque and circular than the samples shaken without NaCl, as shown in Figures 2.4 and 2.5. These stressed samples contained little to no covalently linked aggregates with largely native-like secondary structure and low surface hydrophobicity (Figs 2.6-2.8) even after three days of shaking stress. While shaking generated higher number of aggregates and particles than freeze-thaw, there were not many differences in the biophysical characteristics of the aggregates generated by these two stresses compared to the unstressed, native protein. This result is similar to data published previously with other proteins.[17,22,54]

Stirring stress was a harsher condition on the IgG1 compared to freeze-thaw and shaking. In addition, the particles generated from this stress were predominantly spherical in morphology which was not observed with other stresses. From the MFI morphology data, NaCl did not notably affect particle morphology (in terms of aspect ratio and intensity) of the stirred samples in the micron size range as shown by the radar chart analysis in Figure 2.4. Biophysical differences were also observed in protein from the pellet fraction and supernatant fraction of the centrifuged stirred IgG mAb samples. The protein in the pellet fraction displayed greater surface

hydrophobicity (Figure 2.8) and contained an increased amount of reducible high molecular weight covalently linked aggregates (Figure 2.6) than the supernatant fraction. The ANS fluorescence data suggest that the population of aggregates present in the pellet may be more structurally altered compared to the aggregates present in the supernatant. The isolated stir-stressed particles showed some loss in overall intramolecular beta sheet structure content and some increase in the formation of intermolecular beta sheet structures (non-native, aggregated structures) as shown by FTIR analysis (Figure 2.7). One study with a different mAb reported that the overall secondary structure of the stirred sample was similar to that of the unstressed sample, contrary to our results with this IgG.[17] In addition to rapid transportation of aggregates into bulk solution from the interface, protein also encounters the harsh shear force of the stir-bar and the resulting thermal and cavitation effects.[17,55] All of these factors could account for higher aggregation and particulation with stirring stress compared to shaking.

For the heated samples of the IgG mAb, the supernatant fraction contained less non-native covalently linked aggregates compared to the pellet fraction which possessed higher levels of this type of disulfide cross-linked aggregate as measured by SDS-PAGE (Figure 2.6). The variability in the micron particle concentration was very high due to heating, so it is difficult to make definitive conclusions about the aspect ratio or intensity of these particles, although more elongated and more opaque particles were seen in the presence of NaCl (Figure 2.4). In the presence of NaCl, nanometer sized particles seen by TEM appeared fibrillar in morphology (Figure 2.5). The heat stressed samples displayed a highly perturbed overall secondary structure content consisting of predominantly intermolecular beta sheets as measured by FTIR (Figure 2.7). The increased ANS binding in both the supernatant and pellet of the centrifuged heated samples suggests significant exposure of apolar moieties in both fractions. Hawe et al. noted that

the heat generated aggregates contained non-native covalent cross-linking with significantly increased ANS binding (increase in surface hydrophobicity), as well as a large perturbation in the secondary structure [18,22] Zhang et al. conducted a similar experiment with Bevacizumab and determined that heat generated aggregates had significantly altered structure from their ANS and intrinsic Trp fluorescence data.[53] These results are consistent with our observations

In summary, while there has been a vast growth in our ability to count and size protein aggregates and particles over a wide size range during the past ~5 years, our analytical capabilities to describe the morphology, structural integrity and composition of the protein within these particles is still limited. The goal of this study was to provide a case study to examine the effect of different environmental stresses on an IgG1 mAb solution in terms of the morphology of particles formed as well the extent of structural alterations of the protein within the particles. We confirmed results of previous studies [17,18,22,52,55] that the type of stress a mAb solution experiences greatly influences many of its physical properties in distinct ways. There are still many gaps in our understanding that need to be addressed, [56] especially if there is a relationship between a particular particle count, particle size range, particle weight or perhaps the physicochemical or morphological trait(s) of protein particles/aggregates and their potential to generate an immune response *in vivo*.[56-62]

2.5 TABLES AND FIGURES

Table 2.1. Turbidity measurements and visual assessments of visible particles for control and stressed IgG1 mAb samples. Samples contained 1 mg/mL antibody in 10 mM sodium acetate, pH 5 in absence and presence of 150 mM NaCl. The turbidity data are an average of three independent experiments (n=3) with standard deviation. For visual assessments of visible particles, "-" is no change observed relative to unstressed sample; "+" is some change observed relative to unstressed sample (2-5 particles detected); "++" notable change observed relative to unstressed sample (> 5 particles detected).

	No NaCl			**With 150mM NaCl**		
	Turbidity (NTU)		**Visual Assessment**	**Turbidity (NTU)**		**Visual Assessment**
mAb Samples	*Average*	*Stdev*		*Average*	*Stdev*	
Buffer Alone (no mAb)	0.2	0.1	-	0.7	0.6	-
Day 0	0.6	0.1	-	0.7	0.1	-
Freeze-Thaw Cycle 1	1.3	0.3	-	0.7	0.1	-
Freeze-Thaw Cycle 3	1.5	0.5	-	1.6	0.2	-
Agitation Day 1	8.1	1.6	++	22.4	2.1	++
Agitation Day 3	7.6	0.4	++	25.0	10.5	++
Stirring Day1	13.2	5.4	++	217.7	17.0	++
Stirring Day3	64.4	7	++	756.7	71.9	++
Heating Day1	0.9	0.1	-	82.4	3.4	+
Heating Day3	0.9	0.1	-	212.3	5.9	++

Table 2.2. Summary of formation of soluble aggregates and nanometer, subvisible (microns), and visible (>100μm) sized particles in IgG1 mAb solutions as measured by SEC, NTA, MFI, Turbidity, and Visual Assessments, respectively. Symbols describe whether a change was observed (+) or not observed (-) compared to the unstressed mAb sample with the given analytical technique. Eight types of measurements are shown in the table and the last column summarizes, for each stress, the number of notable effects (+ vs. -) due to the presence versus absence of NaCl. Samples contained 1 mg/mL antibody in 10 mM sodium acetate, pH 5 in absence and presence of 150 mM NaCl.

	SEC[a]				NTA	MFI	Turbidity	Visual Assessment	# Results Differing due to NaCl
	%M	%I	%A	%F					
Freeze/Thaw									
-NaCl	-	-	-	-	-	-	-	-	**3/8**
+NaCl	-	+	-	-	+	+	-	-	
Agitation									
-NaCl	-	-	-	-	-	+	+	+	**1/8**
+NaCl	-	+	-	-	-	+	+	+	
Stirring									
-NaCl	-	+	-	-	+	+	+	+	**1/8**
+NaCl	+	+	-	-	+	+	+	+	
Heating									
-NaCl	-	+	-	+	-	+	-	-	**6/8**
+NaCl	+	+	+	-	+	+	+	+	

[a] %M, %I, %A, %F correspond to percent monomer, insoluble aggregate, soluble aggregate, and fragment, respectively.

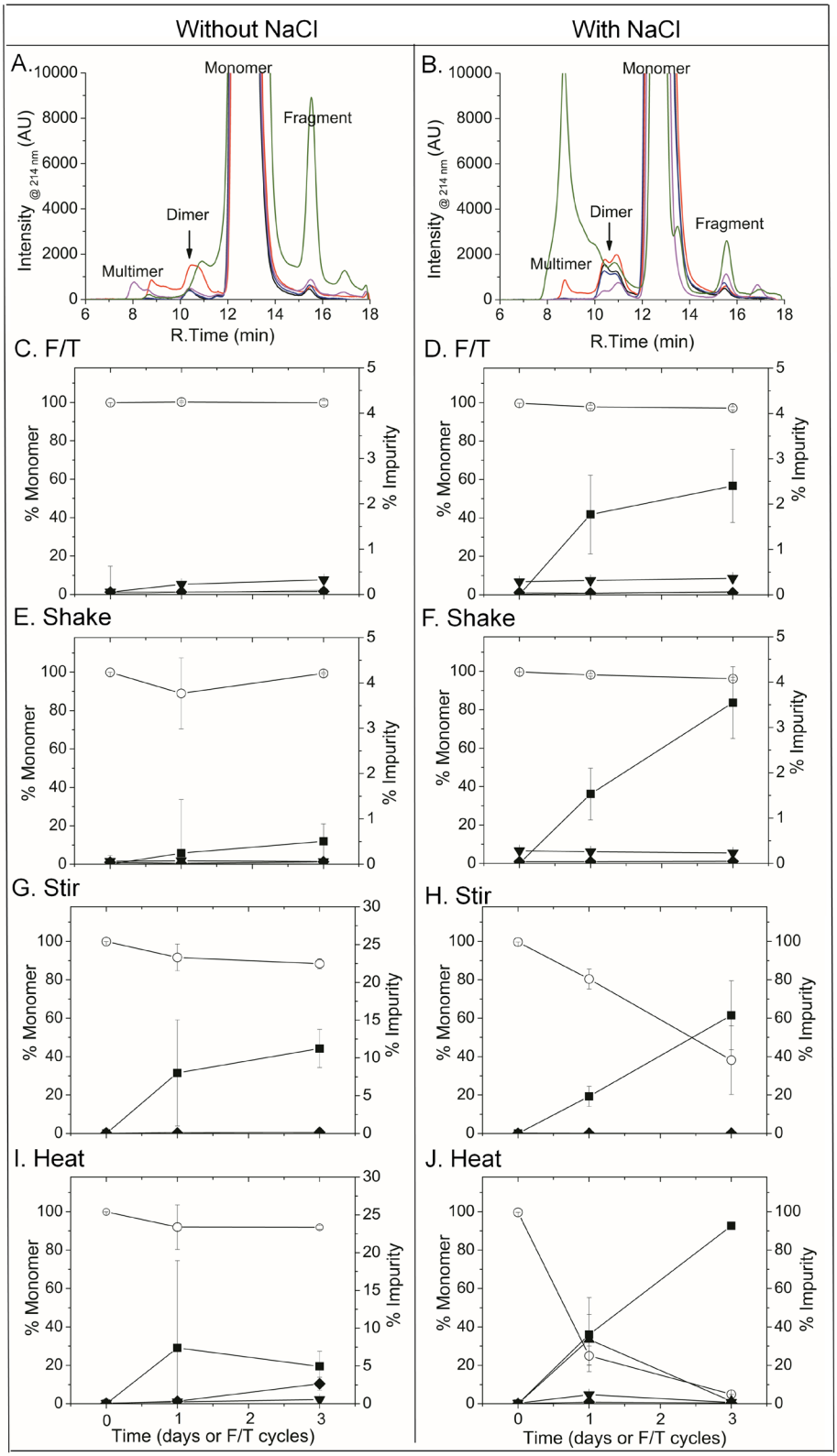
Without NaCl
With NaCl
A.
B.
Monomer
Dimer
Fragment
Multimer
Intensity @ 214 nm (AU)
R.Time (min)
C. F/T
D. F/T
E. Shake
F. Shake
G. Stir
H. Stir
I. Heat
J. Heat
% Monomer
% Impurity
Time (days or F/T cycles)

Figure 2.1. Formation of soluble and insoluble aggregates in IgG1 mAb solutions exposed to different stresses as measured by SEC. Representative SEC chromatograms monitored at 214 nm of 1 mg/mL antibody in 10 mM sodium acetate, pH 5 in absence (a) and presence (b) of 150 mM NaCl. Key: day 0 control (—), F/T cycle 3 (—), agitation day 3 (—), stirring day 3 (—), heating day 3 (—). Plots of monomer loss and changes in amounts of impurities as a function of different stresses are shown: freeze-thaw cycles (c) without NaCl and (d) with NaCl; days of agitation (e) without NaCl and (f) with NaCl; days of stirring (g) without NaCl and (h) with NaCl; days of heating (i) without NaCl and (j) with NaCl. Key for c-j: ⬭ -% monomer; impurity: ■ - % insoluble; ▲- % multimer; ▼- % dimer; ◆- % fragment. Each graph represents the average of three separate experiments (n=3). Error bars represent one standard deviation.

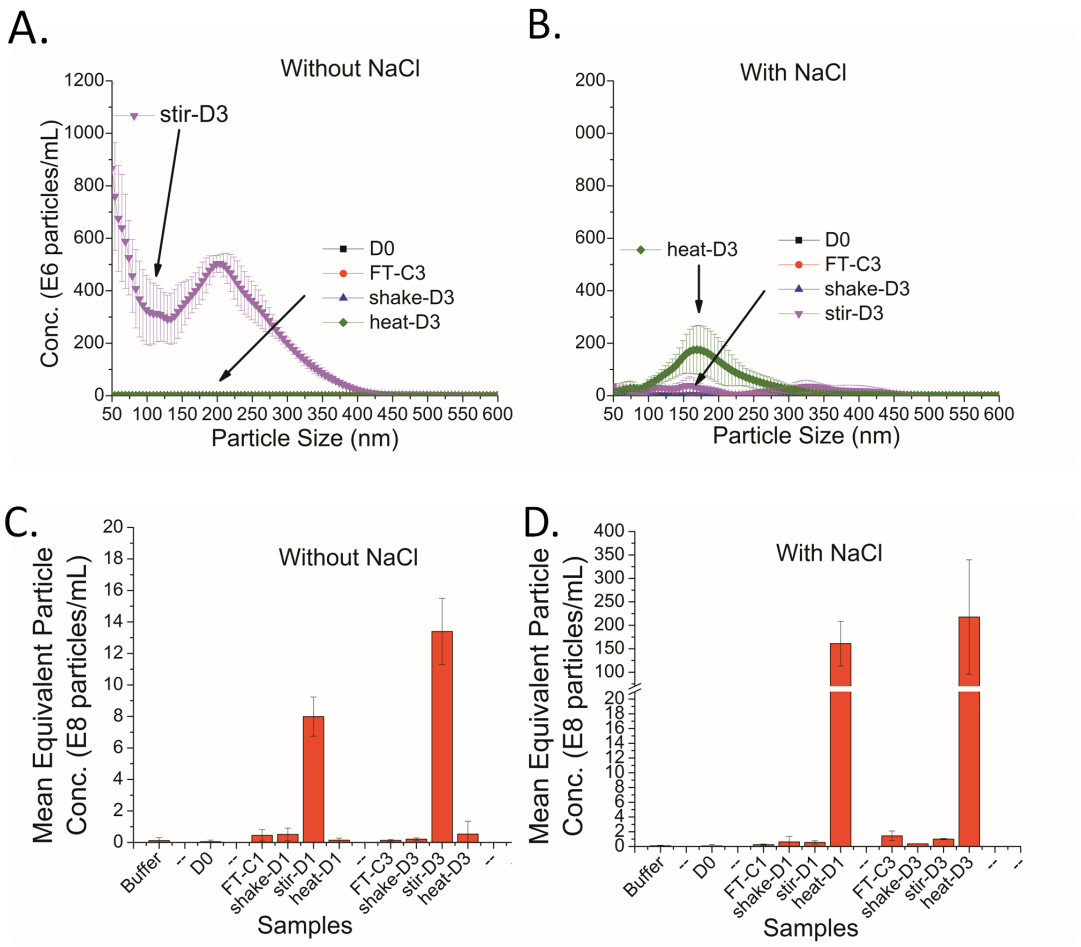

Figure 2.2. Formation of submicron-sized particles in IgG1 mAb solutions exposed to different stresses as measured by NTA. Representative NTA data showing the formation of nanometer sized particles due to four indicated stresses applied to 1 mg/mL antibody solution in 10 mM sodium acetate, pH 5 in the (a) absence of NaCl and (b) in the presence of NaCl. Concentration of nanometer-sized protein particles formed due to each stress at day 1 (D1) and (D3) in the (c) absence and (d) presence of NaCl. Each data set is the average of three separate experiments (n=3) and the error bars for each data point represents one standard deviation.

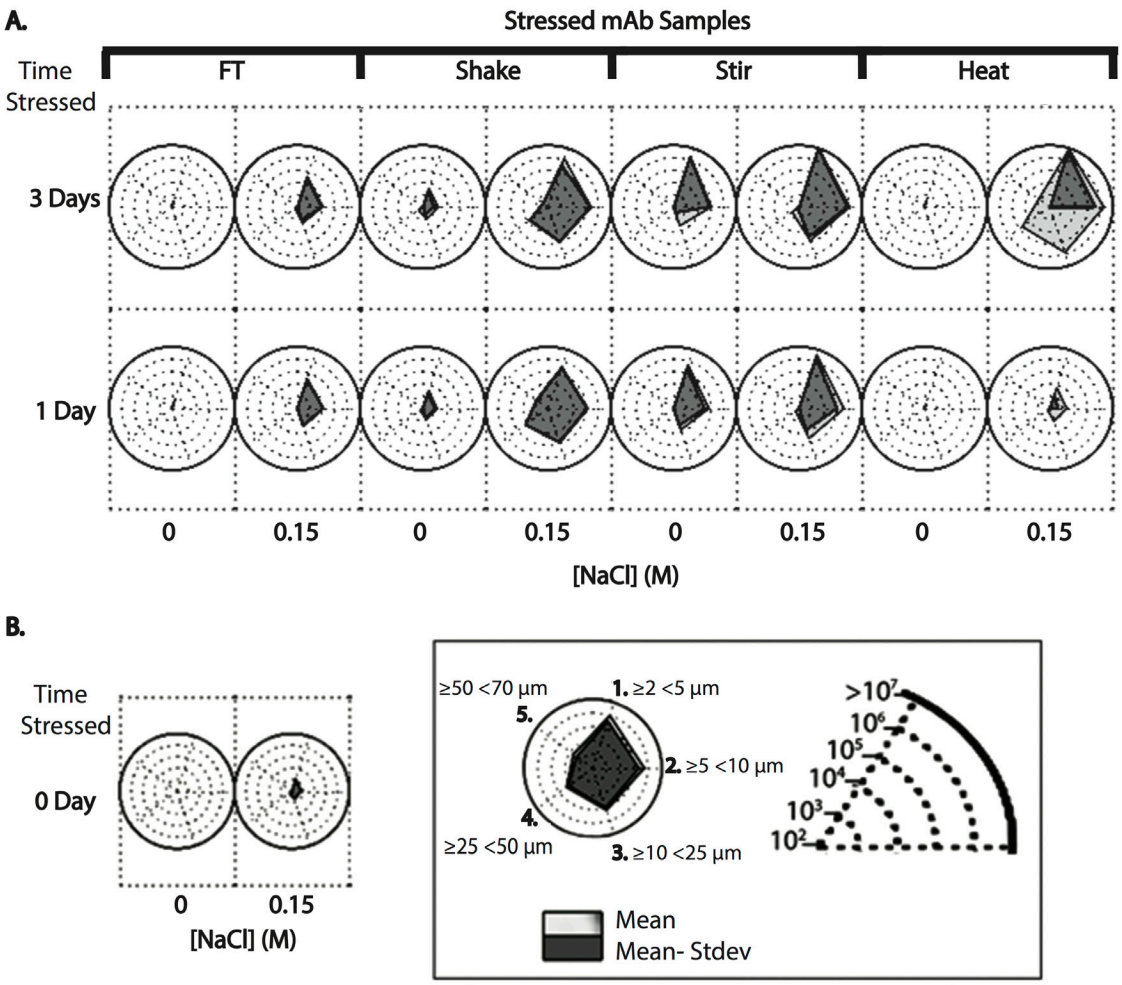

Figure 2.3. Radar plots for visualizing formation of subvisible particles (concentration and size distributions) in IgG1 mAb solutions exposed to different stresses as measured by MFI. Radar plots show MFI particle concentration and size data distributions as generated by four indicated stresses when applied to 1 mg/mL antibody solution in 10 mM sodium acetate, pH 5 with and without 150 mM NaCl. See the text for details of radar plot analysis. The data shown are the average of three separate experiments (n=3) and the error represents one standard deviation.

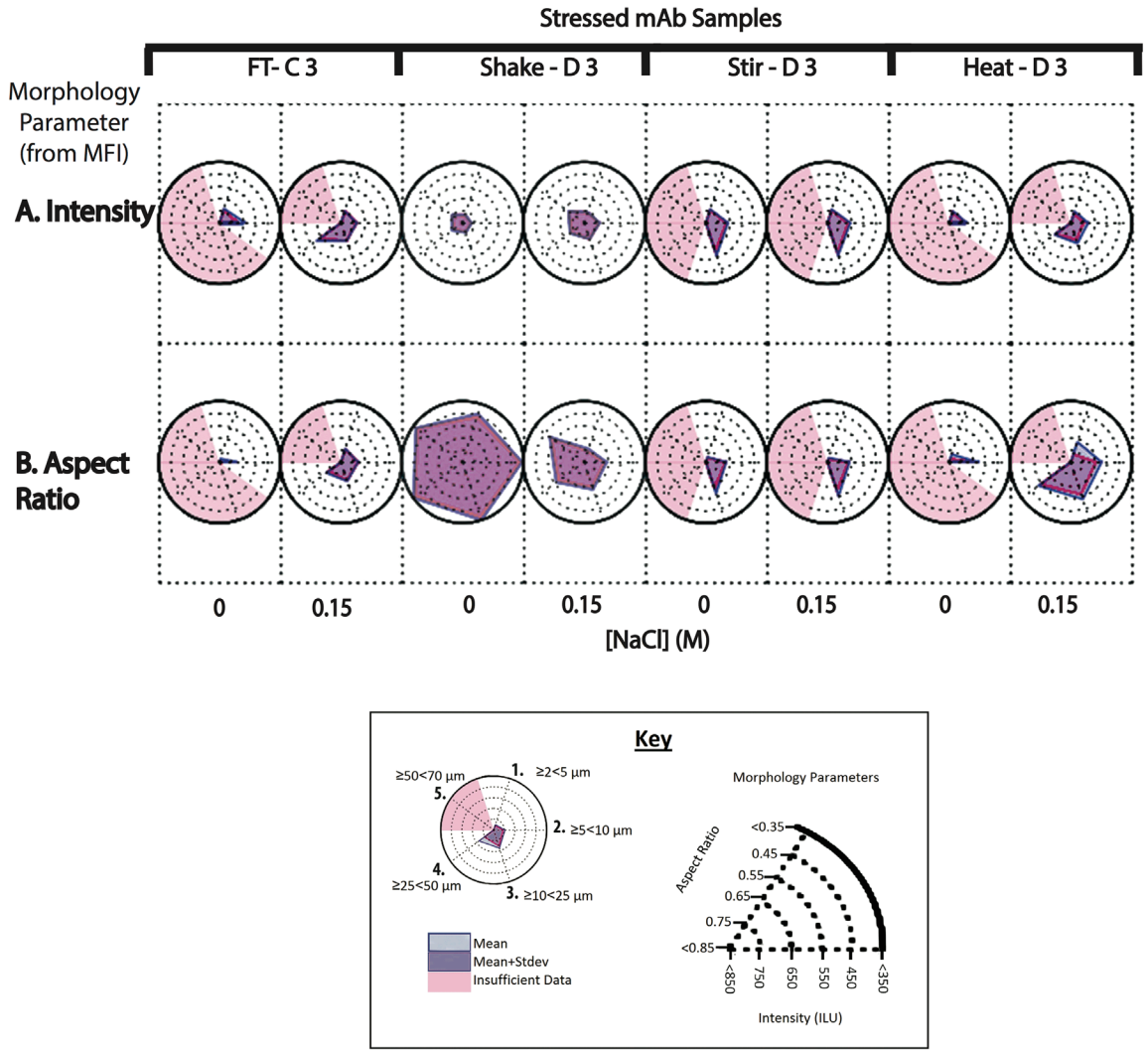

Figure 2.4. Radar plots for visualizing morphology parameters of subvisible particles (aspect ratio and intensity) in IgG1 mAb solutions exposed to different stresses as measured by MFI. Radar plots show MFI morphology data distributions as generated by four indicated stresses when applied to 1 mg/mL antibody solution in 10 mM sodium acetate, pH 5 with and without 150 mM NaCl. See text for details of radar plot analysis. The data shown are the average of three separate experiments (n=3) and the error represents one standard deviation.

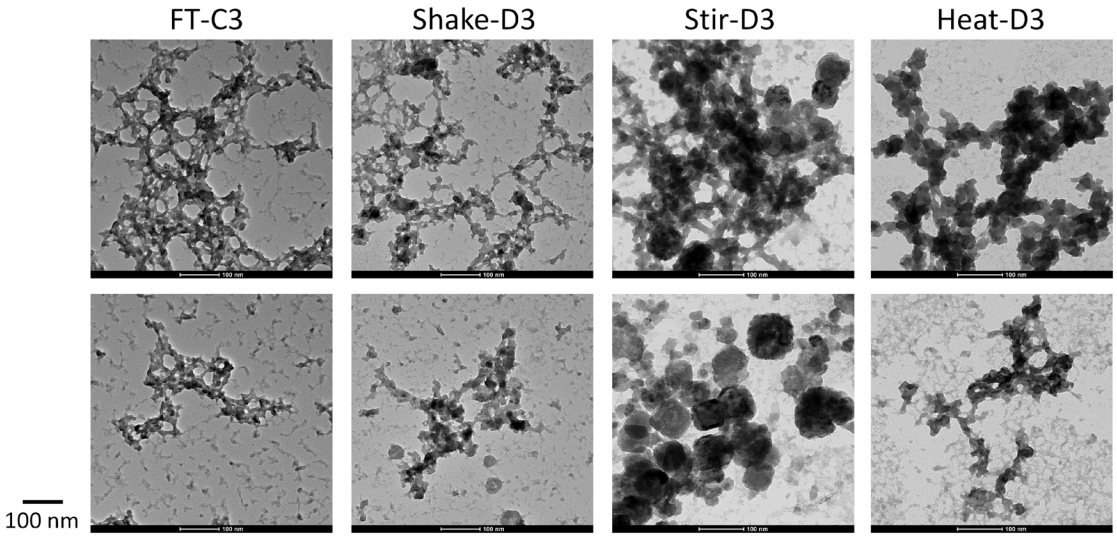

Figure 2.5. Representative TEM images of IgG1 mAb aggregates and particles formed after three freeze-thaw cycles or three days of each indicated stress. Particles were isolated from 1 mg/mL antibody solution in 10 mM sodium acetate, 150 mM NaCl, pH 5.

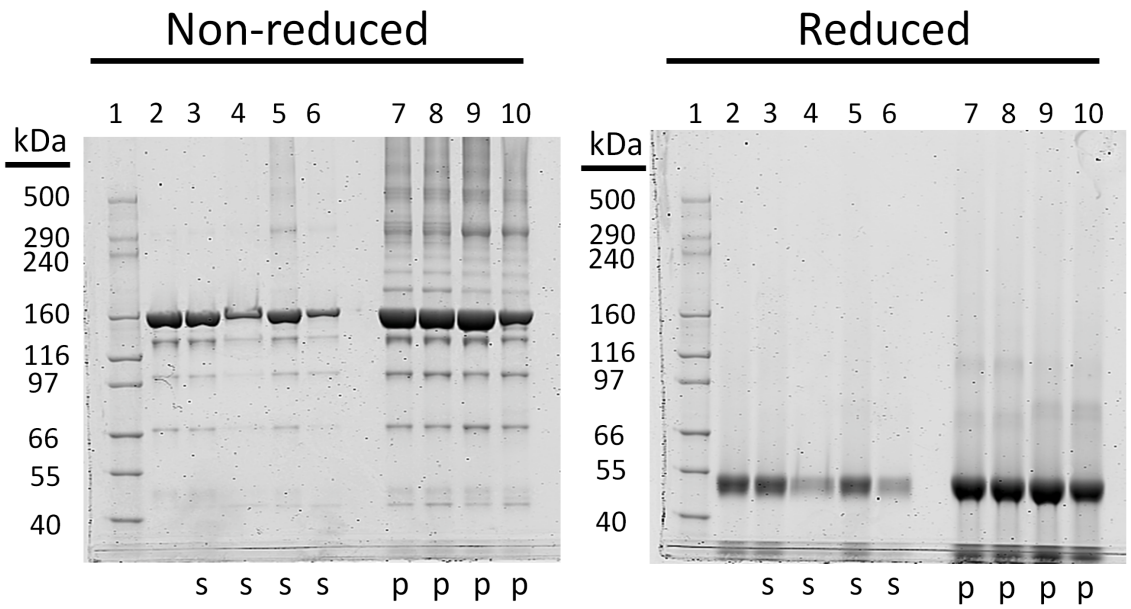

Lane	Sample
1	Ladder (MW standards)
2	D0
3	stir-D1 (supernatant)
4	stir-D3 (supernatant)
5	heat-D1 (supernatant)
6	heat-D3 (supernatant)
7	stir-D1 (pellet)
8	stir-D3 (pellet)
9	heat-D1 (pellet)
10	heat-D3 (pellet)

Figure 2.6. Reduced and non-reduced SDS-PAGE gels of IgG1 mAb samples exposed to four different stresses. Samples contained 1 mg/ml antibody in 10 mM sodium acetate, 150 mM NaCl, pH 5. High molecular weight aggregates formed by disulfide linkages were observed in pellet of stir-day 1, stir-day 3, heat-day 1 and heat-day 3 samples. Stressed samples were centrifuged to separate supernatant (S) from pellet (P), run on SDS-PAGE, and stained as described in the *Methods* section.

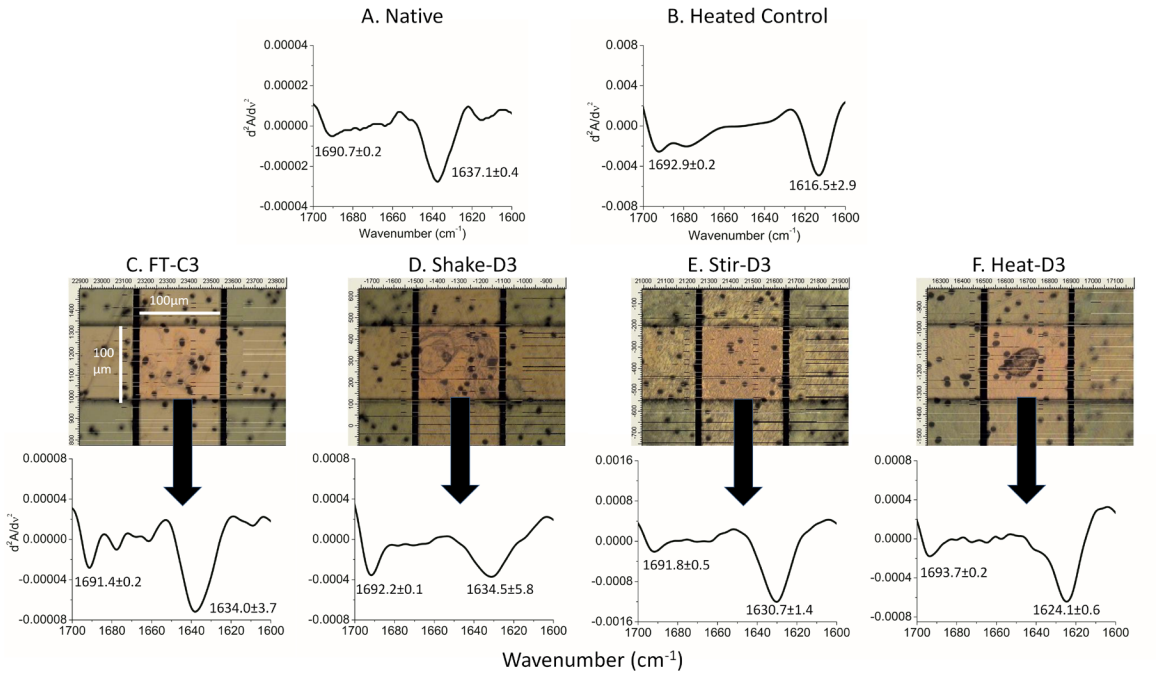

Figure 2.7. FTIR analysis of overall secondary structure of IgG mAb solutions and isolated particles as generated from four indicated stresses. Samples contained 1 mg/ml antibody in 10 mM sodium acetate, 150 mM NaCl, pH 5. Second derivative FTIR spectrum of (a) native, unstressed protein in solution, and (b) particle isolated from mAb heated at 80°C for 20 min to determine the maximum extent of secondary structure loss in solution. (c-f) Representative optical images of isolated mAb particles (by passing through gold filter) as generated from the four indicated stresses and their corresponding second derivative FTIR spectra from FTIR microscope. Numerical values are the average of three separate experiments (n=3) with error associated with the wavenumbers representing one standard deviation.

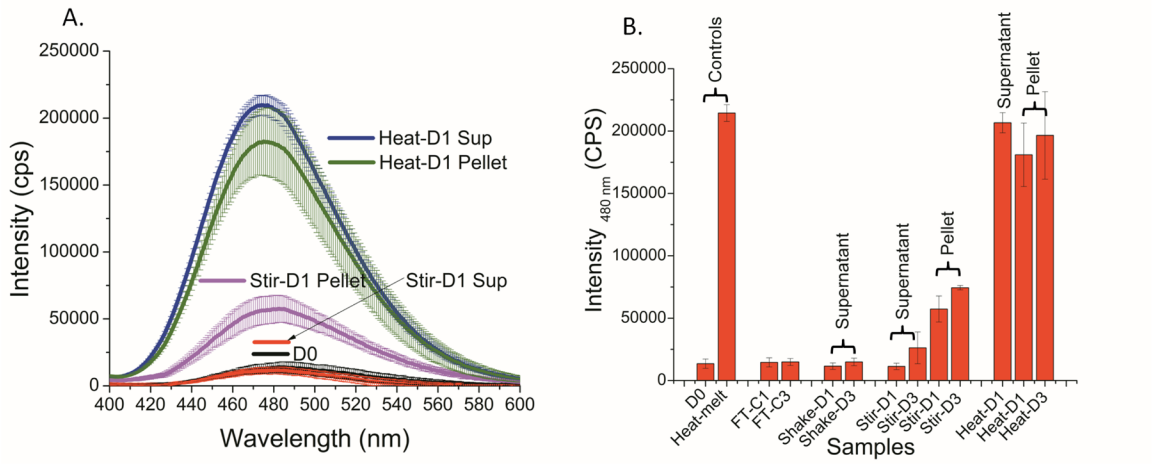

Figure 2.8. ANS extrinsic fluorescence analysis of IgG1 mAb samples (supernatant and pellet components) before and after indicated stress was applied to samples. Samples contained 1 mg/ml mAb in 10 mM sodium acetate, 150 mM NaCl, pH 5. (a) Representative ANS spectra, and (b) ANS fluorescence intensity values (at 480 nm) for each stressed mAb sample compared to the two controls: unstressed (D0) and extensively heated samples (heat-melt). The average intensities shown are based on three separate experiments (n=3). The error bars represent one standard deviation.

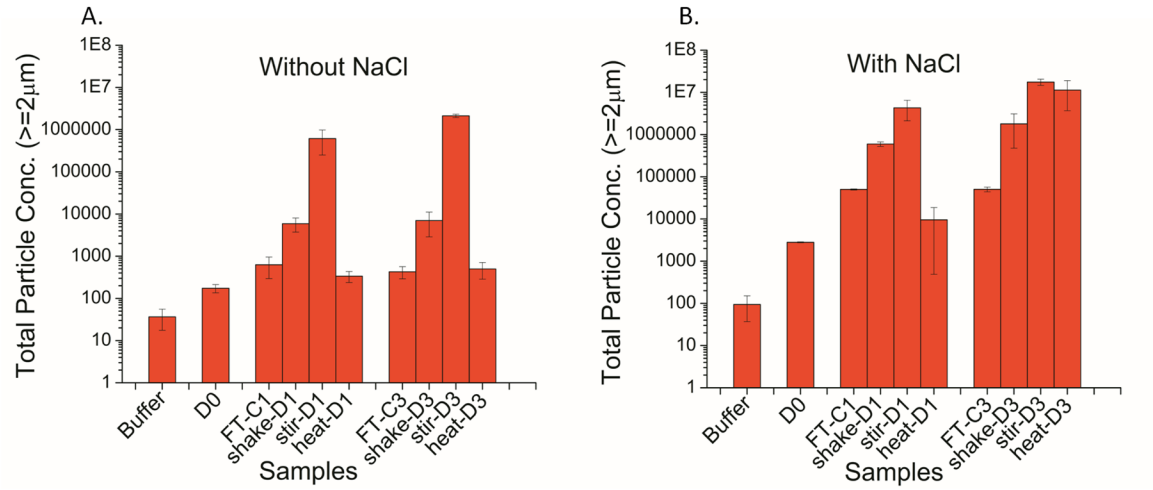

Figure 2.9. Total concentration of subvisible particles (greater than 2 µm as measured by MFI) formed in IgG1 mAb solutions as generated by indicated stress at different time points. Samples contained 1 mg/ml antibody in 10 mM sodium acetate, pH 5 in the absence (A) or presence (B) of 150 mM NaCl. The MFI particle data shown are the average of three separate experiments (n=3) and the error bars represent one standard deviation.

2.6 REFERENCES

1. Hermeling S, Crommelin DJ, Schellekens H, Jiskoot W 2004. Structure-immunogenicity relationships of therapeutic proteins. Pharm Res 21(6):897-903.
2. Rosenberg AS 2006. Effects of protein aggregates: an immunologic perspective. Aaps J 8(3):E501-507.
3. Schellekens H 2002. Bioequivalence and the immunogenicity of biopharmaceuticals. Nat Rev Drug Discov 1(6):457-462.
4. Schellekens H 2003. Immunogenicity of therapeutic proteins. Nephrol Dial Transplant 18(7):1257-1259.
5. Cromwell ME, Hilario E, Jacobson F 2006. Protein aggregation and bioprocessing. Aaps J 8(3):E572-579.
6. Mahler HC, Friess W, Grauschopf U, Kiese S 2009. Protein aggregation: pathways, induction factors and analysis. J Pharm Sci 98(9):2909-2934.
7. Wang W 2005. Protein aggregation and its inhibition in biopharmaceutics. Int J Pharm 289(1-2):1-30.
8. Shire SJ, Shahrokh Z, Liu J 2004. Challenges in the development of high protein concentration formulations. J Pharm Sci 93(6):1390-1402.
9. Chi EY, Krishnan S, Randolph TW, Carpenter JF 2003. Physical stability of proteins in aqueous solution: mechanism and driving forces in nonnative protein aggregation. Pharm Res 20(9):1325-1336.
10. Arosio P, Rima S, Morbidelli M 2013. Aggregation mechanism of an IgG2 and two IgG1 monoclonal antibodies at low pH: from oligomers to larger aggregates. Pharm Res 30(3):641-654.
11. Strambini GB, Gonnelli M 2007. Protein stability in ice. Biophys J 92(6):2131-2138.
12. Pikal-Cleland KA, Cleland JL, Anchordoquy TJ, Carpenter JF 2002. Effect of glycine on pH changes and protein stability during freeze-thawing in phosphate buffer systems. J Pharm Sci 91(9):1969-1979.
13. Kreilgaard L, Frokjaer S, Flink JM, Randolph TW, Carpenter JF 1998. Effects of additives on the stability of recombinant human factor XIII during freeze-drying and storage in the dried solid. Arch Biochem Biophys 360(1):121-134.
14. Hillgren A, Lindgren J, Alden M 2002. Protection mechanism of Tween 80 during freeze-thawing of a model protein, LDH. Int J Pharm 237(1-2):57-69.
15. Kueltzo LA, Wang W, Randolph TW, Carpenter JF 2008. Effects of solution conditions, processing parameters, and container materials on aggregation of a monoclonal antibody during freeze-thawing. J Pharm Sci 97(5):1801-1812.
16. Wang W, Roberts CJ editors. 2010. Aggregation of Therapeutic Proteins. Hoboken, NJ: Wiley.
17. Kiese S, Papppenberger A, Friess W, Mahler HC 2008. Shaken, not stirred: mechanical stress testing of an IgG1 antibody. J Pharm Sci 97(10):4347-4366.
18. Hawe A, Kasper JC, Friess W, Jiskoot W 2009. Structural properties of monoclonal antibody aggregates induced by freeze-thawing and thermal stress. Eur J Pharm Sci 38(2):79-87.
19. Eppler A, Weigandt M, Hanefeld A, Bunjes H 2010. Relevant shaking stress conditions for antibody preformulation development. Eur J Pharm Biopharm 74(2):139-147.

20. Brych SR, Gokarn YR, Hultgen H, Stevenson RJ, Rajan R, Matsumura M 2010. Characterization of antibody aggregation: role of buried, unpaired cysteines in particle formation. J Pharm Sci 99(2):764-781.
21. Hawe A, Wiggenhorn M, van de Weert M, Garbe JH, Mahler HC, Jiskoot W 2012. Forced degradation of therapeutic proteins. J Pharm Sci 101(3):895-913.
22. Joubert MK, Luo Q, Nashed-Samuel Y, Wypych J, Narhi LO 2011. Classification and characterization of therapeutic antibody aggregates. J Biol Chem 286(28):25118-25133.
23. Wang W, Nema S, Teagarden D 2010. Protein aggregation--pathways and influencing factors. Int J Pharm 390(2):89-99.
24. Demeule B, Messick S, Shire SJ, Liu J 2010. Characterization of particles in protein solutions: reaching the limits of current technologies. Aaps J 12(4):708-715.
25. Narhi LO, Schmit J, Bechtold-Peters K, Sharma D 2012. Classification of protein aggregates. J Pharm Sci 101(2):493-498.
26. Bond MD, Panek ME, Zhang Z, Wang D, Mehndiratta P, Zhao H, Gunton K, Ni A, Nedved ML, Burman S, Volkin DB 2010. Evaluation of a dual-wavelength size exclusion HPLC method with improved sensitivity to detect protein aggregates and its use to better characterize degradation pathways of an IgG1 monoclonal antibody. J Pharm Sci 99(6):2582-2597.
27. Wang T, Joshi SB, Kumru OS, Telikepalli S, Middaugh CR, Volkin DB. 2013. Case Studies Applying Biophysical Techniques to Better Characterize Protein Aggregates and Particulates of Varying Size. In Biophysics for therapeutic protein development; Narhi LO, ed.: Springer New York, p 205-243.
28. Zolls S, Tantipolphan R, Wiggenhorn M, Winter G, Jiskoot W, Friess W, Hawe A 2012. Particles in therapeutic protein formulations, Part 1: overview of analytical methods. J Pharm Sci 101(3):914-935.
29. Wuchner K, Buchler J, Spycher R, Dalmonte P, Volkin DB 2010. Development of a microflow digital imaging assay to characterize protein particulates during storage of a high concentration IgG1 monoclonal antibody formulation. J Pharm Sci 99(8):3343-3361.
30. Sharma DK, Oma P, Pollo MJ, Sukumar M 2010. Quantification and characterization of subvisible proteinaceous particles in opalescent mAb formulations using micro-flow imaging. J Pharm Sci 99(6):2628-2642.
31. Ohno O, Cooke TD 1978. Electron microscopic morphology of immunoglobulin aggregates and their interactions in rheumatoid articular collagenous tissues. Arthritis Rheum 21(5):516-527.
32. Flatman S, Alam I, Gerard J, Mussa N 2007. Process analytics for purification of monoclonal antibodies. J Chromatogr B Analyt Technol Biomed Life Sci 848(1):79-87.
33. Piekarska B, Skowronek M, Rybarska J, Stopa B, Roterman I, Konieczny L 1996. Congo red-stabilized intermediates in the lambda light chain transition from native to molten state. Biochimie 78(3):183-189.
34. Hawe A, Sutter M, Jiskoot W 2008. Extrinsic fluorescent dyes as tools for protein characterization. Pharm Res 25(7):1487-1499.
35. He F, Phan DH, Hogan S, Bailey R, Becker GW, Narhi LO, Razinkov VI 2010. Detection of IgG aggregation by a high throughput method based on extrinsic fluorescence. J Pharm Sci 99(6):2598-2608.
36. Schule S, Friess W, Bechtold-Peters K, Garidel P 2007. Conformational analysis of protein secondary structure during spray-drying of antibody/mannitol formulations. Eur J Pharm Biopharm 65(1):1-9.

37. Matheus S, Mahler HC, Friess W 2006. A critical evaluation of Tm(FTIR) measurements of high-concentration IgG1 antibody formulations as a formulation development tool. Pharm Res 23(7):1617-1627.
38. Vermeer AW, Bremer MG, Norde W 1998. Structural changes of IgG induced by heat treatment and by adsorption onto a hydrophobic Teflon surface studied by circular dichroism spectroscopy. Biochim Biophys Acta 1425(1):1-12.
39. Kalonia C, Kumru OS, Kim JH, Middaugh CR, Volkin DB 2013. Radar Chart Array Analysis to Visualize Effects of Formulation Variables on IgG1 Particle Formation as Measured by Multiple Analytical Techniques. J Pharm Sci.
40. Luo Q, Joubert MK, Stevenson R, Ketchem RR, Narhi LO, Wypych J 2011. Chemical modifications in therapeutic protein aggregates generated under different stress conditions. J Biol Chem 286(28):25134-25144.
41. Kumru OS, Liu J, Ji JA, Cheng W, Wang YJ, Wang T, Joshi SB, Middaugh CR, Volkin DB 2012. Compatibility, physical stability, and characterization of an IgG4 monoclonal antibody after dilution into different intravenous administration bags. J Pharm Sci 101(10):3636-3650.
42. Kim JH, Iyer V, Joshi SB, Volkin DB, Middaugh CR 2012. Improved data visualization techniques for analyzing macromolecule structural changes. Protein Sci 21(10):1540-1553.
43. Chi EY, Krishnan S, Kendrick BS, Chang BS, Carpenter JF, Randolph TW 2003. Roles of conformational stability and colloidal stability in the aggregation of recombinant human granulocyte colony-stimulating factor. Protein Sci 12(5):903-913.
44. Vonhoff S, Condliffe J, Schiffter H 2010. Implementation of an FTIR calibration curve for fast and objective determination of changes in protein secondary structure during formulation development. J Pharm Biomed Anal 51(1):39-45.
45. Murphy BM, Zhang N, Payne RW, Davis JM, Abdul-Fattah AM, Matsuura JE, Herman AC, Manning MC 2012. Structure, stability, and mobility of a lyophilized IgG1 monoclonal antibody as determined using second-derivative infrared spectroscopy. J Pharm Sci 101(1):81-91.
46. van Stokkum IH, Linsdell H, Hadden JM, Haris PI, Chapman D, Bloemendal M 1995. Temperature-induced changes in protein structures studied by Fourier transform infrared spectroscopy and global analysis. Biochemistry 34(33):10508-10518.
47. Hamada H, Arakawa T, Shiraki K 2009. Effect of additives on protein aggregation. Curr Pharm Biotechnol 10(4):400-407.
48. Weinbuch D, Zolls S, Wiggenhorn M, Friess W, Winter G, Jiskoot W, Hawe A 2013. Micro-flow imaging and resonant mass measurement (archimedes) - complementary methods to quantitatively differentiate protein particles and silicone oil droplets. J Pharm Sci 102(7):2152-2165.
49. Hawe A, Romeijn S, Filipe V, Jiskoot W 2012. Asymmetrical flow field-flow fractionation method for the analysis of submicron protein aggregates. J Pharm Sci 101(11):4129-4139.
50. Wilson GA, Manning MC 2013. Flow imaging: moving toward best practices for subvisible particle quantitation in protein products. J Pharm Sci 102(3):1133-1134.
51. Hamrang Z, Rattray NJ, Pluen A 2013. Proteins behaving badly: emerging technologies in profiling biopharmaceutical aggregation. Trends Biotechnol.
52. Barnard JG, Singh S, Randolph TW, Carpenter JF 2011. Subvisible particle counting provides a sensitive method of detecting and quantifying aggregation of monoclonal antibody

caused by freeze-thawing: insights into the roles of particles in the protein aggregation pathway. J Pharm Sci 100(2):492-503.
53. Zhang A, Singh SK, Shirts MR, Kumar S, Fernandez EJ 2012. Distinct aggregation mechanisms of monoclonal antibody under thermal and freeze-thaw stresses revealed by hydrogen exchange. Pharm Res 29(1):236-250.
54. Serno T, Carpenter JF, Randolph TW, Winter G 2010. Inhibition of agitation-induced aggregation of an IgG-antibody by hydroxypropyl-beta-cyclodextrin. J Pharm Sci 99(3):1193-1206.
55. Mahler HC, Muller R, Friess W, Delille A, Matheus S 2005. Induction and analysis of aggregates in a liquid IgG1-antibody formulation. Eur J Pharm Biopharm 59(3):407-417.
56. Bee JS, Goletz TJ, Ragheb JA 2012. The future of protein particle characterization and understanding its potential to diminish the immunogenicity of biopharmaceuticals: a shared perspective. J Pharm Sci 101(10):3580-3585.
57. Ripple DC, Dimitrova MN 2012. Protein particles: what we know and what we do not know. J Pharm Sci 101(10):3568-3579.
58. Rosenberg AS, Verthelyi D, Cherney BW 2012. Managing uncertainty: a perspective on risk pertaining to product quality attributes as they bear on immunogenicity of therapeutic proteins. J Pharm Sci 101(10):3560-3567.
59. Marszal E, Fowler E 2012. Workshop on predictive science of the immunogenicity aspects of particles in biopharmaceutical products. J Pharm Sci 101(10):3555-3559.
60. Wang W, Singh SK, Li N, Toler MR, King KR, Nema S 2012. Immunogenicity of protein aggregates--concerns and realities. Int J Pharm 431(1-2):1-11.
61. Joubert MK, Hokom M, Eakin C, Zhou L, Deshpande M, Baker MP, Goletz TJ, Kerwin BA, Chirmule N, Narhi LO, Jawa V 2012. Highly aggregated antibody therapeutics can enhance the in vitro innate and late-stage T-cell immune responses. J Biol Chem 287(30):25266-25279.
62. Filipe V, Jiskoot W, Basmeleh AH, Halim A, Schellekens H 2012. Immunogenicity of different stressed IgG monoclonal antibody formulations in immune tolerant transgenic mice. MAbs 4(6).

CHAPTER 3: Characterization of the Physical Stability of a Lyophilized IgG1 mAb After Accelerated Shipping-like Stress

3.1 INTRODUCTION

When a protein therapeutic is appropriately lyophilized with stabilizing excipients, the solid dosage form typically displays increased physicochemical stability during storage and shipping, compared to a liquid formulation counterpart, resulting in a longer shelf life including a lower propensity toward aggregation.[1-3] Many proteins, including monoclonal antibodies (mAbs), have been shown to be more stable during exposure to elevated temperatures in the lyophilized than in the liquid state[1,4-7], although there are some exceptions to this general rule.[6] Despite protein lyophilization being a relatively well-established formulation technology, there remains numerous challenges both in terms of developing an improved understanding of protein degradation pathways in the solid state as well as better optimizing lyophilization process design and scale-up [1,5,8,9].

The lyophilization process typically consists of freezing, primary and secondary drying, and reconstitution steps, each of which may structurally damage proteins[10-14]. Freezing of bulk water in a protein solution can cause cryoconcentration of protein and excipients, pH changes, and/or adsorption of protein to the surface of ice crystals[10,13,14]. Primary drying removes the frozen bulk water and further concentrates the protein and stabilizers, allowing the possibility of unfavorable interactions [5,11]. Protein instability is also possible during secondary drying, during which the non-frozen water bound to the protein or excipients is removed. The composition of the reconstitution medium and it's rate of addition may also affect the stability of a lyophilized protein upon reconstitution back into the liquid state[15]. For example, if the reconstitution medium is added too rapidly, the dried protein may not be given sufficient time to rehydrate and assume its native conformation, and the presence of this improperly rehydrated protein may lead to aggregation. [6,16]. The aggregation of monoclonal antibodies in the lyophilized state, and/or

upon reconstitution, has also been correlated with formation of non-native intermolecular disulfide bonds[17] as well as the appearance of aggregates of different sizes including an increased number of subvisible particles[18].

A freeze-dried cake's physical structure and moisture level are typically optimized as part of protein lyophilization development, since either can potentially affect the extent to which a protein may aggregate in the solid state [6,19-21]. These parameters can be interrelated since changes in residual moisture content may affect not only protein structure, but also the physical integrity of the lyophilized cake itself (i.e., a change from a viscous to a rubbery state where molecular mobility increases[7]). Some lyophilized protein preparations with high moisture content have shown increased chemical degradation due to increased mobility and the ability of water to participate in chemical reactions.[22,23] However, a bell shaped relationship between moisture content and physical stability (aggregation) has also been observed, e.g., lyophilized recombinant human albumin displayed maximum aggregation at ~50% moisture content. [24] In terms of the effect of the physical integrity of a freeze-dried cake on protein stability, it has been shown that when a lyophilized cake of an IgG1 mAb is physically collapsed to different extents by using different amounts of stabilizers and bulking agents during the freeze-drying process, the mAb can still remain stable in the different preparations.[19-21] The method of cake collapse, however, either during the freeze-drying cycle or during storage at elevated temperatures, has been shown to potentially be an important factor in determining protein stability during subsequent storage.[21]

The effect of mechanical stress on the stability of lyophilized proteins has not been as widely examined. In this work, to examine the potential of shipping stress to cause protein aggregation, we implemented a stress shipping test based on considering guidelines in the

vibration testing document D999 proposed by ASTM International Standard Test Methods for Vibration Testing of Shipping Containers[25]. Currently, there are no guidance documents available that are specific for pharmaceutical products that outline the testing criteria to use when evaluating product quality impact of shipping-related stress. Initially, we examined the physical stability of an IgG1 mAb formulation in both a liquid and lyophilized state after exposure to shaking stress with the expectation that the protein in the lyophilized state would be more stable in terms of aggregation and particle formation. Surprisingly, the lyophilized preparation also displayed mAb physical instability (upon reconstitution).

The focus of this work was to better understand the effect of shaking stress, used to mimic extreme shipping conditions, on the physical stability of a lyophilized mAb preparation. A wide variety of analytical characterization techniques were used to size and count protein aggregates and particles across a wide size range including size-exclusion chromatography (SEC), dynamic light scattering (DLS), Nanoparticle Tracking Analysis (NTA), Resonant Mass Measurement (Archimedes), Microflow-Imaging (MFI), and turbidity. We also used data visualization tools (e.g., radar plots) to display and compare the number and size of protein particles formed under different conditions. The composition of the protein found in particles was further examined using SDS-PAGE and FTIR Microscopy. We determined how formulation variables such as residual moisture content, reconstitution speed, and composition of the reconstitution medium affected the formation of subvisible particles and solution turbidity when the lyophilized mAb was exposed not only to shaking stress, but also to subsequent storage for three months at various temperatures.

3.2 EXPERIMENTAL SECTION

3.2.1 Materials

Lyophilized IgG1 mAb samples prepared at 0.6% and 6.8% moisture content, and their corresponding matching placebos without protein, were supplied in stoppered 20 mL glass vials by Human Genome Sciences (currently GlaxoSmithKline). Upon reconstitution with 5 mL of deionized water from Water Pro PS Station (Labconco, Kansas City, MO), the target concentration was approximately 30 mg/mL protein, in a formulation consisting of 0.08 mg/mL citric acid monohydrate (Avantor Performance Materials, JT Baker 0115, Center Valley, PA), 1.6 mg/mL sodium citrate dihydrate (Avantor Performance Materials, JT Baker 3647), 11 mg/mL glycine (Avantor Performance Materials, JT Baker 0581), 3 mg/mL sucrose (Avantor Performance Materials, JT Baker 4005), and 0.12 mg/mL polysorbate-80 (Croda International, SR48833, England) at pH 6.5. Lyophilized samples were stored at 4 °C unless otherwise indicated. The IgG1 mAb has a pI of ~8.4 and protein concentrations were determined by UV spectroscopy at 280 nm with an extinction coefficient of $\varepsilon^{0.1\%} = 1.58\ (g/100mL)^{-1}\ cm^{-1}$.

3.2.2 Methods

3.2.2.1 Shaking stress studies

Glass vials containing lyophilized and liquid IgG1 protein samples and corresponding placebo controls were taped horizontally inside of a lightweight, cryogenic box (13 x 13 x 5 cm) , which was then taped to the cuphead of a 4.9 mm orbit Fisher Scientific Analog Vortex Mixer (Waltham, MA) and shaken vigorously at 3200 rpm for different periods of times at ambient temperature. Depending on the experiment, the shake-stressed samples were either in the lyophilized (solid) state or in the reconstituted (liquid) state. Unstressed and stressed samples of

lyophilized protein and placebos were reconstituted with 5 mL of deionized water (Labconco) over 10 s, unless otherwise noted. To prepare the liquid samples, the lyophilized protein formulation was reconstituted with 5 mL of deionized water (Labconco) prior to shaking.

To study the effect of reconstitution medium type and addition rate, shake-stressed (for 24 h) and unstressed lyophilized IgG1 mAb samples were reconstituted by adding 5 mL of four different diluents (deionized water, 150 mM NaCl, 150 mM NaCl + 0.05% polysorbate 80, and 500 mM NaCl) at two rates (5 mL injected over 10 s and 5 mL injected over 2.5 min). To study the effect of shake-stress on subsequent storage stability, lyophilized mAb samples in stoppered glass vials were shaken for 2.5 min or 24 h and placed at 4, 40, or 55°C for up to 3 months at ambient humidity. Intact, unstressed samples (no cake breakage) were also stored up to 3 months at these temperatures. At time zero in the stability study, intact cake samples, 2.5 min shaking, and 24 h shaking samples were analyzed immediately (no storage). Placebos were also analyzed after 3 months storage at 55°C.

3.2.2.2 Turbidity

To monitor solution turbidity of samples, a HACH 2100 AN turbidimeter (HACH, Loveland, CO) was used. Prior to analyzing the experimental samples, StableCal calibration standards (Hach, Loveland, CO), ranging from <0.1 to 4000 Nephelometric Turbidity Units (NTU), containing hexamethylenetetramine and demineralized water, were used for generating a standard curve. The method is based on comparing intensity of light scattered by a sample under defined conditions with the intensity of light scattered by a standard reference suspension. Samples were not centrifuged or diluted for analysis.

3.2.2.3 Size-exclusion HPLC (SE-HPLC)

A Shimadzu UFLC HPLC system equipped with a diode-array detector and a Tosoh Bioscience (Tokyo, Japan) TSK-Gel G3000SW_{XL} (7.8 mm ID x 30.0 cm, 5μm) and the corresponding guard column (TSK-Gel Guard Column $SW_{XL,}$ 6.0 mm ID x 4.0 cm, 7μm) were used to monitor for the presence of soluble aggregates (< 100 nm). Prior to sample runs, the columns were rinsed for 60 min with deionized water followed by equilibration at 30^{o}C for 1 h using mobile phase (10 mM sodium phosphate, 450 mM sodium chloride, pH 7.4) at a flow rate of 0.5 ml/min. Molecular weight standards (Biorad Laboratories, Hercules, CA) were run to test for efficacy of separation and resolution. Samples were centrifuged at 16,000 x g for 5 min and 10μL of supernatant was injected for analysis and monitored at 280 nm for each 35 min sample run. Aggregates, monomers, and fragment peaks were quantified using the LC Solutions data analysis software provided with the instrument.

3.2.2.4 Nanoparticle Tracking Analysis (NTA)

Submicron sized particles (50-1000 nm) were measured using a Nanosight LM-14 (Nanosight, Amesbury, UK) with a CCD camera. Stressed samples and controls were centrifuged at 16,000 x g for 5 min, to separate larger aggregates outside the instrument sizing range. The supernatant was diluted 100 fold in formulation buffer (η=1.08 mpa$\cdot$ S for formulation buffer and η=1.36 mpa$\cdot$ S for the unstressed sample). Three hundred microliters of the 100 fold diluted supernatants were injected into the sample holder. Three 30 s movies were taken at ambient temperature for each sample. All samples were corrected for dilution. Data analysis was performed using the NTA 2.3 software, provided with the instrument, with detection threshold of 16, a screen gain of 7, and a minimum expected particle size of 50 nm.

3.2.2.5 Dynamic Light Scattering (DLS)

DLS measurements were performed to monitor small nanometer sized particles (1-1000nm) using a DynaPro™ Plate Reader (Wyatt Technologies, Santa Barbara, CA). Prior to analysis, the protein samples and controls were centrifuged at 16,000 x g for 5 min to remove large aggregates. The supernatant was separated and 30µL of the supernatant was loaded into a clear bottom 384 well assay plate (Corning Incorporated, Corning, NY). The plate was then centrifuged at 1177 x g for 3 min to remove air bubbles. Measurements were performed at 20°C with auto attenuation using the globular protein model and with the viscosity values determined using an Anton Parr Stabinger Viscometer 3000 (Anton Parr Inc., Ashland, VA). The data were collected using the Dynamics V 7.1.6 software, provided with the instrument, and analyzed using multimodal analysis.

3.2.2.6 Resonant Mass Measurements

Analysis of 0.25 to 3 micron sized particles was accomplished using an Archimedes particle metrology system (Affinity Biosciences, Santa Barbara, California). The instrument was first calibrated with NIST standard 1 µm polystyrene beads prior to analyzing experimental samples. To prevent clogging of the Hi-Q micro sensors, samples were centrifuged at 16,000 x g for 5 min and supernatants were analyzed. Triplicates of each sample were allowed to run until 500 particles were counted to obtain statistically significant data. Particle Lab software, provided with the instrument, was used to obtain particle size and concentration.

3.2.2.7 Micro-flow Digital Imaging and Radar Chart Analysis

Micron sized subvisible particles (2-100 µm) were analyzed and imaged using an MFI DPA-4200 (Protein Simple, Santa Clara, CA). See the method described in Telikepalli et al. 2014[26] for further details. Protein containing samples were diluted 100 fold prior to analysis and

this dilution factor was accounted to determine particle concentration. MFI's MVAS 1.3 software was used to collect particle imaging data, which was then analyzed by radar plots to assess the particle size and concentration distribution for the unstressed and stressed samples using in-house software (Middaugh Suite) as described in detail elsewhere[26-28]. Additional radar plot analysis was performed in which the particle concentrations in each size bin for the stressed samples were normalized relative to its "control," an unstressed sample that is similar in all other parameters. This normalization helps in visualizing and rank ordering the relative impact of a particular formulation parameter (e.g., stress) on the relative extent and size distribution of particle formation.

3.2.2.8 SDS-PAGE

Samples were mixed with 4X NuPAGE LDS sample buffer (Life Technologies, Carlsbad, CA) with and without, 50mM dithiothreitol (BioRad Laboratories, Hercules, CA) and incubated at 80^{o}C for 90 s. Approximately 10 μg of each sample was separated on a 3-8% Tris-Acetate gel using Tris-Acetate Buffer (Life Technologies, Carlsbad, CA). Hi-Mark Unstained Protein Standard (Life Technologies, Carlsbad, CA) was used as a molecular weight ladder. Protein bands were visualized by staining the gels with Bio-safe Coomassie Blue G250 stain (BioRad Laboratories, Hercules, CA).

3.2.2.9 FTIR

Unstressed lyophilized mAb, after being reconstituted with 5 mL deionized water over 10 s, was analyzed for overall secondary structure content as a function of temperature by Fourier transform infrared spectroscopy (FTIR) using instrumentation and methodology presented in Telikepalli et al. 2014[26].

3.2.2.10 FTIR Microscopy-15X Objective-Reflectance mode

The method from Telikepalli et al. 2014[26] was used to prepare and isolate protein particles from stressed samples, and then to perform overall secondary structure analysis of proteins within individual isolated particles using a Bruker Hyperion FTIR Microscope (Bruker Biosciences, Billerica, MA) with a 15X objective in reflectance mode to image individual particles on gold coated filters (Pall Corporation, Port Washington, NY).

3.3 RESULTS

3.3.1 Comparison of the physical stability of an IgG1 mAb formulation in the solid and liquid state during shaking

Samples of the IgG1 mAb were shaken (to simulate extreme shipping stress conditions) in the same formulation in the liquid or solid state for 5 min, 2h, 6h, and 15 h. Upon shaking, the solid state lyophilized cake increasingly turned into a finer, broken down powder after each of these shaking conditions. The physical stability of the mAb was assessed by a combination of analytical techniques including SE-HPLC, DLS, NTA, MFI, and turbidity. These techniques were used to determine differences in the aggregation behavior of protein from lyophilized and liquid shake-stressed samples across a wide aggregate size range of nanometers to hundreds of microns[29]. Aggregate formation in the size range of 1-1000 nm (detectable by a combination of SE-HPLC, DLS, and NTA) was minimal with similar results in both types of stressed samples (data not shown). For example, with SE-HPLC, approximately 99% monomer and 1% aggregate was noted at time zero with no change after shake-stress. Additionally, no changes in the total area of the SEC peaks were observed, suggesting no detectable change in the total protein

concentration by this method. DLS showed predominantly monomers (approximately 5 nm radius), with no changes in hydrodynamic size of protein in these samples after shake-stress. For NTA analysis, submicron sized particles in the range of 100-300 nm were observed in the samples with no changes noted in particle concentration and size distribution as a function of shake-stress (data not shown).

In contrast, differences in solution turbidity and micron size particle concentrations (detected by MFI) were observed between the liquid and lyophilized mAb samples after shaking as shown in Figure 3.1A and 3.1B, respectively. The turbidity of the liquid sample does not appear to change even after 15 h of shaking. In contrast, for the lyophilized sample, the turbidity of the solution (upon reconstitution) increases as a function of shaking time (Figure 3.1A). After stressing the liquid and lyophilized samples for 5 min up to 15 h, the liquid and lyophilized samples both showed a small increase in the total number of micron sized particles as measured by MFI (Figure 3.1B). Given the variability in the particle concentration determinations, it was concluded that both the liquid and lyophilized stressed samples generated similar levels of micron particles, with the 15 h time point showing a trend such that the lyophilized stressed sample may actually produce a greater number of micron sized particles than the liquid stressed samples.

The relative instability of the lyophilized protein was not anticipated. In fact, it was assumed that the protein in liquid state would be more susceptible to physical degradation by shaking, compared to the lyophilized state, even though the formulation contained polysorbate 80, a non-ionic surfactant which is known to stabilize against shaking-induced degradation in liquid formulations. To better understand these observations, a series of experiments were performed as described below to examine the effect of shaking the lyophilized formulation on

the physical stability of the IgG1 mAb (measured upon reconstitution) as determined by solution turbidity and formation of micron sized particles (MFI).

3.3.2 Characterization of particle formation in shake stressed lyophilized mAb samples

In an initial set of experiments, the effect of moisture content on the physical stability of the lyophilized mAb after shaking was assessed. Both "low" moisture (0.6%) and "high" moisture (6.8%) freeze-dried samples were prepared and then shaken for 24 h, turning both lyophilized samples into broken apart, finer powders, prior to reconstitution. No increases in size or in concentration of soluble aggregates or submicron particles were observed as a function of stress or moisture content by SE-HPLC and NTA, respectively (data not shown). In addition, DLS analysis did not show the presence of species other than the monomer across the four samples (data not shown). Twenty-four hours of shaking increased the solution turbidity and micron sized particle counts for both samples (Figure 3.2). The shake-stressed 6.8% moisture lyophilized mAb sample showed somewhat increased levels of turbidity and particle counts when compared to the 0.6% moisture samples.

The MFI total particle concentration data displayed in Figure 3.2 were further analyzed and displayed as a radar chart to better visualize the particle size distributions in the four samples as shown in Figure 3.3. Two different scales, shown on the right side of the figure, are used to analyze these MFI data. The "particle number" scale, used to display the actual MFI particle size and concentration data for samples at time 0 and after 24 hours of shaking, has the innermost circle representing the lowest particle concentration of ~0 particles/mL and the outermost corresponding to the highest concentration of ~2.5 x 10^6 particles /mL. The 2-5 μm size bin starts at the top and increases clockwise up to a 25-40 μm size bin. The "normalized" scale shows particle concentrations of the stressed sample relative to its unstressed control for each size bin.

Thus the scale increases from 0x (innermost circle) to 50x (outermost circle), where the latter indicates the number of particles in a size bin after shake-stressing are 50x greater than the number of particles in the same size bin at time 0 (no shaking).

For both the low and high moisture samples, the lyophilized mAb shows a low number of micron-sized particles upon reconstitution. After 24 h of shaking, the number of 2-5 μm particles increased (along with a small increase in 5-10 μm particles) in both moisture level samples. However, the 6.8% moisture samples formed more 2-5 μm particles than the 0.6% samples after shaking. This effect is more clearly reflected in the normalized radar plots where, it can be seen that the shake-stressed 6.8% moisture sample shows a larger relative increase in particles compared to its control than the shake-stressed 0.6% moisture sample. For example, there is an ~40 fold increase in the formation of 2-5 μm particles compared to the unstressed control for the 6.8% moisture sample, but only about a 10 fold increase of the 2-5 μm for the shaken 0.6% moisture sample. Similarly, a larger relative increase is observed for the formation of 5-10 μm sized particles, with an almost 35 fold increase for the higher moisture sample after shaking.

In addition to sizing and counting particles, the nature of the protein within the particles formed was examined by SDS-PAGE and FTIR analysis. In both the control and shake-stressed lyophilized samples at the two different moisture levels, non-reduced and reduced SDS-PAGE gels were compared. In the non-reduced gel, mostly IgG1 monomers with some fragments and dimers were observed. Upon reduction with dithiothreitol, however, dimers were reduced and only heavy and light chains of the IgG1 can be seen (see Figure 3.9). However, it appeared that these dimers were not forming as a function of the shake-stress and were present in all of the samples. Additionally, upon centrifugation of samples into supernatant and pellet components,

no notable differences were seen in both the non-reduced and reduced SDS-PAGE gels for the supernatant, pellet, or the non-centrifuged samples.

FTIR and FTIR Microscopy were used for the evaluation of overall secondary structure of the mAb in solution and of the mAb within the particles formed as a function of shaking stress in the lyophilized samples, respectively. Representative FTIR spectra, and corresponding wavenumber positions from triplicate measurements, are shown for two control samples and for the 0.6% and 6.8% moisture lyophilized mAb samples in Figures 3.4A and 3.4B, respectively. The solid black line corresponds to the FTIR second derivative spectrum of the Amide I band of the unstressed, control mAb in solution and shows spectra with minima around 1636 and 1690 cm^{-1}, which correspond to the intramolecular beta sheets that are in the main secondary structure of antibodies. To determine the extent of secondary structure loss that is possible with this mAb, the mAb solution was extensively heated and the resulting isolated particles were analyzed by FTIR Microscopy. The second derivative spectra, depicted as blue dotted graphs, possess minima at 1622 cm^{-1} and 1619 cm^{-1} and 1692 cm^{-1} and 1693 cm^{-1} indicating loss of intra-molecular beta sheets and formation of inter-molecular beta sheets (i.e., aggregation). The red dotted lines are the second derivative spectra of the isolated protein particles obtained from each of the two shake-stressed samples by FTIR Microscopy (after reconstitution of the low and high moisture lyophilized mAb samples followed by filtration and capture of particles on a gold filter). Compared to the two control samples (unstressed sample in solution and heat control), the IgG1 in the protein particle from the T=24 h shake-stressed sample has similar overall secondary structure to the unstressed control. However, these isolated protein particles may have a slightly altered overall secondary structure content compared to the protein in the unstressed sample since their spectra show a small shift in the average minima around 1633 cm^{-1} and 1691

cm^{-1}. Importantly, the particles obtained from the 0.6 and 6.8% moisture samples showed similar levels of change in protein secondary structure indicating that for this IgG1 mAb, moisture content in conjunction with shake stress do not seem to largely impact the secondary structure of the protein within the particles.

3.3.3 Characterization of particle formation in shake stressed lyophilized mAb samples as function of reconstitution medium type and addition time.

For both the low and high moisture containing lyophilized mAb samples, the control (unstressed) vials fully reconstituted in about 30 s, while the shake-stressed vials took ~ 1.5 min. This was similar regardless of the medium type or medium addition rate. There was no difference in reconstitution time as a result of moisture content, so the effect of medium type and addition rate were further examined with the low moisture lyophilized sample. The 0.6% moisture lyophilized sample was shaken for 24 h and reconstituted with 5 mL of different mediums at two different rates and then monitored for their effects on physical stability of the mAb by measuring solution turbidity and the concentration of micron-sized particles. As shown in Figures 3.5A and 3.5B, the shake stressed lyophilized samples were more turbid and contained higher concentrations of micron-sized particles than the non-shaken samples upon reconstitution. Reconstitution with water consistently led to higher solution turbidity and higher micron-sized particle concentrations than reconstitution with the other diluents. In addition, the role of medium addition rate was examined and no effects were observed for most of the conditions with two exceptions: (1) for the 24 h shake-stressed lyophilized samples reconstituted at a slow rate with 150 mM NaCl + 0.05% polysorbate 80, higher turbidity and increased particle counts were observed compared to the fast addition of this medium, and (2) while the turbidity did not

change, reconstituting the shake-stressed lyophilized sample slowly with 150 mM NaCl solution produced more micron-sized particles than the same sample reconstituted at the fast rate.

Radar plot analysis of the MFI particle data showed some distinct relative changes in particle size distribution depending on the medium selection and the rate of addition (Figures 3.6 for water as the medium and Figure 3.7 for the other diluents; note the scale differences in the two figures). Regardless of medium type, predominantly 2-5 μm particles are formed upon shake-stress lyophilized samples upon both the slow and fast medium addition. When water was used as the reconstitution medium (Figure 3.6), there was almost a 15 fold increase in the formation of 5-10 μm particles upon slow reconstitution compared to the unstressed sample similarly reconstituted. In contrast, rapid addition of water resulted in a smaller relative increase in particles formed in this same size range. For the other medium types, the addition rate was found to have some effect on the micron particle concentration as shown in Figure 3.7. Slow reconstitution of the shake-stressed lyophilized samples with 150 mM NaCl and 150 mM NaCl+0.05% polysorbate 80 produced a larger relative increase (as seen by the normalized plot) in the formation of micron particles across the size bins. Such a relative increase in particle formation was not observed upon more rapid addition of these reconstitution media.

3.3.4 Effect of shake stressing lyophilized mAb samples on subsequent storage stability.

A three month stability study was performed using the lyophilized mAb samples (0.6% moisture) after exposure to different amounts of shake stress. Intact lyophilized cakes (unstressed controls), slightly broken cakes (shaken for 2.5 min) and completely broken lyophilized cakes (shaken for 24 h) were stored at 4, 40, and 55^{o}C for 3 months (at ambient humidity) in stoppered glass vials. Representative pictures of the physical integrity of these lyophilized cakes corresponding to the varying levels of shake stress are shown in Figure 3.8A.

Upon fast addition with 5 mL deionized water, samples were analyzed by a combination of NTA, MFI, and turbidity. NTA showed no changes in aggregation due to stress (data not shown). In contrast, solution turbidity (Figure 3.8A) and micron-sized particles measured by MFI (Figure 3.8B) did reveal some stability differences as a function of shake stress and storage temperature (in addition, at the higher temperatures and longer time periods, slight yellow color changes were noted in all of the samples upon reconstitution; data not shown). As shown in Figure 3.8A, all samples showed an increase in turbidity with increasing storage temperature (4°C < 40°C < 55°C). If samples stored for identical time periods are considered, turbidity did not significantly increase in the intact and 2.5 min shaken samples. The samples stored at 55°C were the most turbid, followed by the samples stored at 40°C (4°C < 40°C < 55°C). Figures 3.8C and 3.8D show normalized turbidity and normalized micron particle concentrations obtained by taking a ratio of turbidity (or micron particle concentration) of the stressed sample to its control (T=0) for a given shaking duration. This shows the change in turbidity or number of micron particles in a sample relative to its unstressed control. At 40°C, after three months of storage, the relative change in turbidity and total subvisible particle concentration for all shaken samples is approximately 1.5x and 2-3x, respectively. At 55°C after three months, the relative change for the shaken samples is about 3.5-5x and 7-15x for turbidity and total micron particle concentration, respectively.

In summary, Figures 3.8A and 3.8B show increasing turbidity and particle counts with increasing shaking duration, storage time, and temperature. However, the T=0 samples themselves show an increase in turbidity and micron sized particle counts with increasing shaking duration (T=0 Intact cake < T=0 2.5 min shaking < T=0 24 h shaking). Higher temperatures and longer storage show an increase in turbidity and particle counts relative to the

control (4°C < 40°C < 55°C and T=0 ~ T=1 month < T=3 months) within each shaking time. When different shaking times are compared, in terms of relative changes versus time zero (Figures 3.8C and 3.8D), however, both relative turbidity and relative micron particle concentration changes stay constant or even decrease, especially for the samples stored at 55°C for three months as the cake structure is increasingly collapsed.

3.4 DISCUSSIONS

The focus of this work was to better characterize how shaking of a freeze-dried IgG1 mAb formulation can affect protein stability upon reconstitution. We first examined the lyophilized IgG1 mAb control (no shake-stress), which showed minimal levels of physical instability after reconstitution. These initial results indicated the formulation composition and lyophilization cycle resulted in a stable protein preparation. While there is a plethora of literature on how to effectively formulate and stabilize protein drugs during the lyophilization process and subsequent long term storage,[1,5,17,24,30] the effect of subsequent mechanical stresses applied to the lyophilized dosage form on physical stability and aggregation of mAb, which could potentially occur during shipping and handling, has not been examined to the same extent.

3.4.1 Physical stability of shake-stressed mAb in lyophilized state

In this work, mechanical shaking-stress was applied to the liquid and lyophilized state of an IgG1 mAb formulation, and a variety of analytical techniques were used to assess the physical stability of the mAb. These results highlight the need to examine protein aggregation across a wide size range since no one analytical approach covers the different size ranges of protein aggregates and particles that may form[26,29,31]. SEC and DLS, two very commonly used techniques to monitor soluble, nanometer sized aggregates, along with NTA, to detect submicron

sized particles, showed no differences in particle levels between control (unstressed) and shake-stressed samples across the various experiments. Interestingly, although the shaking stress had minimal effects on the formation of soluble aggregates and smaller submicron sized particles, physical instability was detected by turbidity measurements and by formation of larger micron size particles (as shown by MFI). Thus, shake-stressing the lyophilized mAb, followed by reconstitution, led to increased levels of protein particles in the subvisible size range (~2-100 microns) but not in the smaller, submicron size ranges. These results highlight the need to examine protein aggregation across a wide size range since no one analytical approach covers the different size ranges of protein aggregates and particles that may form[26,29,31]

The shake-stress had minor effects on the conformation and composition of the protein contained within these particles as evidenced by SDS-PAGE and FTIR analysis. Upon shake stressing freeze-dried cakes, the resulting protein particles, formed in two different moisture level samples, showed similar levels of non-native disulfide crosslinks (SDS-PAGE) and the presence of slightly altered overall secondary structure content compared to the native protein (FTIR analysis). In contrast, the role of non-native disulfide bond formation in the generation of aggregates appears less influential than has been observed previously with other lyophilized mAbs[17]. A recent study performed in our laboratory studied the aggregation behavior of a mAb undergoing shaking stress. While this was a different IgG1 mAb, in a liquid solution and in a different formulation, shake stress also led to formation of particles with only minor changes in overall conformational integrity of the protein within the particles as seen by SDS-PAGE, FTIR and by ANS fluorescence spectroscopy[26].

The effect of the residual moisture content of the lyophilized cake on the physical stability of the mAb after shake-stress was also evaluated. There is an abundance of literature

describing the effects of moisture content on the stability of lyophilized protein therapeutics[19-22] Improved protein stability is often observed at lower moisture contents of a lyophilized cake, with values not exceeding 2.0% [6], However, exceptions have been noted. For example, when the stability of a lyophilized humanized mAb produced with varying moisture contents and stored at elevated temperatures up to a year was analyzed,[22] no cake collapse or changes in protein secondary structure were observed[22] but the intermediate moisture level samples were more resistant to aggregation. The relationship between moisture content and protein aggregation potential is complex and may be very dependent on the protein itself, formulation composition and freeze-drying conditions[1,5-7,22]. In our study with an IgG1 mAb, the physical stability of the 6.8% moisture sample was not drastically different than the 0.6% moisture sample during lyophilization or upon exposure to subsequent mechanical stress.

3.4.2 Effect of reconstitution on shake-stressed degradation of lyophilized mAb

The choice of medium used to reconstitute the lyophilized IgG mAb was an important factor in this study[6,32]. Using water as the diluent for both the unstressed and shake-stressed lyophilized mAb samples resulted in higher solution turbidity, and in an increased concentration of micron sized particles, compared to the use of other diluents. The addition of sodium chloride solutions partially inhibited the formation of micron particles in our studies probably because the sodium chloride reduces protein-protein colloidal interactions.[6 33] Previous studies have shown the importance of ionic strength in reconstitution solutions where either increased or decreased ionic strength of the reconstitution medium inhibited protein aggregation, highlighting the protein and formulation specific nature of these observations. [32-36] However, sodium chloride containing diluents result in reconstituted mAb solutions with higher solution osmolality, which might be a concern depending on the route of administration (e.g., subcutaneous injection into

the patient). The presence of polysorbate 80 in the reconstitution buffer perhaps had a small stabilizing effect on the formation of subvisible particles upon reconstitution. Numerous studies have shown that polysorbate can decrease aggregation when used in the reconstitution medium.[33,34,37-39]. It has been suggested that surfactants may increase wettability of powders leading to increased dissolution rate of lyophilized powders, inhibit surface induced denaturation during reconstitution, or stabilize the native state of the protein by increasing the free energy of unfolding. [34,37,39] Stabilizing compounds, such as polysorbate 80 or NaCl, in the diluent may prevent or reduce protein-protein interactions, and/or the physical dilution imparted by their addition can lead to separation of protein molecules and hinder aggregation[7].

Upon reconstitution, the type of diluent and the rate of diluent addition can affect not only protein stability [6,36], but also reconstitution times. The rate of diluent addition on the physical stability of the reconstituted, lyophilized IgG1 mAb in this study was, in general, not an important factor. However, the time required for reconstitution was longer for the shake-stressed lyophilized samples than the unstressed vials (approx. 0.5 vs. 1.5 minutes), regardless of the rate of addition or the type of diluent used. Since the physical state of the lyophilized mAb impacts dissolution time upon reconstitution, it is possible this results in differences in local protein or excipient concentrations and subsequently to the observed differences in subvisible particle formation. The higher surface area and porosity present in the lyophilized cake, compared to the finer powder formed after shaking, may allow it to dissolve faster than the powder[40]. However, disruption of lyophilized cake structure may not be the only destabilizing mechanism. Vibrational forces, or local heating effects generated from shaking itself, can potentially increase the contact area of powder particles allowing increased interactions between them[41] leading to a cohesive powder that is "sticky."[42]

These differences in reconstitution time did not change, however, when the samples were reconstituted at different rates and with different diluents. While this lyophilized protein formulation had a relatively short reconstitution time, for other lyophilized protein samples in which the reconstitution time is longer and may be problematic during clinical administration, techniques mentioned by Cao et al[15] could be beneficial. For example, reconstituting under vacuum, adding wetting agents, and/or using low diluent volumes were observed to be methods that can decrease reconstitution times in a high concentration lyophilized formulation of a Fc-fusion protein[15]. Additionally, three reconstitution procedures were described, in which the reconstitution medium is added and the vial is gently swirled for different periods of time, resulting in different reconstitution times[15]. In addition to reconstitution time, such reconstitution procedures could be evaluated in the future to assess their ability to minimize subvisible particle formation during reconstitution of shake stressed lyophilized protein powders.

3.4.3 Storage of shake-stressed lyophilized mAb samples

The effects of the extent of shaking stress on subsequent storage stability of the freeze dried IgG1 formulation were also analyzed in this work. Lyophilized mAb samples were prepared as follows: (1) unstressed, physically intact cakes, (2) brief shaking (2.5 min) resulting in some cake breakage, and (3) extensive shaking (24 h) resulting in the cake being broken down to a powder. These samples were stored at different temperatures over a three month period, and at each time point, were reconstituted rapidly with 5 mL of water. Increasing shaking stress on the freeze dried cake showed some small differences with increased levels in turbidity and subvisible particles. Solution turbidity and subvisible particle concentration increased with increasing storage (T=0 < T=1 month <T=3months), especially for the samples stored at 40°C and 55°C. Similar to Schersch et al[19-21], we also noticed a color change during storage of the

lyophilized protein at higher temperatures in this formulation, which they reasonably attributed to the well-known non-enzymatic browning (Malliard-type) reaction between reducing end sugars (potentially due to degraded sucrose) and lysine residues in the protein. The turbidity levels and subvisible particle concentrations are highest for the 24h shaken samples compared to the intact and 2.5 min shaken samples (Intact ~ 2.5 min shaking < 24 h shaking). Even though Figures 3.8A and 3.8B show increasing turbidity and particle counts with increasing shaking duration, storage time, and temperature, comparing samples to appropriate controls provides fuller understanding of the importance of shaking stress in inducing turbidity and micron particle formation. Figure 3.8C and Figure 3.8D compare a particular sample with its relevant control (T=0). Within each shaking time, higher temperatures and longer storage show increase in turbidity and particle counts relative to the control (4°C < 40°C < 55°C and T=0 ~ T=1 month < T=3 months). When different shake times are compared, however, both turbidity and micron particle counts stay relatively constant or decrease, especially for the samples stored at 55°C for three months. This is largely because the controls themselves (T=0) increase in both turbidity and particle counts with increasing shaking duration so the instability associated with storage temperature and storage duration appear less profound.

In comparison, Schersch et al. have examined the effect of cake collapse (due to a variety of causes) during freeze-drying and subsequent storage at elevated temperatures on the stability of a different IgG1 mAb.[19-21] For example, when lyophilized cakes were collapsed by using different amounts of excipients or by using different freeze-drying protocols, the stability of protein in the collapsed and non-collapsed cakes were not different from one another. In addition, conformational integrity of the IgG1, as measured by FTIR analysis of the overall secondary structure, was also not affected by cake collapse.[19] Additionally, when the effect of

cake collapse on long-term storage at various temperatures ranging from 2-50°C up to 6 months was analyzed, protein stability was retained in the collapsed and non-collapsed cakes after storage.[20] In addition, the stability of the freeze-dried samples that were collapsed during freeze-drying vs. samples collapsed only during subsequent storage at 40 and 50°C for 3 months were compared to determine if the method of collapse affected protein stability. In this case, the stability of the proteins in the collapsed lyophilized cakes (collapse due to freeze-drying) was better than the stability of protein in the storage-collapsed samples. Overall, the authors concluded that the collapse (freeze-dried) samples appeared to be more stable than the collapsed (storage) samples.[21]

The method of cake collapse could be another important parameter to consider as well in terms of effects on storage stability. In this work, we mechanically stressed the samples to alter the cake integrity to different extents and then stored the cakes (with varying levels of physical collapse) at different temperatures. In comparison, Schersch et al. have examined in detail the effect of different methods of cake collapse on the stability of a different IgG mAb.[19-21] The stability of the samples collapsed during freeze-drying compared to samples during subsequent storage at elevated temperatures showed that the stability of the protein in the freeze-drying collapsed cake was better than the protein in the storage-collapsed samples. Overall, the authors concluded that the collapse (freeze-dried) samples appeared to be more stable than the collapsed (storage) samples[21].

3.5 CONCLUSIONS

This case study highlights that post-lyophilization mechanical stresses, potentially encountered during shipping and transportation excursions, can result in physical instability of a

lyophilized protein upon reconstitution. For this particular IgG1 mAb formulation, a liquid dosage form (5 mL of a 30 mg/mL protein solution in a 20 mL stoppered glass vial) showed instability due to shaking stress, despite the presence of stabilizers including polysorbate 80. The common sense approach of lyophilization did not successfully address the issue since the lyophilized dosage form of the same formulation was also shake-sensitive. The increase in subvisible particle formation seen with the shake-stressed lyophilized IgG1 mAb upon reconstitution correlated with the formation of a finer powder and increased dissolution times, while no major differences in the structural integrity of the protein within the particles was noted. Thus, local differences in protein and excipient concentrations, upon the wetting and dissolution of the shake-stressed vs. control lyophilized cakes, likely contribute to these observations.

It is acknowledged that the level of shake stress that the cakes were exposed to in this study was relatively high, but this was a useful means of rapidly characterizing various conditions with respect to product quality impact (e.g., cake moisture, reconstitution rate, medium type, etc). The level of mechanical stress that a product will be exposed to during typical shipping and handling can be variable, and it is easier to interpret their effects by comparing to stressed, worst-case study designs. In addition, within the general ASTM shipping guidance documents[25], which are not specific for pharmaceutical products, the level of stress these documents suggest may be relatively high based on the schedule rating a user chooses to analyze.

The observations highlight the importance of considering shake sensitivity of lyophilized cakes in terms of protein stability as part of formulation development activities including the formulation composition, lyophilization process and reconstitution medium selection. Potential degradation is expected to be manageable by implementing an appropriate packaging and

shipping configuration that will minimize or prevent extensive cake breakage. The use of orthogonal subvisible particle counting and sizing techniques such as light obscuration (HIAC) and/or coulter counters are suggested for future work for comparison to the MFI analytical results. Additional work is also required to further elucidate the nature of the physical degradation pathway(s) leading to protein particle formation during reconstitution of shake-stressed lyophilized mAb preparations, as well as to evaluate how this physical instability may vary with different IgG mAbs, other proteins and in the presence of different excipients and stabilizers.

3.6 FIGURES

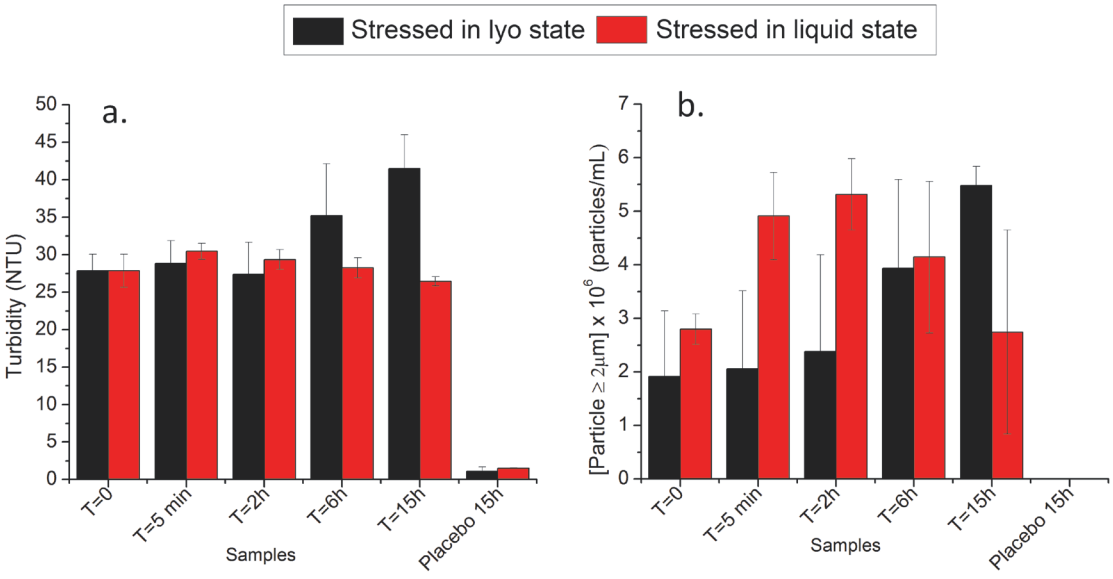

Figure 3.1. Physical instability of an IgG1 mAb formulation after shaking in the solid (freeze-dried cake) or liquid state for 5 min, 2h, 6h, and 15h. Samples were monitored by (A) solution turbidity and (B) total concentration of subvisible particles (≥2 µm as measured by MFI). Lyophilized samples were reconstituted prior to analysis. Each graph represents the average of three separate experiments (n=3) and error bars represent one standard deviation. Placebo samples were measured after 15 h of shaking showed negligible turbidity and concentration of micron sized particles compared to the protein containing samples.

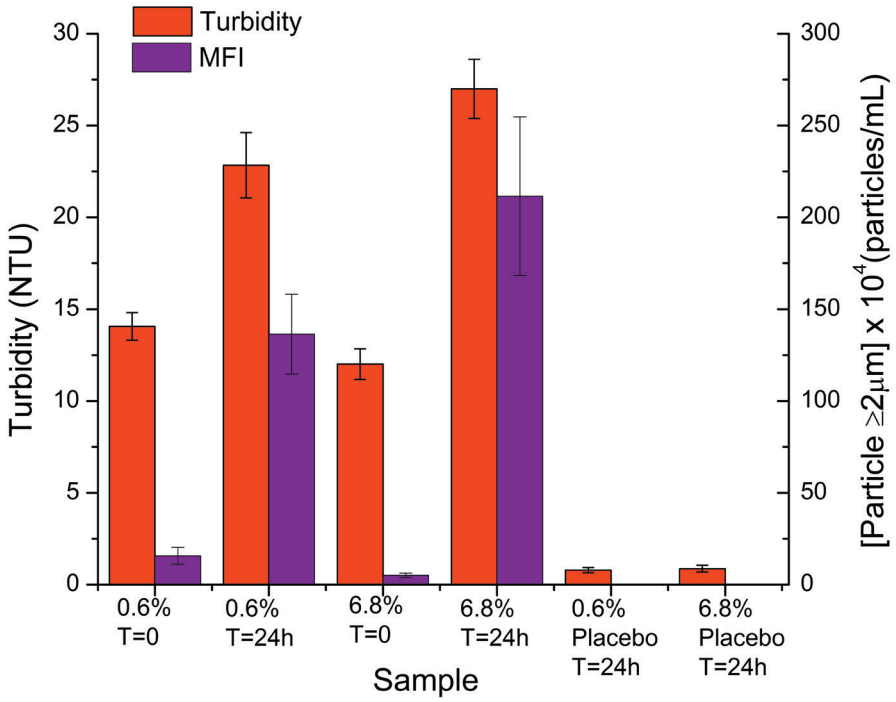

Figure 3.2. Physical instability of a lyophilized IgG1 mAb samples prepared with 0.6% and 6.8% moisture content and shake-stressed for 24 h in the solid state. Samples were reconstituted with water and monitored for solution turbidity (left Y- axis) and subvisible particles by MFI (right Y-axis). Placebo samples were measured after 24 h of shaking and showed negligible turbidity and concentration of micron sized particles compared to the protein containing samples. The graph represents the average of three separate experiments (n=3) and error bars represent one standard deviation.

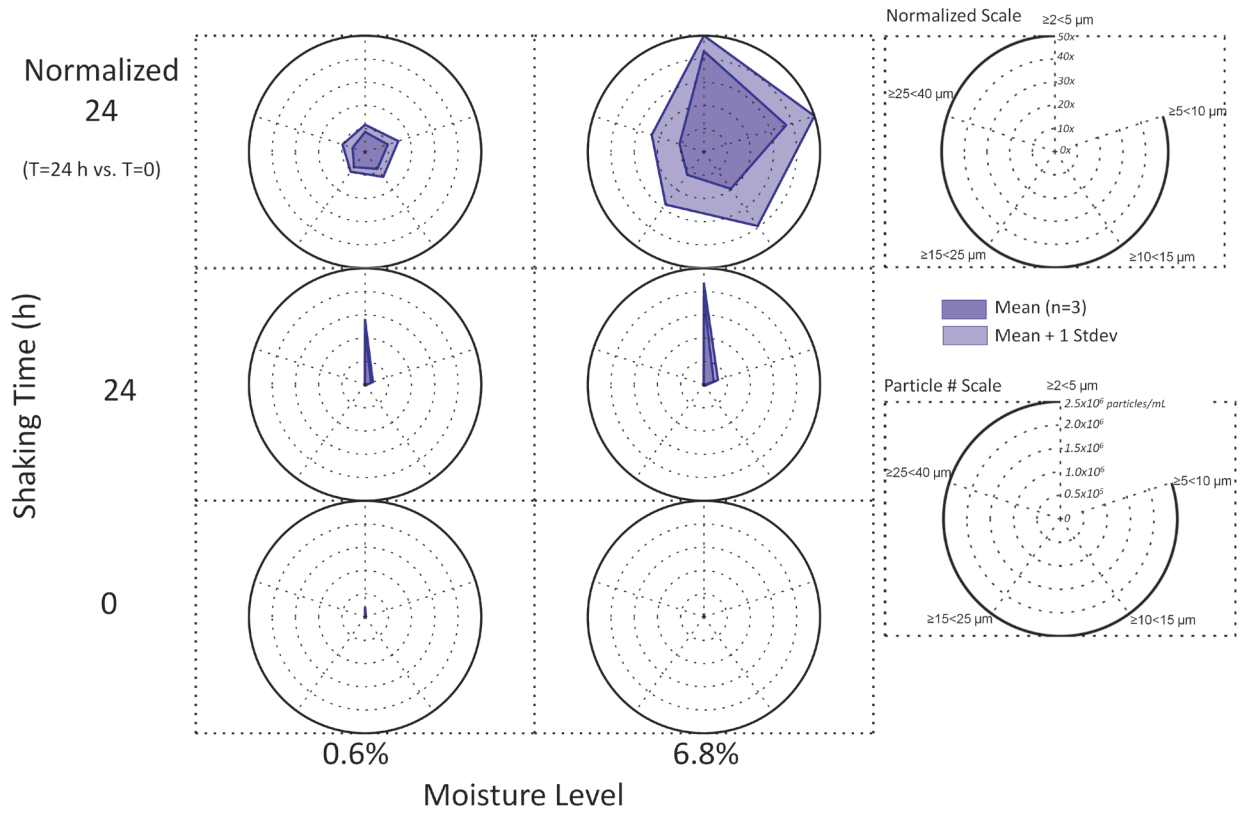

Figure 3.3. Radar plot analysis of MFI particle concentration and size distribution results before and after shake-stressing lyophilized mAb samples. IgG1 mAb lyophilized samples were prepared with 0.6% and 6.8% moisture content, shake-stressed for 24 h, reconstituted with water, and subvisible particle levels were measured by MFI (See Figure 3.2). The "particle # scale" radar plot shows actual particle concentration values in different size ranges and the "normalized scale" radar plot shows relative change in subvisible particle concentration and size distribution of shake stressed samples compared to the corresponding T=0 sample (unstressed control).

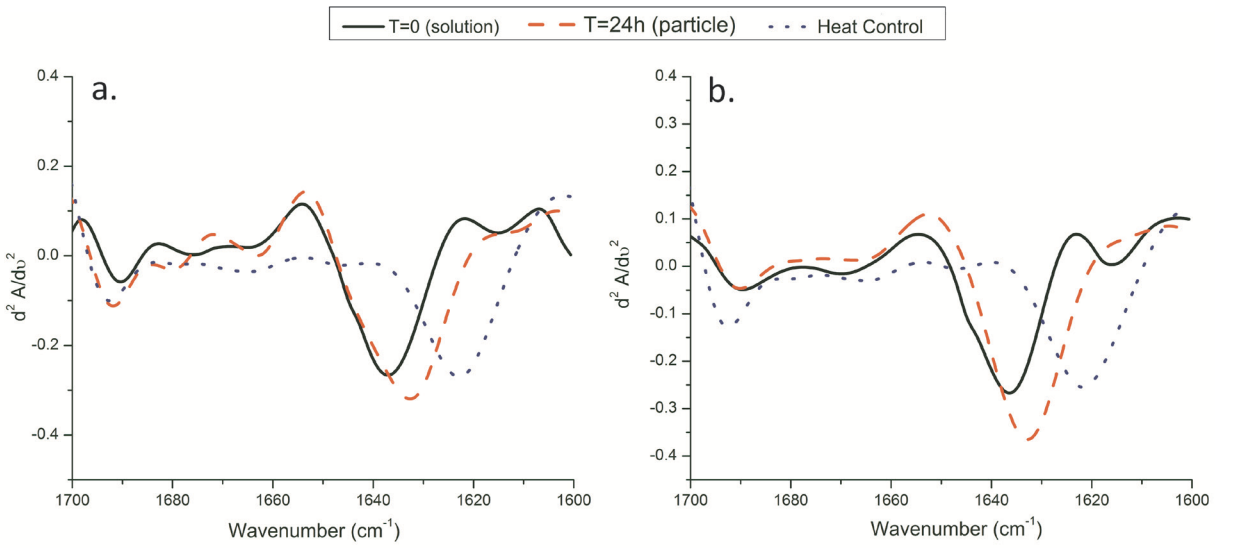

	Sample	Wavenumber 1 (cm^{-1})	Wavenumber 2 (cm^{-1})
	T=0 (solution)	1636.8 ± 0.4	1690.1 ± 0.3
0.6%	Heat Control	1622.1 ± 1.1	1692.4 ± 0.3
	T=24h (particle)	1633.2 ± 0.8	1691.7 ± 1.8

	Sample	Wavenumber 1 (cm^{-1})	Wavenumber 2 (cm^{-1})
	T=0 (solution)	1636.5 ± 0.7	1690.1 ± 0.1
6.8%	Heat Control	1619.3 ± 3.9	1692.9 ± 0.5
	T=24h (particle)	1633.4 ± 0.9	1691.1 ± 1.2

Figure 3.4. Representative second-derivative FTIR spectra of protein particles isolated from lyophilized IgG1 mAb samples containing 0.6% and 6.8% moisture levels after shake-stress. Samples include: native, unstressed protein in solution (T=0); protein particles isolated from shake stressed lyophilized mAb (a) 0.6% and b) 6.8% moisture) after reconstitution (T=24h); and particles isolated from mAb solution heated at 80°C for 20 min (heat control). The characteristic peaks in the Amide I region indicative of intra and inter molecular beta sheet secondary structure are shown in the table. Values in table represent the average of three separate experiments (n=3) along with one standard deviation.

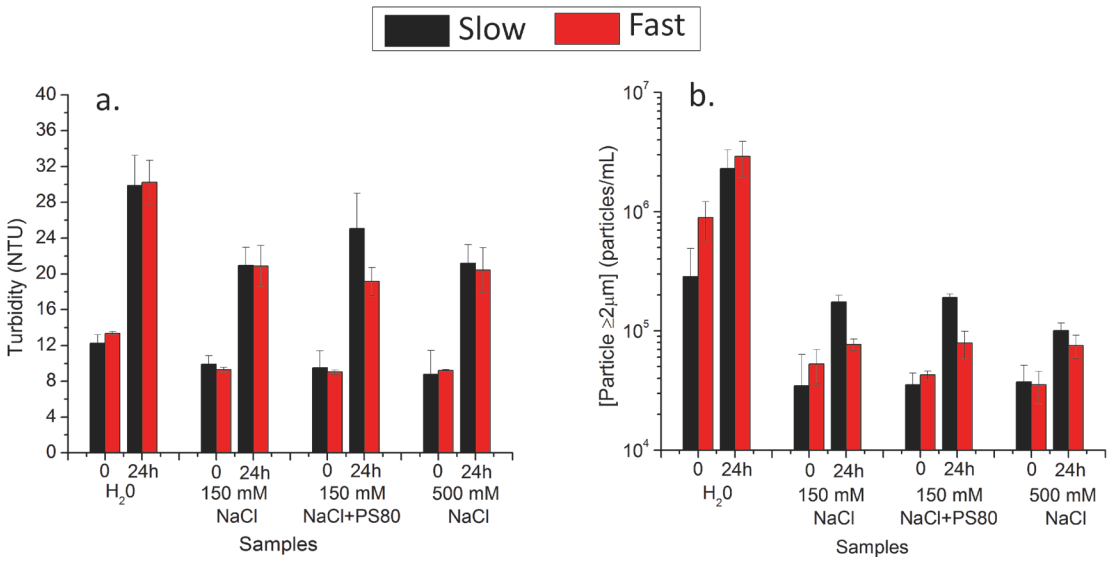

Figure 3.5. Effect of reconstitution medium and addition rate on the physical instability of a lyophilized IgG1 mAb samples reconstituted after shaking. Lyophilized IgG1 mAb samples were shake-stressed for 24 h and reconstituted slow (5 mL over 2.5 minutes) or fast (5 mL over 10 seconds) conditions with the following mediums: (1) deionized H_20, (2) 150 mM NaCl, (3) 150 mM NaCl containing 0.05% polysorbate 80, and (4) 500 mM NaCl. The resulting (A) solution turbidity and (B) total concentration of subvisible particles (≥2 μm as measured by MFI) values are shown. Each graph represents the average of three separate experiments (n=3) and error bars represent one standard deviation.

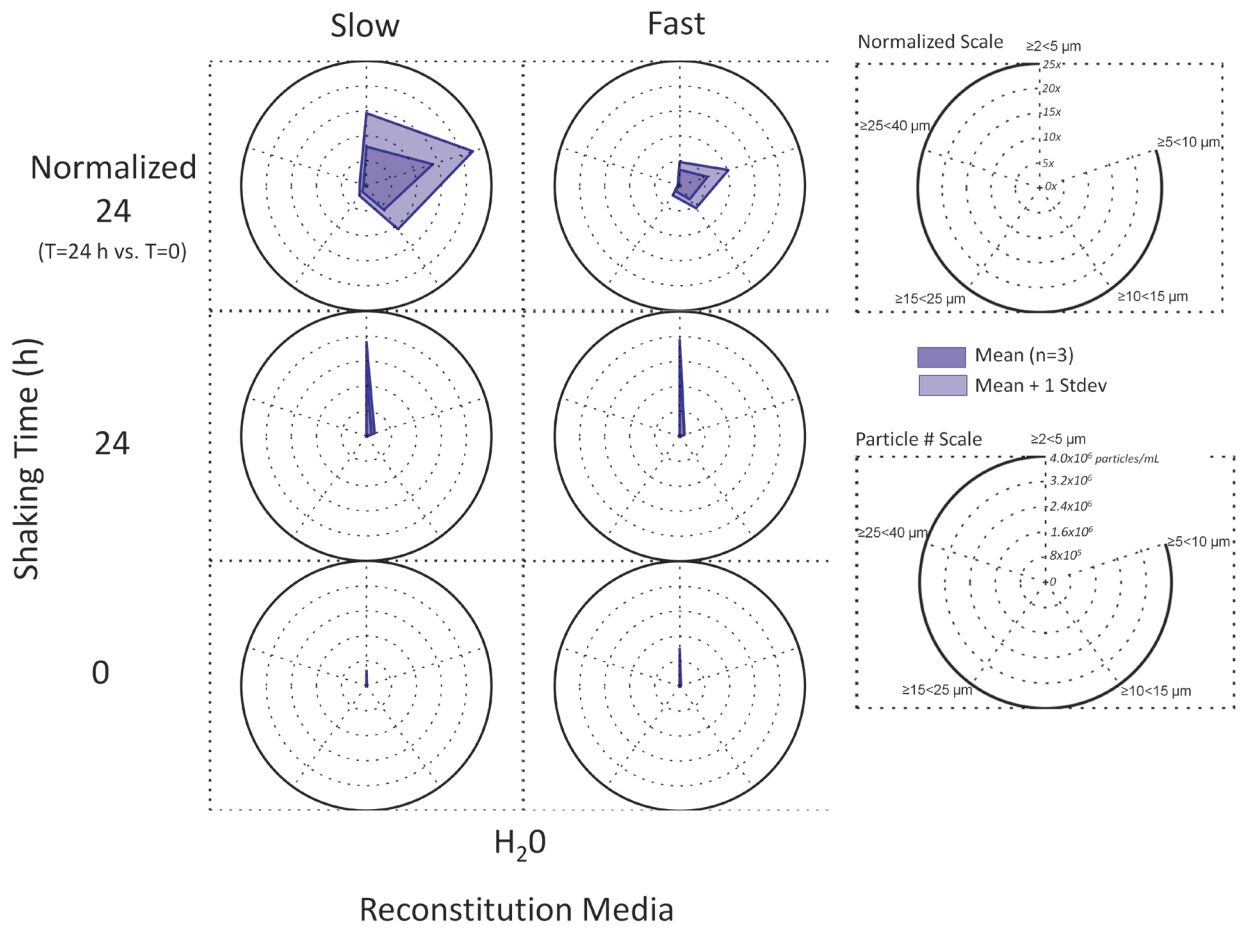

Figure 3.6. Radar plot analysis of MFI particle concentration and size distribution results as a function of the rate of reconstitution of shaking-stressed lyophilized mAb samples. Lyophilized IgG1 mAb samples (without shaking, T=0) and 24 h of shaking (T=24) were reconstituted with deionized H_20 slowly (5 mL over 2.5 min) or rapidly (5 mL over 10 s) are shown. The "particle # scale" radar plot shows actual particle concentration values in different size ranges and the "normalized scale" radar plot shows relative change in subvisible particle concentration and size distribution of shake stressed samples compared to the corresponding T=0 sample (unstressed control).

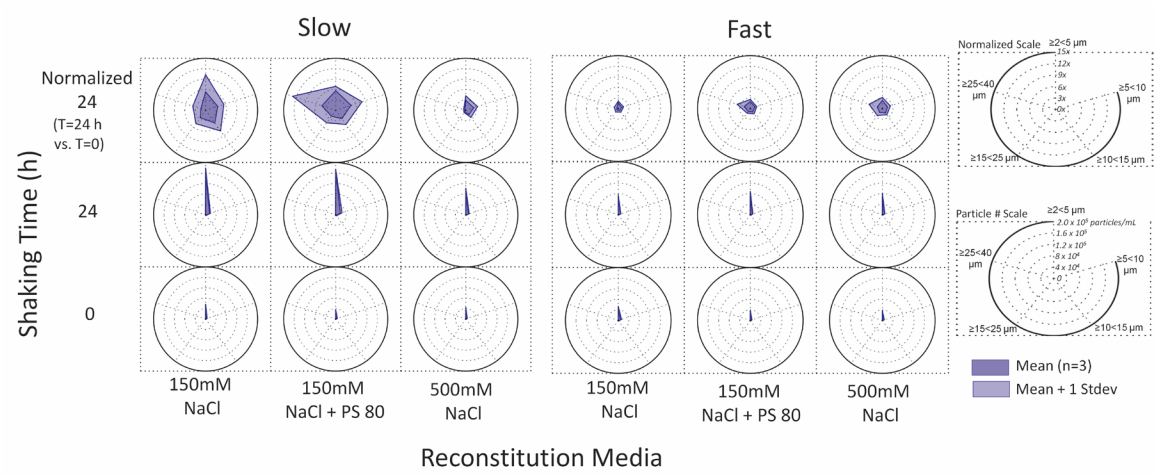

Figure 3.7. Radar plot analysis of MFI particle concentration and size distribution results as a function of diluent type used to reconstitute shake-stressed lyophilized mAb samples. Lyophilized IgG1 mAb samples (without shaking, T=0) and 24 hours of shaking (T=24) were reconstituted with various mediums under slow (5 mL over 2.5 min) or fast (5 mL over 10 s) conditions as indicated in the figure. Reconstitution diluents included: (1) 5 mL of 150 mM NaCl, (2) 5 mL of 150mM NaCl + 0.05% Polysorbate 80, and (3) 5 mL 500 mM NaCl. The "particle # scale" radar plot shows actual particle concentration values in different size ranges and the "normalized scale" radar plot shows relative change in subvisible particle concentration and size distribution of shake stressed samples compared to the corresponding T=0 sample (unstressed control).

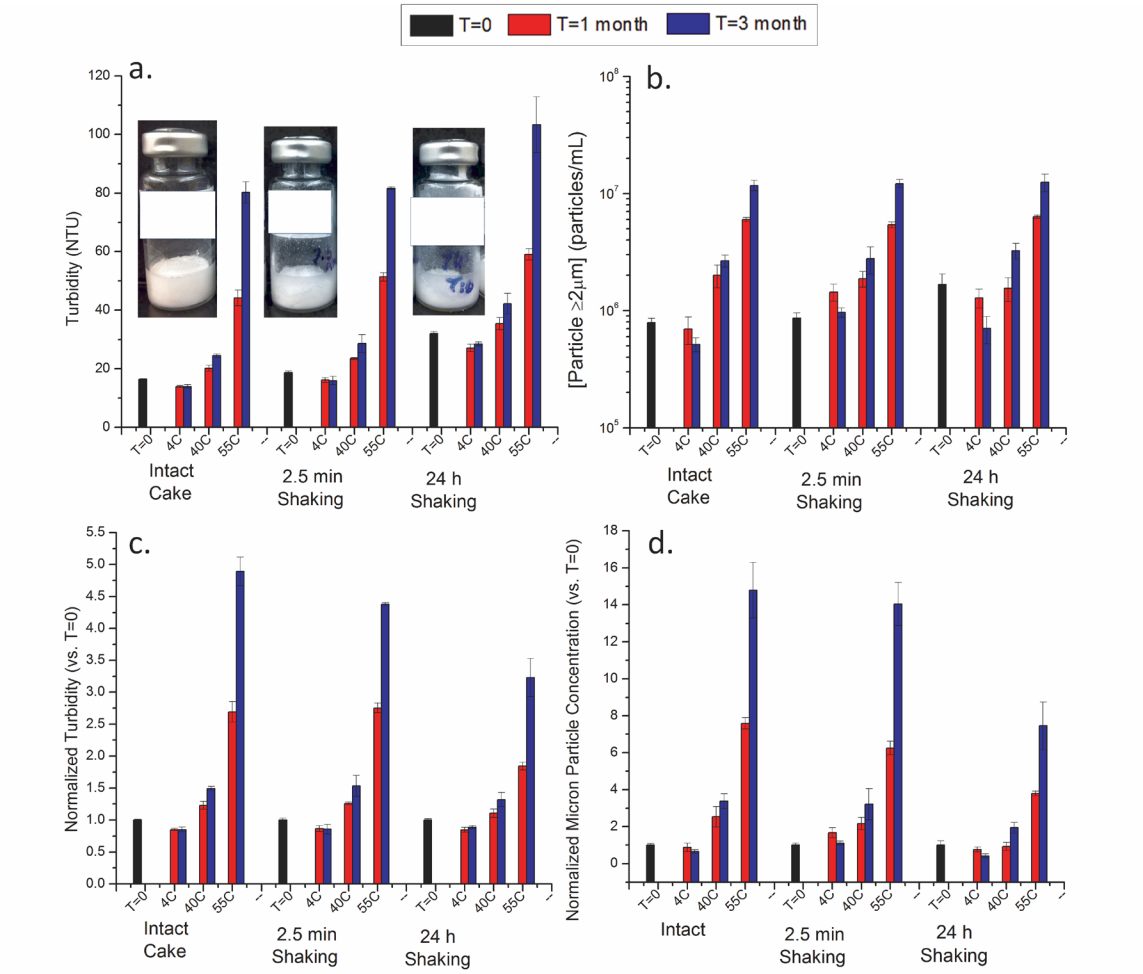

Figure 3.8. Storage stability of lyophilized IgG1 mAb samples as a function of cake integrity. Lyophilized samples included unstressed control (Intact cake), shake stressed for 2.5 min, and shake stressed for 24 hrs. Representative pictures of intact cake, 2.5 min shaking, and 24h shake stressed cakes at time zero are shown. Samples were then stored for up to 3 months at three different temperatures (4, 40, 55°C), reconstituted and monitored for (A) solution turbidity and (B) total concentration of subvisible particles (≥2 μm as measured by MFI). Stressed samples, which have been shaken for a certain amount of time and stored at different temperatures, were compared to controls (T=0, but with shaking) and resulting C) normalized turbidity or D) normalized subvisible particle concentrations are shown. The y-axis values for both (C) and (D) were obtained by dividing the turbidity values (or micron particle concentration) of a stored

sample by its relevant control at time zero experiencing similar duration of shaking. Each graph represents the average of three separate experiments (n=3) and error bars represent one standard deviation. Placebo samples were measured after 3 months storage at 55°C h and showed low turbidity (~1 NTU) and a relatively low number of micron sized particles (~12,000 particles/mL).

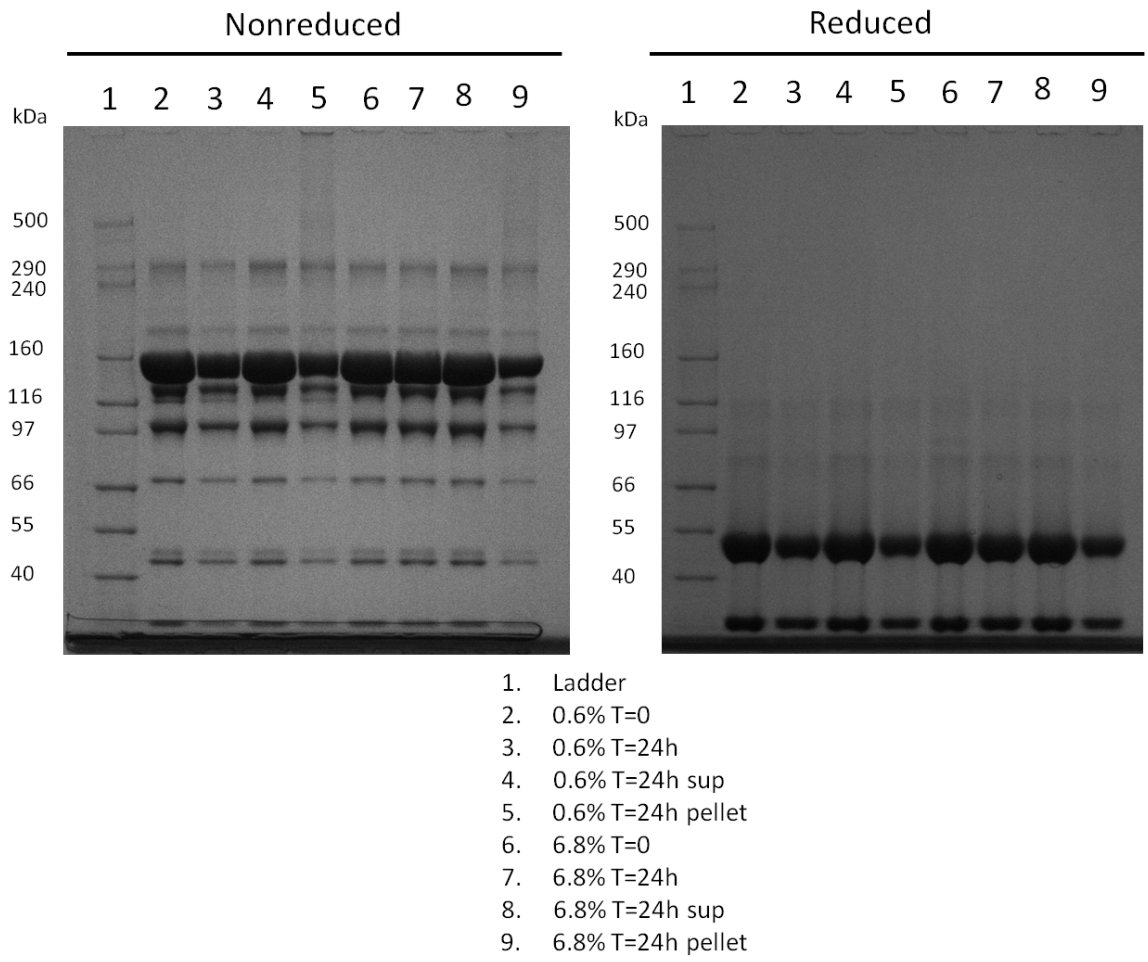

Figure 3.9. Nonreduced and reduced SDS-PAGE gels of lyophilized shake-stressed (T=24 h) and unstressed (T=0) IgG1 mAb samples prepared with 0.6% and 6.8% moisture levels are shown. Samples were also centrifuged to separate supernatant from pellet and run on SDS-PAGE and stained as described in the *Methods* section. See text for description of results.

3.7 REFERENCES

1. Carpenter JF, Chang BS, Garzon-Rodriguez W, Randolph TW 2002. Rational design of stable lyophilized protein formulations: theory and practice. Pharm Biotechnol 13:109-133.
2. Matejtschuk P 2007. Lyophilization of proteins. Methods Mol Biol 368:59-72.
3. Tang X, Pikal MJ 2004. Design of freeze-drying processes for pharmaceuticals: practical advice. Pharm Res 21(2):191-200.
4. Chang LL, Pikal MJ 2009. Mechanisms of protein stabilization in the solid state. J Pharm Sci 98(9):2886-2908.
5. Carpenter JF, Pikal MJ, Chang BS, Randolph TW 1997. Rational design of stable lyophilized protein formulations: some practical advice. Pharm Res 14(8):969-975.
6. Wang W 2000. Lyophilization and development of solid protein pharmaceuticals. Int J Pharm 203(1-2):1-60.
7. Wang W, Roberts CJ, Eds. 2010. Aggregation of therapeutic proteins. Hoboken, New Jersey: Wiley.
8. Kasper J, Winter G, Friess W 2013. Recent advances and further challenges in lyophilization. Eur J Pharm Biopharm 85:162-169.
9. Awotwe-Otoo D, Agarabi C, Wu GK, Casey E, Read E, Lute S, Brorson KA, Khan MA, Shah RB 2012. Quality by design: impact of formulation variables and their interactions on quality attributes of a lyophilized monoclonal antibody. Int J Pharm 438(1-2):167-175.
10. Mahler HC, Friess W, Grauschopf U, Kiese S 2009. Protein aggregation: pathways, induction factors and analysis. J Pharm Sci 98(9):2909-2934.
11. Heljo VP, Harju H, Hatanpaa T, Yohannes G, Juppo AM 2013. The effect of freeze-drying parameters and formulation composition on IgG stability during drying. Eur J Pharm Biopharm 85(3):752-755.
12. Abdul-Fattah AM, Dellerman KM, Bogner RH, Pikal MJ 2007. The effect of annealing on the stability of amorphous solids: chemical stability of freeze-dried moxalactam. J Pharm Sci 96(5):1237-1250.
13. Awotwe-Otoo D, Agarabi C, Read EK, Lute S, Brorson KA, Khan MA, Shah RB 2013. Impact of controlled ice nucleation on process performance and quality attributes of a lyophilized monoclonal antibody. Int J Pharm 450(1-2):70-78.
14. Bhatnagar BS, Bogner RH, Pikal MJ 2007. Protein stability during freezing: separation of stresses and mechanisms of protein stabilization. Pharm Dev Technol 12(5):505-523.
15. Cao W, Krishnan S, Ricci MS, Shih LY, Liu D, Gu JH, Jameel F 2013. Rational design of lyophilized high concentration protein formulations-mitigating the challenge of slow reconstitution with multidisciplinary strategies. Eur J Pharm Biopharm 85(2):287-293.
16. Cleland JL, Powell MF, Shire SJ 1993. The development of stable protein formulations: a close look at protein aggregation, deamidation, and oxidation. Critical reviews in therapeutic drug carrier systems 10(4):307-377.
17. Andya JD, Hsu CC, Shire SJ 2003. Mechanisms of aggregate formation and carbohydrate excipient stabilization of lyophilized humanized monoclonal antibody formulations. AAPS PharmSci 5(2):E10.
18. Davis JM, Zhang N, Payne RW, Murphy BM, Abdul-Fattah AM, Matsuura JE, Herman AC, Manning MC 2013. Stability of lyophilized sucrose formulations of an IgG1: subvisible particle formation. Pharm Dev Technol 18(4):883-896.

19. Schersch K, Betz O, Garidel P, Muehlau S, Bassarab S, Winter G 2010. Systematic investigation of the effect of lyophilizate collapse on pharmaceutically relevant proteins I: stability after freeze-drying. J Pharm Sci 99(5):2256-2278.
20. Schersch K, Betz O, Garidel P, Muehlau S, Bassarab S, Winter G 2012. Systematic investigation of the effect of lyophilizate collapse on pharmaceutically relevant proteins, part 2: stability during storage at elevated temperatures. J Pharm Sci 101(7):2288-2306.
21. Schersch K, Betz O, Garidel P, Muehlau S, Bassarab S, Winter G 2013. Systematic investigation of the effect of lyophilizate collapse on pharmaceutically relevant proteins III: collapse during storage at elevated temperatures. Eur J Pharm Biopharm 85(2):240-252.
22. Breen ED, Curley JG, Overcashier DE, Hsu CC, Shire SJ 2001. Effect of moisture on the stability of a lyophilized humanized monoclonal antibody formulation. Pharm Res 18(9):1345-1353.
23. Towns JK 1995. Moisture content in proteins: its effects and measurement. J Chromatogr A 705(1):115-127.
24. Costantino HR, Langer R, Klibanov AM 1995. Aggregation of a lyophilized pharmaceutical protein, recombinant human albumin: effect of moisture and stabilization by excipients. Biotechnology (N Y) 13(5):493-496.
25. International A. 2008. ASTM Standards. Standard Test Methods for Vibration Testing of Shipping Containers
D 999-08, ed., West Conshohocken, PA: ASTM International. p 1-5.
26. Telikepalli SN, Kumru OS, Kalonia C, Esfandiary R, Joshi SB, Middaugh CR, Volkin DB 2014. Structural Characterization of IgG1 mAb Aggregates and Particles Generated Under Various Stress Conditions. J Pharm Sci 103(3):796-809.
27. Kalonia C, Kumru OS, Kim JH, Middaugh CR, Volkin DB 2013. Radar Chart Array Analysis to Visualize Effects of Formulation Variables on IgG1 Particle Formation as Measured by Multiple Analytical Techniques. J Pharm Sci 102(12):4256-4267.
28. Kim JH, Iyer V, Joshi SB, Volkin DB, Middaugh CR 2012. Improved data visualization techniques for analyzing macromolecule structural changes. Protein science : a publication of the Protein Society 21(10):1540-1553.
29. Wang T, Joshi SB, Kumru OS, Telikepalli S, Middaugh CR, Volkin DB. 2013. Case studies applying biophysical techniques to better characterize protein aggregates and particulates of varying size. In Biophysics for therapeutic protein development; Narhi LO, Ed.: Springer New York, p 205-243.
30. Costantino HR, Carrasquillo KG, Cordero RA, Mumenthaler M, Hsu CC, Griebenow K 1998. Effect of excipients on the stability and structure of lyophilized recombinant human growth hormone. J Pharm Sci 87(11):1412-1420.
31. Kumru OS, Liu J, Ji JA, Cheng W, Wang YJ, Wang T, Joshi SB, Middaugh CR, Volkin DB 2012. Compatibility, physical stability, and characterization of an IgG4 monoclonal antibody after dilution into different intravenous administration bags. Journal of pharmaceutical sciences 101(10):3636-3650.
32. Zhang MZ, Wen J, Arakawa T, Prestrelski SJ 1995. A New Strategy for Enhancing the Stability of Lyophilized Protein: The Effect of the Reconstitution Medium on Keratinocyte Growth Factor. Pharm Res 12(10):1447-1452.
33. Roy S, Jung R, Kerwin BA, Randolph TW, Carpenter JF 2005. Effects of benzyl alcohol on aggregation of recombinant human interleukin-1-receptor antagonist in reconstituted lyophilized formulations. J Pharm Sci 94(2):382-396.

34. Sarciaux JM, Mansour S, Hageman MJ, Nail SL 1999. Effects of buffer composition and processing conditions on aggregation of bovine IgG during freeze-drying. J Pharm Sci 88(12):1354-1361.
35. Prestrelski SJ, Pikal KA, Arakawa T 1995. Optimization of lyophilization conditions for recombinant human interleukin-2 by dried-state conformational analysis using Fourier-transform infrared spectroscopy. Pharm Res 12(9):1250-1259.
36. Zhang MZ, Pikal K, Nguyen T, Arakawa T, Prestrelski SJ 1996. The effect of the reconstitution medium on aggregation of lyophilized recombinant interleukin-2 and ribonuclease A. Pharm Res 13(4):643-646.
37. Chang BS, Kendrick BS, Carpenter JF 1996. Surface-induced denaturation of proteins during freezing and its inhibition by surfactants. J Pharm Sci 85(12):1325-1330.
38. Jones LS, Randolph TW, Kohnert U, Papadimitriou A, Winter G, Hagmann ML, Manning MC, Carpenter JF 2001. The effects of Tween 20 and sucrose on the stability of anti-L-selectin during lyophilization and reconstitution. J Pharm Sci 90(10):1466-1477.
39. Webb SD, Cleland JL, Carpenter JF, Randolph TW 2002. A new mechanism for decreasing aggregation of recombinant human interferon-gamma by a surfactant: slowed dissolution of lyophilized formulations in a solution containing 0.03% polysorbate 20. J Pharm Sci 91(2):543-558.
40. Sinko PJ, Singh Y editors. 2011. Martin's Physical Pharmacy and Pharmaceutical Sciences. 6 ed., Baltimore, MD: Lippincott Williams & Wilkins. p 659.
41. Duran J. 2000. Sands, Powders, and Grains: An Introduction to the Physics of Granular Materials. ed., New York: Springer-Verlag. p 214.
42. Chaudhuri B, Mehrotra A, Muzzio FJ, Tomassone MS 2006. Cohesive effects in powder mixing in a tumbling blender. Powder Technology 165(2):105-114.

CHAPTER 4: Physical characterization and *in vitro* biological impact of highly aggregated antibodies separated into size enriched populations by FACS

4.1 INTRODUCTION

The presence of aggregates in recombinant protein therapeutics is a serious concern due to their potential immunogenicity risk in patients.[1-10] The most notable clinical examples of immunogenicity include Factor VIII[7], and human growth hormone (hGH),[8] and most likely erythropoietin (EPO). [2,3] Unfortunately, exactly how aggregates produce an immune response, and the extent of their impact in *in-vivo* responses, is not fully understood. Aggregates can arise at all steps of protein production: fermentation, expression, purification, formulation, filling, transport, storage, and administration.[11,12] Since each protein is different, it may aggregate differently depending on the environmental stresses and solution conditions, which may expose various epitopes that may be more immune reactive than others. For example, different solution conditions can lead to formation of different types and sizes of aggregates and particles.[13-15] Various environmental stresses including interfaces, temperatures, freeze-thaw, containers, pH, ionic strength, excipients, and concentration can all lead to protein aggregation.[16-22]

Our knowledge of the immunogenic potential of protein therapeutics is confounded by the fact that in addition to the presence of aggregates, immunogenicity risk can be contributed by factors that may arise from many patient related factors such as genetics, age, disease-related factors, and other concomitant medications the patient may be taking. The route of administration, dose, and the frequency of administration are also important factors. Product related factors such as non-human T-cell epitope content in sequence, origin of the active substance, process related contaminants, and formulation can impact immunogenicity as well. [23-26] The presence of so many variables complicates our understanding of the immunogenic potential of various therapeutic proteins. Therefore, determining the potential impact of aggregates by themselves on immunogenicity is very challenging. Despite these obstacles, a

combination of *in silico* predictions [27-30], *in vitro* cell-based assays[27,31-33], and *in vivo* transgenic animal models[34-38] are currently being extensively evaluated to assess the relative potential of different protein aggregates and particles to elicit immune responses in humans.

One particularly promising *in vitro* approach is the use of human Peripheral Blood Mononuclear Cells (PBMC) derived from a healthy donor population with heterozygous MHC genotypes to screen antigens or mAb candidates for their propensity to stimulate certain features of the immune system[1]. In-vitro models have been previously used to examine the immunogenicity of recombinant human erythropoietin-alpha[39], recombinant Factor VIII[39] and IgG mAbs[40] with a certain degree of success. The correlation of clinical immunogenicity with the *in vitro* PBMC output was also investigated for immunogenic human fusion protein. Subjects that induced IFN-gamma secreting T cells in PBMC were associated with a higher magnitude of immune response (as detected by binding and neutralizing anti-drug antibody) in clinical trials.[31] These *in-vitro* assays are relatively cheaper and faster to perform than *in-vivo* animal model based studies, can incorporate the diversity of the genetic polymorphism of alleles in the representative human population, can be used to screen a large number of candidate biotherapeutic mAbs during early development, and can be employed to compare the relative immunogenicity of different pharmaceuticals.[27,31-33]

Most of the studies to date have focused on evaluation of immune activation by challenging with heterogeneous sized aggregates. However, there is still a gap where the actual aggregate size associated with the immune activation has not been as thoroughly addressed. Previous work using three different IgG mAbs, including the one used in this study, were stressed by a variety of different methods and the resulting particles were characterized in terms of size, particle counts, conformation, morphology, and reversibility.[13,41] Different types of

aggregates formed depending on the type of stress applied. [13] These different stressed mAbs were tested in an *in vitro* system to compare their relative response in human PBMC.[40] It was found that aggregates, prepared by stirring for all three mAbs, displayed the highest response compared to the aggregates generated by all the other stresses tested.[40] These results indicated that the presence of a high number of 2-10 μm particles, which were partially reversible, with retention of some folded structure in the stir-induced sample may be responsible for the increased PBMC response.[40]

The purpose of this study was to further examine the impact of protein particle size on signature cytokine secretions of human PBMC at different stages of the immune response.[40] An IgG2 monoclonal antibody (mAb2) solution was stirred to generate protein particles of varying sizes. The mAb2 particles were then separated into various size enriched populations using (1) low speed centrifugation to enrich for nanometer vs. micron sized particles, and (2) Fluorescence Activated Cell Sorting (FACS) to separate enriched fractions of micron-sized protein particles. FACS is a promising approach for protein particle characterization as recently described by Rombach-Riegraf et al [42] for size separation and for related applications such as to detect and differentiate subvisible protein particles from silicone oil protein particles. [43-45] [46] The stirring induced mAb particles were also physically characterized, before and after FACS separation, in terms of their particle number, size distribution, mass distribution, morphology and composition using a combination of techniques including Microflow imaging (MFI) with radar chart analysis, FTIR microscopy, and multiple electron microscopy analyses (TEM and SEM-EDS).

4.2 EXPERIMENTAL SECTION

4.2.1 Materials

The IgG2 mAb, subsequently referred to as mAb2, was supplied by Amgen Inc. at 10.1 mg/mL. This mAb has been used previously to characterize the immune potential of different mAbs and their aggregates.[40,47] The antibody was highly purified[48] and endotoxin levels were confirmed to be in an acceptable range (< 1.00 EU/mL) for use in these cell based assays. The stock mAb2 solution was stored at 4 °C prior to use.

4.2.2 Methods

4.2.2.1 Generation of aggregates

The stock mAb2 was diluted to 1 mg/mL with 10 mM sodium acetate pH 5.0 (A5 buffer) and stressed by stirring (referred to as stir-20h) as described previously by Joubert et al.[13] Stirring stress was chosen since previous work showed that stirring of this IgG mAb produced aggregates that induced the highest response from PBMC.[40] Additionally, for biophysical comparison purposes, a 1 mg/mL solution of mAb2 was heated extensively at 90°C for 30 min (labeled heat control).

4.2.2.2 Size separation of mAb particles

Two techniques were used to enrich different size populations of stirring induced particles: (1) slow speed centrifugation, and (2) gravitational settling of the samples combined with Fluorescence Activated Cell Sorting (FACS), subsequently referred to as "FACS". For method (1), one mL of stir-20h mAb2 sample was centrifuged at 2500 RCF using a Baxter Hereaus Biofuge 15 Model 3604 (Deerfield, IL) for 5 min. The supernatant was removed and the pellet was resuspended in one mL of A5 buffer. For method (2), 5 mL of stir-20h mAb2

sample was gently pipetted into 12x75mm polypropylene tubes and allowed to settle in a disturbance-free environment for 3 h at room temperature. After 3 h, 200 uL aliquots were removed carefully from the top to the bottom using a pipetteman with gel loading tips and collected into eppendorf tubes. The last aliquot in the tube (referred to as "bottom") contained a greater number of larger micron-sized particles and this sample was then further size fractionated by FACS as described below.

4.2.2.3 Fluorescent Activated Cell Sorting (FACS)

A Beckman Coulter MoFlo XDP (Brea, CA) was set up as described in the instrumentation manual with calibrations done according to the manufacturer's specifications. A flow cytometry size calibration kit from Invitrogen (Molecular Probes, Carlsbad, CA) was used for general size correlation between reference beads and protein particles. The bottom sample was filtered through a 70 µm nylon mesh filter into a 12 x 75 mm polypropylene tube, and then diluted 15-20x with A5 buffer (called "pre-sort"). Four polypropylene tubes, each containing 200 uL of A5 were placed at 4°C in a sterile FACS sorting chamber. Samples were FACS sorted under the purify mode using a ceramic 70 µm nozzle tip at a pressure of 60 psi and at a speed of 5000-10,000 events/sec. The gain and sensitivity values of the detectors were optimized to maximize the protein particle detection and threshold. The charge plates were set to 4000V. Intellisort I was used to determine drop delay using flow check fluorospheres. All experiments used phosphate buffered saline (PBS) at pH 7.2, as the sheath fluid, daily prepared using deionized water (Labconco, Kansas City, MO) under aseptic conditions. The sheath fluid passed through an inline 0.22 µm filter just prior to mixture with pre-sort. Endotoxin levels were tested in each part of the instrument and were found to be at an acceptable range after the rigorous cleaning procedure as described below. Summit software version 5.2 (Beckman Coulter) was

used for data collection and data analysis was performed using Kaluza Flow Analysis (Beckman Coulter).

4.2.2.4 Endotoxin cleaning and testing

4.2.2.4.a Removing endotoxins

Prior to using the stir-stressed mAb samples in the *in-vitro* cell-based assay, the samples were tested for endotoxins. High levels of endotoxins (>10 EU/mL) were present in the FACS sorted samples despite sterilization of all instrument components and use of aseptic procedures. Therefore a protocol was developed to remove endotoxins by washing the instrument and all of its components with various solutions in the following sequence: 1) 10% bleach for 2 hours 2) deionized (Labconco) water for 2 hours 3) 70% ethanol for 2 hours 4) deionized water for 2 hours, 5) 1% Triton-X 114 (Sigma, St. Louis, MO) for 2 hours, 6) deionized water for 3 hours 7) approximately 1 mg/mL polymyxin B sulfate solution (Sigma, St. Louis, MO) for 3 hours, and 8) final flushing with deionized water for 3 hours.

4.2.2.4.b Endotoxin testing

All protein samples and buffers were assessed for endotoxin levels by a LAL (Limulus amebocyte lysate) test with the Charles River Endosafe®-PTS™(Charles River, Wilmington, MA) system prior to being used in the biological assay. The analysis was performed according to the manufacturer's instructions.

4.2.2.5 Particle counting and sizing of mAb particles

4.2.2.5.a HIAC-Royco Liquid Particle Counter

HIAC/Royco liquid particle counter model 9703 with a HRLD-150 sensor and PharmSpec software PharmSpec (HACH Ultra Analytics, Grants Pass, OR) was used for obtaining particle counts and size distribution in some experiments. The HIAC method is described in detail by Joubert et al.[13,40]

4.2.2.5.b MicroFlow Imaging (MFI)

Particle images, size distribution, and counts were obtained using MFI System DPA4200 (Protein Simple, Santa Clara, CA). For analysis, stir-stressed mAb2 samples, generated at 1mg/mL, were diluted 100x in A5 buffer. Unstressed, buffer, and FACS sorted sample were not diluted, while the heat generated sample was diluted 25x prior MFI analysis. After obtaining a clean base line, three hundred microliters of each sample was loaded using the peristaltic pump. No notable differences were observed in degassed versus non-treated samples (data not shown), so samples were not degassed for these studies.

4.2.2.5.c MFI data analysis

MFI particle concentration data are displayed as either bar charts or radar carts, all corrected for all dilution factors. Additionally, a plot of % Particles vs Sample (size bin) is displayed. The percentage of particles as detected by MFI was calculated by dividing the concentration of particles of a certain size range by the total number of particles in all size ranges. This percentage is referred to as "enrichment" throughout this manuscript. MFI morphology radar charts were generated in the size ranges 2-5, 5-10, and >10 μm to evaluate changes in particle intensity and aspect ratios as described previously.[15,49] Finally, MFI particle data were used to calculate the estimated mass of protein within the particles, in the following

four size bins: 1-2, 2-5, and 5-10, >10μm, using the ellipsoid volume method recently described.[50]

4.2.2.5.d Resonant Mass Measurement (RMM)

A Particle Metrology System (Affinity Biosensors, Santa Barbara, California) was used with a Hi-Q micro sensor to quantify submicron and small micron particles from 0.2 to 1.85 μm. Sensor calibration and reference solution preparations were done according to the manufacturer's instructions. After a clean frequency trace was obtained, protein sample was loaded for 30 s, with a stop trigger of 200 particles. This limit of detection was empirically determined and used throughout the study. A density value for mAb of 1.41 g/mL was used.

4.2.2.6 Biological testing of mAb particles using PBMC (in vitro comparative immunogenicity assessment assay, IVCIA)

4.2.2.6.a Isolating Peripheral Blood Mononuclear Cells (PBMC)

PBMC from healthy human donors were obtained from Amgen's environmental health and safety department. PBMC were isolated according to the procedure described previously.[40]

4.2.2.6.b. Challenging PBMC with protein samples and controls

PBMC from up to 8 donors were plated and acclimatized in 96-well culture plates as described previously.[40] Acclimatized cells were then challenged with control (unstressed), and stir-20h mAb2 samples at equal volume, equal protein concentration at 40 μg/ml (total protein in solution determined by OD280 measurements), or equal particle number (based on light obscuration or MFI measurements). Negative controls, consisting of buffers isolated by FACS or medium-treated cells, and positive controls, such as lipopolysaccharide (LPS) or phytohemagglutinin (PHA). LPS and PHA were controls at the early or late-stage immune

response, respectively. Samples were incubated for either 20 h or 7 days, to assess an early stage or late stage immune response, respectively, as described by Joubert et al.[40]

4.2.2.6.c. Meso-Scale Discovery Assay

A 96-well human cytokine electro-chemiluminescence assay kit K151AYB-1 (Meso-Scale Discovery, Gaithersburg, MD) was used, according to the manufacturer's instructions, to quantify the concentration of monocyte chemotactic protein-1 (MCP-1) that was secreted by PBMC in response to the samples. The 96 well plates were analyzed using an MSD Sector Imager 6000 instrument (Meso Scale Discovery, Gaithersburg, MD) and MSD Discovery Workbench Software 4.0 (Meso Scale Discovery). SoftMax Pro was used for data analysis to convert the output luminescent units into protein concentration (pg/mL) using a standard curve. Responses were presented in terms of concentration of MCP-1 secreted and percentage of responding donors. To determine the percentage of responding donors, the stimulation index (SI) was also calculated. The SI was calculated by dividing the amount of cytokine detected (pg/mL) in the sample of interest by the cytokine detected in the unstressed sample. For these studies, a response was considered to be positive if the SI $\geq$ 2.0 (i.e., response of the PBMC to the stressed sample is at least 2 fold higher than the control). The percentage of donors (% donors) that responded was calculated by taking the total number of donors that had an SI $\geq$ 2.0 as a percentage of the total number of donors tested. The cutoff of SI $\geq$ 2.0 was determined by statistical analysis as described elsewhere.[40]

4.2.2.6.d. Multiplex Cytokine Analysis

Quantification of cytokines released from PBMC was performed using a multiplex plate format using Milliplex (EMD Millipore, Billerica, MA) human panel kits and a Luminex Multiplexing instrument (specifically a Luminex FLEXMAP 3D instrument from EMD Millipore) as described by Joubert et al.[40] For analysis of the PBMC supernatants at the early phase (after 20h incubation), the following cytokines were monitored: IL-10, IL-1ra, IL-1α, IL-1β, IL-6, IL-8, MCP-1, MIP-1α, MIP-1β, TNF-α, and TNF-β. For analysis of the PBMC supernatants at the late phase (after 7 days of incubation), the following cytokines were monitored: IFN-γ, IL-10, IL-12p40, IL-12p70, IL-13, IL-2, IL-4, IL-5, IL-6, IL-7, IL-8, and TNF-α. A robust PBMC response was difficult to obtain due to the dilute nature of the FACS purified samples. Therefore, the concentration of cytokines released by the PBMC was directly reported and the percentage of responding donors was calculated differently than for the MSD results. The cytokine response was analyzed as follows: for each cytokine monitored, the number of donors, who responded the highest (by releasing the largest amount of that same cytokine) to a specific size-enriched particle-containing sample was determined. The number of donors that responded highest to this size bin was then taken as a percentage of the total number of donors that were tested. In all cases, negative controls such as buffer isolated by FACS and medium-treated cells showed minimal response and positive controls such as LPS and/or PHA showed a very high response (SI>>2.0; data not shown). In all cases, PBMC responses induced by the mAb samples were much lower than those induced by the LPS or PHA positive controls (data not shown).

4.2.2.7 Biophysical characterization of mAb particles

4.2.2.7.a Extrinsic fluorescence

8-Anilino-1-naphthalene sulfonate (8,1-ANS) was used to study changes in the accessibility of apolar regions in the protein samples. An Agilent 8453 (Santa Clara, CA) was used with baseline and light scattering corrections.[51] Fluorescence data were obtained as described previously.[15] A spectrum of buffer containing ANS was subtracted from each spectrum prior to data analysis using Microsoft Excel software. ANS peak positions and intensities were monitored and compared to that of the control samples to compare relative similarities or differences in surface hydrophobicity among samples.

4.2.2.7.b FTIR

The control, heat, and stirred mAb2 samples in solution were analyzed with a Bruker Tensor 27 FTIR Spectrometer and Bio-ATR cell. Two hundred fifty-six scans were recorded from 600 to 4000 cm^{-1} with a resolution of 4 cm^{-1} as described in detail in Telikepalli et al.[15] For analyzing mAb particles, 3 μm gold filters (Pall Corporation, Port Washington, NY) were used to capture and wash protein particles and then analyzed by FTIR microscopy as described in detail elsewhere.[15]

4.2.2.7.c SDS-PAGE

Each sample other than the FACS sorted samples was dissolved in NuPAGE LDS sample buffer (Life Technologies, Carlsbad, California) with and without 50 mM dithiothreitol (BioRad Laboratories, Hercules, CA) and incubated at 90°C for 5 min. Approximately 3 μg of each sample was separated on a 3-8% Tris-acetate gel using Tris-acetate running buffer (Life Technologies) for 65 min at 150V. A Hi-Mark unstained molecular weight ladder was used as a

reference (Life Technologies). Protein bands were visualized by staining with Colloidal Coomassie (Invitrogen, Carlsbad, CA) according to the manufacturer's instructions.

4.2.2.7.d Transmission Electron Microscopy (TEM)

Six microliters of samples were placed onto Lacey Carbon 300 Mesh Copper grids (Ted Pella, Redding, CA) and allowed to sit for 2 min, with the excess wicked off by a Kimwipe. Stir-20h and bottom samples were diluted 100x with A5 buffer prior to being loaded onto the TEM grids. FACS sorted samples, heat-stressed, unstressed control, and buffers were loaded directly onto the TEM grids with no dilution. The grids were then placed into filtered 2% uranyl acetate for 2 min and extra stain was removed with a Kimwipe. The wet grids were air-dried for several min prior to being examined by TEM. Samples were imaged on an FEI Technai F20 XT Field Emission Transmission Electron Microscope (Hillsboro, OR) using 200 kV electron acceleration voltage. Images were captured at a standardized, normative electron dose and at a constant defocus value from the carbon-coated surfaces[52].

4.2.2.7.e Scanning Electron Microscopy (SEM)/Energy-dispersive X-ray Spectroscopy (EDS)

A FEI Versa 3D Dual Beam Scanning Electron Microscope/ Focused Ion Beam (Hillsboro, OR) with an XMAX silicon drift detector (Oxford Instruments, UK) was used to obtain information regarding the surface morphology, elemental composition, and distribution of elements of the protein samples. SEM data was obtained at an acceleration voltage of 7 kV and a spot size of 4.0 using an Everthart Thornely (ET) detector for image collection. Elemental mapping and energy spectra were acquired and processed with AZtecEnergy software (Oxford Instruments, UK). For sample preparation, a small square piece of ruby red mica sheet (Electron Microscopy Sciences, Hatfield, PA) was mounted onto a standard SEM pin stub specimen mount

(Ted Pella, Redding, CA). The grids prepared for TEM analysis were placed on top of the mica and a thin coating (3 nm) of electrically conductive material (gold) was deposited on the sample by a low vacuum sputter coater (Quorum Technology, Laughton, UK).

4.3 RESULTS

4.3.1 Initial comparisons of nanometer vs. micron sized mAb particles in a PMBC assay

As an initial experiment, the IgG2 mAb (mAb2) in 10 mM acetate buffer, pH 5 (A5 buffer) was stirred for 20h and the particles generated were fractionated by slow speed centrifugation to separate the supernatant and pellet, containing enriched nanometer and micron-sized particles, respectively. Figure 4.1 shows the size distribution of nanometer and micron sized particles present in the supernatant and pellet components as measured by HIAC and RMM, respectively. There was almost a ten-fold higher number of smaller nanometer sized particles (0.2 to 1.5 μm) in the supernatant than the pellet, which contained more of the micron sized particles (2-10 μm). The percentage values shown in Figure 4.1 were calculated by dividing the number of particles in either the supernatant or pellet by the total number of particles present in both supernatant and pellet in a particular size range. Hence the percentages signify the enrichment of a given size range in the samples. For example, 83% of all the particles detected in the 0.2-1.5 μm range are in the supernatant, while only 17% of particles in this size range are in the pellet. In addition, 70% of the particles detected in the 2-10 μm range are in the pellet, but only 30% of the particles in this size range are in the supernatant. To get a better estimate for the precision of each technique, relative standard deviations (RSD) were calculated by running the stir-stressed mAb2 multiple times (N=10) on RMM; the RSD over the

size range 0.2 – 1.5 μm was about 30%. A similar experiment has been previously done to determine the RSD of particles from another mAb using HIAC, which showed an RSD of 1% for the 2-10 μm particles, and 8 % RSD for particles greater than 10 μm.[53] These samples were then analyzed for their cytokine response using an *in vitro* comparative immunogenicity assessment assay (IVCIA),[40] as described in the Methods section.

For these initial IVCIA studies, we tested the propensity of the supernatant (enriched in nanometer sized particles) and the resuspended pellet (enriched in micron-sized particles) to elicit a response in PBMC by monitoring the level of MCP-1 secreted. MCP-1 was chosen as a representative cytokine since we previously identified this cytokine as part of the cytokine signature that is released by PBMC in response to aggregates at the early phase.[40] PBMC from 8 naïve healthy human donors were challenged with the mAb2 stir-20h total, supernatant and pellet samples and the secretion of MCP-1 was assessed at the early phase (20 hours) by an electro-chemiluminescence assay. These initial results are shown in Figure 4.2. The Y-axis on the left and corresponding colored bars represent the average concentration of MCP-1 detected in response to the different samples, while the Y-axis on the right and the corresponding gray bars refer to the percentage of donors that responded at least two fold higher than the unstressed mAb sample (SI $\geq$ 2.0). The dots represent the individual data points for the 8 human donors. Figure 4.2 highlights the variability of MCP-1 expression levels for individual donors as well as the variability in responsiveness to the different mAb samples.

When the PBMC were challenged with equal sample volumes of the three particle-containing mAb samples (stir-20h total, supernatant, and pellet), the stir-20h total sample (no fractionation) showed the highest response with respect to both the number of responding donors as well as by magnitude of secreted MCP-1 (Figure 4.2A). The stir-20h pellet showed a higher

response than the corresponding supernatant in terms of number of responding donors and magnitude of cytokine concentration. Similar experiments were performed in which PBMC were challenged with equal protein concentrations (Figure 4.2B) or equal particle numbers (Figure 4.2C) of stir-20h supernatant and stir-20h pellet samples. Even though MCP-1 was detected when PBMC were challenged with the supernatant sample, none of the 8 donors responded two fold higher than the control, unstressed sample (Figure 4.2B). In all three cases, (Figure 4.2A-C) the pellet sample induced a higher response than the supernatant sample by both magnitude of cytokine secretion and number of responding donors, suggesting that micron size particles enhance the response of PBMC *in vitro* to a greater extent than nanometer size particles at the early phase. The level of cytokine secretion induced by the mAb2 samples was, however, much lower than that induced by the positive control (lipopolysaccharide, LPS; data not shown).

To further test the wider applicability of these trends, the supernatant and pellet fractions of a second IgG2 monoclonal antibody were also tested in the IVCIA assay (data not shown). For both mAbs, the pellet fraction induced a higher response than the supernatant fraction, indicating that micron size particles induce a more robust response as compared to nanometer sized particles at the early phase.

4.3.2 Size enrichment of various micron sized particles using FACS

Based on the IVCIA data from evaluating stirring induced nanometer vs. micron sized mAb particles, it was observed that the larger micron sized particles showed higher relative responses in the donor population used (see above). We therefore set out to develop a method to size fractionate the micron sized mAb particles for further analysis. A wide variety (>20 conditions) of settling, centrifugation and filtration experiments were evaluated to size fractionate micron-sized, stirring-induced mAb2 particles with limited success (data not shown).

After much trial and error experimentation, a methodology was identified that utilized a combination of gravitational settling under specific conditions combined with FACS, to enrich distinct micron sized particle populations (Figure 4.3A).

The stir-20h mAb2 sample was gravitationally sedimented for 3h under specific conditions (see Methods section). The bottom fraction (referred to as the "bottom" sample) was then collected. The particle concentration and enrichment factor of the bottom sample as measured by MFI, in comparison to the original stir stressed mAb2 sample, is shown in Figures 4.3B and 4.3C, respectively. The bottom sample was then passed through the FACS and the forward scattering area (FSC) vs. side scattering (SSC) area dot plots were obtained as shown in Figure 4.3D. Each dot represents a counted particle and the FSC signal is generally considered to be a good indicator of particle size.[54] Based on some initial correlations between FACS gating schemes and MFI sizing data (data not shown), gating schemes were optimized for best size enrichment and are shown in Figure 4.3D as I, II, III, and IV. Based on these four gatings, the stir-20h bottom samples were sorted and collected. These four sorted samples (I, II, III, and IV) were collected and analyzed by MFI as shown in Figures 4.3E and 4.3F. Sort I contains enriched number of 1-2 μm particles, Sort II contains an enriched number of 2-5 μm particles, Sort III an enriched number of 5-10 μm particles, and Sort IV an enriched number of greater than 10 μm particles (>10 μm); all sizes were calculated based on equivalent circular diameter (ECD). Comparing MFI enrichment results in Figures 4.3C with 4.3F shows a distinct enrichment in all four size ranges with good reproducibility as indicated by error bars. Comparing MFI counts in Figures 4.3B with 4.3E, however, shows a large decrease in particle concentration after FACS separation, due to an extensive dilution of the samples of over ~1000 fold. In this case, the FACS analysis had to be run numerous times (~20 runs over several months) to collect a

sufficient volume of sample, for further analysis. Since so many runs were required for use in the PBMC assay, the FACS samples had to be collected and frozen after each run.

For logistical reasons, FACS samples had to undergo two freeze thaws cycles prior to being evaluated. The frozen FACS sorted samples from each individual FACS run were thawed, pooled with other similar sorts, and frozen again. It was these pooled frozen samples that were then subsequently thawed for biophysical and FACS analysis. These FACS sorted samples contained predominantly subvisible particles in PBS buffer. The overall protein levels were low since mAb particles had been largely separated from free protein by the FACS. For example, total protein levels were too low to be observed in the FACS samples containing mAb particles by OD 280nm measurements, SDS-PAGE or with a colorimetric BCA assay (data not shown). Therefore, protein levels within the subvisible mAb particles could only be estimated by calculation from MFI data.[50] To initially characterize the size measurements with these samples, one of the FACS sorted samples that underwent two F/T cycles, was examined by MFI (N=9) to examine the precision of the MFI results with these FACS samples. RSD values between 20-25% were obtained for the first three size bins (1-2, 2-5, and 5-10 μm), 60% for the largest size bin analyzed, and 20% for the total MFI particle counts (Figure 4.4A). These values give the relative error associated with each of these particle counts in these different size ranges. Additionally, the pools (Sort I, II, III, IV) that underwent 2 F/T cycles were directly analyzed by MFI (N=3). The particle enrichment factor for each of these four FACS samples is maintained after two F/T treatments (See results in Figure 4.3F vs. Figure 4.4B).

Table 4.1 summarizes subvisible particle number, size and mass characteristics, based on MFI analysis, for each of the pools of the four samples (Sort I, II, III, and IV) that went through two F/T cycles. The total particle concentration is shown including estimated ranges (based on

twice the calculated RSD values from Figure 4.4). In addition, the particle concentration in each of the four size ranges (including enrichment values and estimated ranges) are shown. It is apparent here that the experimentally determined total particle concentration results (column 3) falls within the range expected based on RSD calculations (column 4) for nearly all of the FACS Sorts. In addition, the calculated mass of the protein particles in each size range, based on MFI morphology measurements and assumptions of protein particle density as described by Kalonia et al, 2014,[50] is shown in Table 4.1.

4.3.3 IVCIA testing of FACS size-enriched populations of micron sized mAb particles

The four FACS samples described in Table 4.1 (Sort I, II, III, IV) were next evaluated in the IVCIA assay. PBMC from 7 human donors were challenged with equal volumes and similar particle counts of each of these four FACS samples. The response to these FACS enriched micron-sized mAb particles was monitored at two different times, in the early stage (20 h incubation) and late stage (7 days incubation). Multiplex cytokine analysis was used to assess two different panels of cytokines that were specific for each stage of the incubation. The resulting cytokine profiles are shown in Figures 4.5 and 4.6. A head-to-head comparison of the PBMC response to Sort I (containing enriched 1-2 μm particles) and Sort III (containing enriched 5-10 μm particles) is shown in Figure 4.5 at both the early phase (20 h, Figures 4.5A, 4.5B) and late phase (7 days, Figures 4.5C, 4.5D). Since the overall particle counts in each Sort sample were low, the PBMC responses observed were also low (compared to results shown in Figure 4.2).

Comparison of results in Figures 4.5A with 4.5B show that the concentrations of cytokines released (colored bars corresponding to the left-hand Y-axis) by PBMC in response to Sort I vs. Sort III are similar. However, the percentage of donors that responded (shown on the right hand Y-axis) to Sort III is higher as compared to Sort I. Although this result shows that most of the donors responded more to the particles in Sort III than Sort I, it is important to keep in mind that this was not a dramatic response and the donors responded only marginally higher overall. Similar observations can be made by comparing results in Figures 4.5C with 4.5D at the late phase of the PBMC response, which shows additional T-cell effector cytokines that are more specific to the late phase of the immune response. This subtle difference between Sort I and Sort III is thought to be partly due to the low particle counts, which prevented robust cytokine release. However, it is apparent that more donors consistently responded to the Sort III sample than the Sort I sample.

Since Sort I showed a lower response than Sort III (Figure 4.5), it was not assessed further. Sorts II, III, and IV were further assessed (Figure 4.6). PBMC from 8 human donors were challenged with similar particle counts of Sort II, III, and IV and the resulting cytokine profiles are shown in Figure 6 at both the early phase (Figure 4.6A, 4.6B, 4.6C) and the late phase (Figure 4.6D, 4.6E, 4.6F). The overall responses, in terms of cytokine concentrations, were low, probably for the same reasons described above in Figure 4.5. Despite these limitations, a trend of a greater number of responding donors across the different cytokines was observed for the Sort III sample (enriched in 5-10 μm particles) for the PBMC at both the early and late phase of this *in-vitro* assay (Figure 4.6).

4.3.4 Biophysical characterization of FACS size-enriched populations of micron-sized mAb particles

The Sort I, II, III, IV size enriched samples from the FACS contained subvisible particles, but undetectable amount of free protein in solution (as detected by OD280, SDS-PAGE or BCA assay), in PBS buffer, so this provided an opportunity to characterize protein particles without the presence of IgG2 mAb in solution. Consequently, due to these FACS samples' low mAb particle concentration (and thus low protein concentration), only a limited number of physical assays could be used (see below). Therefore, the IgG2 mAb sample generated just prior to FACS separation was first characterized (stirring followed by gravitational settling and selection of the "bottom" sample) to better understand the nature of the micron-sized particles going into the FACS separation. These samples contained both protein particles and soluble IgG2 mAb.

The biophysical analysis of the starting material for FACS analysis focused on four samples: two controls (unstressed and extensively heated mAb2 solutions as negative and positive controls), the stirred antibody solution (stir-20h), and the "bottom" sample from the stirred sample after gravitational settling (i.e., the starting material for the FACS separation). Only the heat-stressed control contained high molecular weight aggregates containing reducible covalent, disulfide linkages, which were not present in the other three samples as measured by SDS-PAGE (Figure 4.10). Figure 4.7 shows TEM, SEM, EDS, FTIR, and ANS fluorescence spectroscopy data for the four samples. The unstressed control (Figure 4.7; first row) contained no particles that could be imaged by TEM and SEM-EDS (see Figures 4.12 and 4.13). The unstressed mAb2 solution contains antibody with largely native secondary structure (intramolecular beta sheets) with characteristic positions of the two peaks at 1691.1 cm^{-1} and

1636.6 cm^{-1}, as determined by second-derivative FTIR spectroscopy. It also shows virtually no extrinsic fluorescence intensity indicating limited exposure of apolar regions for ANS binding.

Similar biophysical analysis was then performed on the subvisible particle containing samples of mAb2. Results from heat stressed, stir-20h, and the bottom samples are shown in Rows 2, 3 and 4 of Figure 4.7, respectively. These particles were observed to be amorphous in nature by TEM and SEM and contained predominantly carbon, nitrogen, and oxygen by EDS analysis (as expected for protein). All protein samples contained trace levels of elemental chlorine, presumably bound to the mAb protein during exposure to NaCl solutions during purification. Interestingly, the stir-20h samples also contain fluorine, probably originating from the Teflon coated stir-bar, while the heated particles did not contain fluorine (unstressed and heat stressed samples also lacked fluorine; see Figures 4.12 and 4.13). The heat control samples contained protein with structurally altered conformation, containing mAb with predominantly intermolecular beta sheets, as indicated by the 1620.7 cm^{-1} peak by FTIR, as well as increase in surface hydrophobicity relative to the unstressed control. The major peak in FTIR spectra of the particles isolated from the two stirred samples (stir-20h and bottom samples) was between the two control samples, even though there was some increased variability in peak position. The bottom sample showed the largest increase in ANS intensity indicating a relatively increased surface hydrophobicity (or aggregation) of protein within this sample (last row in Figure 4.7). Thus, there is some level of structural alteration of the protein contained in the stir-induced protein particles as well as increase in surface hydrophobicity relative to the unstressed and heated controls.

The bottom sample was the starting material for the FACS separation, leading to collection of Sorts I, II, III, and IV containing size enriched micron sized particles. The protein

particles after FACS separation (Sorts I, II, III, and IV) were quite dilute compared to the samples described above, but were in sufficient number to be visualized by TEM and SEM (Figure 4.8). Representative TEM images at two resolutions (200 nm and 1 μm) with protein particles represented by the darker gray regions are shown, while the lighter, smoother, gray regions are due to the TEM grids used for sample preparation. Representative SEM images (5 μm resolution) are shown, and the protein particles appear lighter with unique shapes and are highlighted by the blue boxes. These SEM images provide a unique visual representation of the morphology of the protein particles compared to TEM. Aside from their size, the protein particles from the four FACS samples (Sorts I, II, III, IV) are similar morphologically. This is especially apparent in the 1 and 5 μm resolution TEM and SEM images, respectively. The proteins within the blue boxes in the SEM images were analyzed for chemical composition by EDS (last column). Similar to the starting material used in the FACS separation, the FACS separated particles contain C, N, O, and trace amounts of chlorine and fluorine. Elemental mapping of these particles confirmed that the fluorine was present only in the particles and not in the background or control samples (Figure 4.13).

In addition, MFI data were used to compare the morphology of these purified particles by constructing radar charts.[15,49,55] These radar charts are a data visualization technique, which facilitates comparisons of a specific morphological characteristic in a large number of samples such as their aspect ratio and transparency (intensity). For example, MFI morphology radar chart analysis of the Sort I, II, III, IV FACS samples, and the bottom mAb2 sample (starting material for FACS separation) is shown in Figure 4.9. As shown in the key in Figure 4.9B, size bins start at 2-5 μm at the top of the circle and increase clockwise up to > 10 μm. The outermost circle has four more concentric circles within it and consists of a triangle, located in the center, pointing to

three size bins. The triangle can get larger or smaller within the circle towards one or more size bin. Depending on whether the intensity parameter or aspect ratio parameter are being analyzed, the expanding triangle shows that the particles in that size bin are becoming elongated (aspect ratio; going from 1 to 0) or more opaque (intensity; going from 850 to 350 ILU).

From Figure 4.9A, no differences were observed in intensity or aspect ratio of FACS sorted mAb particles in the 2-5 μm size range although these small sizes approach the limit of MFI resolution for morphology parameters (around 4 μm). For 5-10 μm size bins, particles present in Sort I, III, and IV samples appear slightly more opaque than similarly sized particles in the bottom and Sort II samples. Particles larger than 10 μm in the bottom and Sort IV samples appear more opaque than similarly sized particles in Sort I, II, and III. In terms of aspect ratio, the FACS sorted samples showed some more elongated particles in the largest size bin (>10 μm) compared to the bottom sample. Overall, these differences are relatively minor, and the morphological parameters among the particles in the four FACS samples were similar.

4.4 DISCUSSION

This work evaluated the immune activation potential of protein aggregates of varying size by examining size-enriched populations of stirring-induced mAb2 particles in an *in-vitro* cell based assay, known as IVCIA, with PBMC from human donors. As an initial set of experiments, we showed that micron sized protein particles enhanced cytokine secretion in the IVCIA assay to a greater extent than nanometer-sized particles. To determine which size subset of micron sized aggregates induced the greatest response, we utilized a combination of gravitational settling and FACS separation to obtain different micron size-enriched protein particles from a stirred solution

of mAb2. FACS sorting resulted in isolated protein particles, with no detectable soluble protein in samples as measured by OD 280nm, SDS-PAGE or BCA analysis, offering the opportunity for additional biophysical characterization of isolated protein particles (in addition to testing these particles in the IVCIA assay).

The mAb2 particles induced by stirring were shown, compared to untreated and heat stressed controls, to contain an amorphous morphology with protein within the particles having some structural alterations in their overall secondary structure and increased surface hydrophobicity, but retaining some of the native higher-order structures as well (Figure 4.7). The FACS separation results for these mAb2 particles are consistent with those of Nishi et al. in that this technique involves a relatively mild condition that do not disrupt particles to a detectable extent.[45] In this work, even after two freeze-thaw cycles, significant size-enrichment of mAb particles is maintained within the FACS sorted samples. This result indicates either these aggregates are irreversible, or that the conditions used to enrich and isolate them do not disrupt the reversible interactions. Previous characterization of aggregates of mAb2 generated by stirring demonstrated some reversibility upon dilution, supporting the second conclusion.[40]

FACS separates particles by imparting a charge on the droplet containing them. From our analysis of morphology of the FACS sorted samples, although minor differences from MFI radar chart analysis were noted, it appears FACS does not dramatically alter the overall nature of particles before and after FACS separation. The small differences observed in the radar plots may actually primarily reflect the different amounts of particles in different size bins (Table 4.1). Thus when evaluating the average aspect ratio or intensity in a size bin, one also needs to consider the number of particles present in that bin as well. A combination of TEM, SEM-EDS and MFI analysis of the morphology and composition of mAb2 particles before and after FACS

separation showed no notable differences (Figure 4.7, 4.8, 4.9). Interestingly, particles generated by stirring contained fluorine as measured by SEM-EDS, and this element was not present in the buffer and control mAb2 (unstressed and heat stressed) samples indicating that it was originating from the stir-stress (Teflon-coated stir bars were used in this study) and carried with the particles through the FACS separation. The presence of this element in protein particles and its impact on PBMC responses is a subject for investigation in future work. This result also highlights that generating particles under accelerated conditions (i.e., extensive stirring with a Teflon coated stir bar) does not necessarily mimic mAb particle formation under real-time storage conditions. In fact, fluorine was not observed in control or heat-stressed mAb2 samples.

There are some practical limitations of the FACS technique for preparative isolation of protein particles that need to be improved in the future. First, FACS isolation results in significant dilution of the particle sample (~1000X in these studies) resulting in low particle yields (compare Figure 4.3B to Figure 4.3E). In fact, to prepare sufficient amounts of size-enriched mAb particle samples for biophysical and biological testing in this work, many months of almost continuous FACS runs were required. This in turn required freezing of individual sorts from individual runs, followed by subsequent thawing, pooling and refreezing of particle preparations to obtain the Sorts I, II, III, and IV evaluated in this work. Even then, low particle counts obtained (< 10,000 particles/mL) approached the lower limit of particles required for the IVCIA assay and consequently led to low PBMC responses. In addition, it is also difficult to further concentrate the FACS separated particles without loss of material due to additional processing or inadvertently altering their size distribution. Rombach-Riegraf showed that resorting IgG particle samples increases purity of distinct size bins[42], which was not a viable

option in this work since it would have dramatically decreased particle concentration even more, making the samples unsuitable for the *in-vitro* assay or biophysical characterization.

The dilution from the FACS could result in the loss of reversible aggregates, so that the samples assessed after FACS analysis might be primarily irreversible aggregates. This should present a "worse case" for immunological potential assessment, but might not reflect the original aggregate population. It was found that even after two freeze-thaws, the FACS sorted samples retained a similar distribution of subvisible particles counts, indicating that they are in fairly stable state where they do not appear to either dissociate or aggregate, indicating potential irreversibility. SDS-PAGE gels showed that the "bottom" sample, used as the starting material for FACS separation, did not contain covalently linked high molecular weight aggregates; unfortunately, due to the dilute nature of the FACS samples, they could not be assessed by this technique. It is possible that the bottom sample contained either covalently or non-covalently linked aggregates that dissociated upon sample preparation. In that case, the aggregates should be fairly reversible. However, more work needs to be done to further characterize the reversibility nature of these FACS sorted samples.

These IVCIA results are consistent with other studies that have examined the role of the size of subvisible particles in eliciting an immune response.[35,40,56-63] For example, stressed conditions that generated high levels of subvisible particles elicited ADA titers in various mouse models with heat stressed allergens[57], human growth hormone [58], and recombinant human interferon alpha 2b.[35] Further evidence suggests that larger sized subvisible particles are more likely to elicit various immune responses. For example, when high pressure was applied to aggregates of human or murine growth hormone, subvisible particle counts declined along with a corresponding decrease in immunogenicity in mice. [58,64] These results agree with prior work

using protein coated spheres as a model system for protein aggregates of different sizes where antibody-coated 5 μm microspheres induced a greater response in (1) the IVCIA assay compared to heterogeneous stress-induced aggregate populations[40] , and (2) in a Xeno-het mouse model system compared to antibody-coated nanospheres (20-50 nm).[47] In this work, 5-10 μm sized protein particles displayed elevated levels of cytokine responses compared to the other sized mAb2 particles tested in the same IVCIA assay.

The role of structural integrity of protein molecules within particles on immune responses has also been widely studied. [35,40,56,57,59,61-63,65] Results from one of our laboratories have previously shown that aggregated solutions with high numbers of 2-10 μm particles and the retention of at least some folded protein structure caused the highest PBMC immune response. [40] In another study, Filipe et al. subjected a fully human IgG1 to various stresses and found that the stress that formed the most micron sized particles, which were mostly native in structure, actually did not show a high immune response[59]. Instead copper-catalyzed aggregates, containing little to no visible and micron sized particles, low surface hydrophobicity, and large changes in secondary and tertiary structures were the ones that showed the highest ADA response in transgenic mice.[59] This aggregate type was shown to contain a high level of copper and histidine oxidation,[13,14] a modification not found in other types of stress treated aggregates. These results highlight the importance of aggregate type in inducing an immune response, which may be more important than size, amount, or morphology of the aggregates.[59] In our work, the stirring induced mAb2 particles contained protein structural alterations in secondary and tertiary structure as shown by FTIR microscopy and extrinsic ANS fluorescence spectroscopy, respectively. Compared to the heat control, the stirred samples displayed some retention of native higher-order structures, which may be necessary for the observed PBMC response.

The inter-relationship of protein particle size, number and mass presents a challenge in determining the most important factors in generating an immune response. Rombach-Riegraf showed that the mass of protein present in subvisible particles may be an important property. They saw a positive correlation between protein mass in subvisible particles, generated by stressing an IgG mAb, and the amount of antigen processed and presented by the dendritic cells (DC).[61] The more subvisible particles there are, the greater the mass of protein, and consequently, the greater the presentation of peptide by DC, which can influence DC maturation and activation of CD4+ T cells[61]. While we did not design the IVCIA assay to examine the effect of protein mass of the FACS sorted samples, we subsequently estimated the weight of protein particles in Sorts I-IV using MFI morphology data using a new method from one of our laboratories.[50] As shown in Table 4.1, Sort III, which showed the greatest response in the IVCIA assay, contained both the highest number of particles and the highest mass of protein present in the 5-10 μm size range (Table 4.1). Even then, roughly 25% of the total protein mass in this sample was estimated to be from the particles larger than 10 μm. Additionally, even though Sort IV contained a significant mass of protein calculated from the 5-10 μm particles, this sample showed a lower relative response in this PBMC *in-vitro* assay. Sort IV contained an enriched number of particles greater than 10 μm, and consequently most of the mass of the protein was present in these particles. This highlights that both protein mass and number of particles are important factors for consideration in monitoring cytokine responses in this assay.

In summary, we observed that size-enriched fractions of stirring-induced mAb2 particles greater than 2 μm, especially in the 5-10 μm range, elicited a relatively greater cytokine responses in a number of PBMC donors in the *in-vitro* assay. However, many questions remain. In terms of physical characteristics of the mAb aggregates, it would be beneficial to use the

methods established in this work to perform additional case studies with FACS size-enriched mAb particle populations (e.g., with different mAbs and different stresses and thus different physicochemical characteristics) to determine if the trends in size and immune potential observed in this work are generally observed across different types of mAb aggregates. In terms of biological readouts, even though this PBMC in-vitro model avoids the challenges associated with animal models, accounts for human genetic diversity, and mimics administration of the drug, it still requires a large number of particles, perhaps much more than clinically relevant, to obtain a strong signal.[40] Additionally, it is important to note that the cytokines monitored in this study serve as biomarkers of early and late phases of the immune response in this *in-vitro* system. They are useful tools to assess the relative response of a diverse human population of PBMC and to rank responses relative to different types of aggregates. However, how the PBMC cytokine responses correlate with various *in-vivo* immune processes or immunogenicity is currently unknown due to the complexities arising from the pleiotropic nature of cytokines and the complexity of the immune system where the T cell driven B cell response and consequent signaling and antibody formation cannot be reproduced *in-vitro*. A combination of this *in-vitro assay* with other *in-silico* and *in-vivo* models, however, should result in enhanced predictive value in determining the relative immunogenic potential of different therapeutics.

4.5 TABLES AND FIGURES

Table 4.1. Various characteristics of the FACS sorted samples I, II, III, and IV used in the IVCIA assay are shown. The average particle concentration, experimental concentration range obtained from N=2, and estimated concentration range based on 2RSD from N=9 from Figure 4.4 measurements using the same protein are shown. The average concentration, range of particles in each of the size bins (1-2, 2-5, 5-10, >10 μm), their corresponding enrichment values, mass of protein in each bin (as calculated from Kalonia et al[50]), and the range of mass of protein within those size bins is shown.

	Total particle conc. (#)			**Size bin**	**Particle conc. & enrichment by size bin**				**Calculated particle mass by size bin**	
Sorts	**Avg conc. (#/mL)**	**Exp. conc. range (#/mL) N=2**	**Est. conc. range based on (2 RSD) (#/mL) N=9**	**ECD (μm)**	**Avg conc. (#/mL**	**Avg enrichment (%)**	**Conc. range (#/mL)**	**Enrichment range (%)**	**Avg mass protein (ng)**	**mass range protein (ng)**
				1-2	67400	94	56000-79000	92-97	2.9	2.4 - 3.3
				2-5	3500	5	2700-4400	3-7	1.5	1.0-1.9
		61100-	49000-	*5-10*	280	0	60-500	0-1	2.1	0.5-3.6
I	71300	81400	110000	*>10*	100	0	50-150	0	5.1	2.4-7.8
				1-2	14400	47	12700-16000	44-50	1	0.8-1.2
				2-5	16300	52	12400-20100	49-55	9.6	6.8-12
		25500-	22000-	*5-10*	400	1	360-380	1	1.3	1.2-1.4
II	31000	36500	51000	*>10*	20	0	13-30	0	7.5	1.0-14
				1-2	30000	28	25200-34700	26-29	1.7	1.4-2.0
				2-5	28200	26	23000-33800	25-26	28	21-36
		85900-	81000-	*5-10*	48000	43	35300-60700	41-45	345	241-449
III	110400	13500	190000	*>10*	4200	4	2900-5600	3-4	119	90-147
				1-2	21200	46	16100-26200	42-51	1.2	0.9-1.5
				2-5	14300	31	10300-18300	30-32	11	7.3-14
		32000-	37000-	*5-10*	8000	16	4100-12000	13-19	71	32-110
IV	46900	62000	87000	*>10*	3400	7	1400-5500	4-9	103	45-162

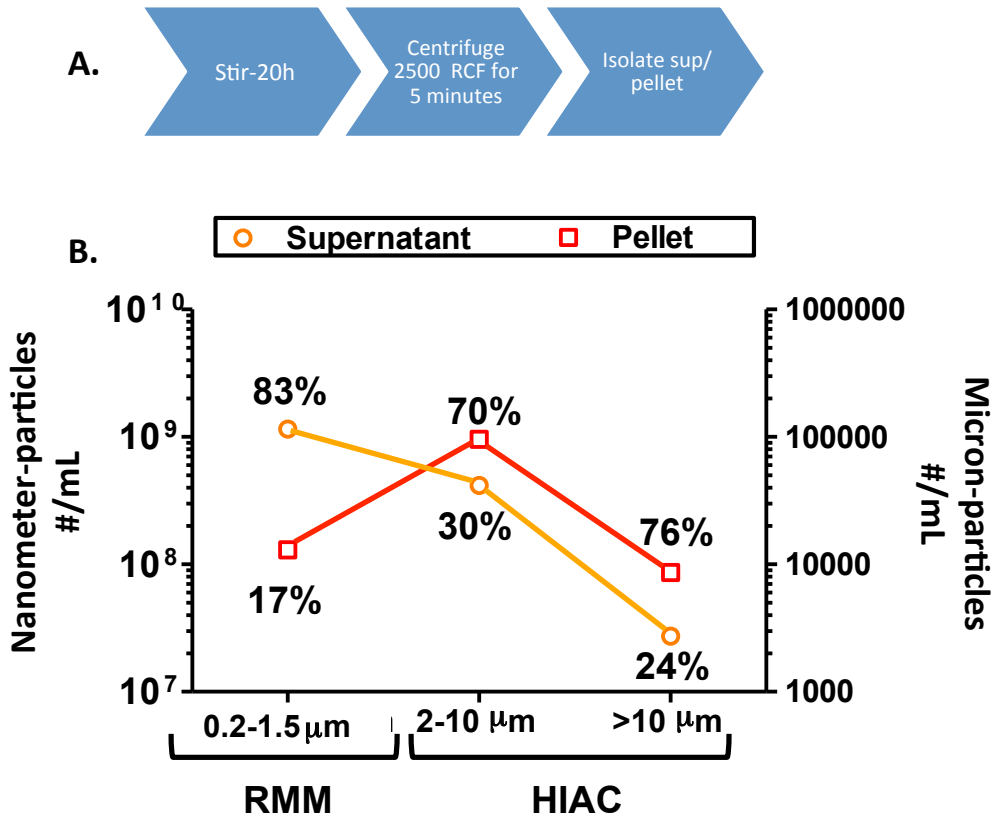

Figure 4.1. Separation of nanometer vs. micron sized stirring induced particles of mAb2 by low speed centrifugation. (A) Schematic of experimental setup, (B) particle number and size distributions of the fractionated samples are shown in three different size ranges. The concentration of smaller particles (0.2-1.5µm) for both supernatant and pellet were obtained by Resonant Mass Measurement (RMM; estimated RSD ~30 %, see text). The concentration of particles 2 to >10 µm was obtained from light obscuration measurements (HIAC; estimated RSD 1-8%, see text). The percentages were calculated by dividing the number of particles in either the supernatant or pellet by the total number of particles present in both supernatant and pellet at a particular size range.

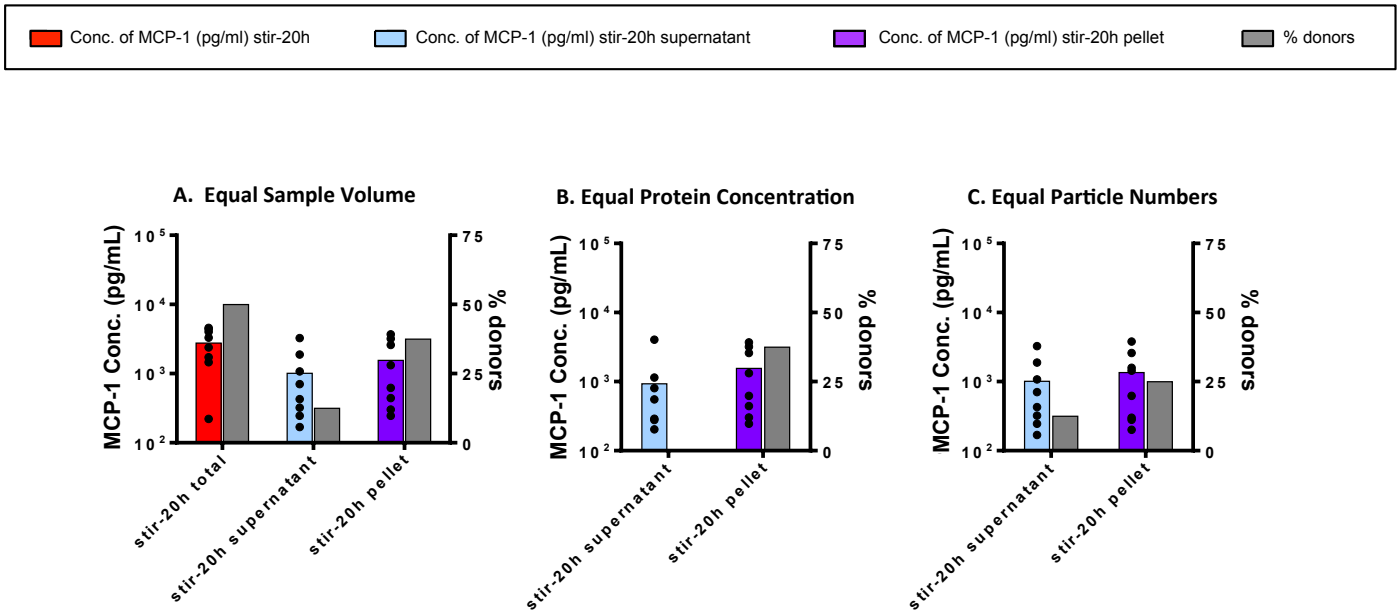

Figure 4.2. Peripheral blood mononuclear cells (PBMC) from 8 human donors were incubated with solutions of mAb2 particles (see Figure 4.1) and examined for the release of MCP-1. MCP-1 was measured by electro-chemiluminescence at the early phase (20 h incubation) at (A) equal sample volume, (B) equal protein concentration, and (C) equal particle numbers. The average concentration (n=8, *colored bars*) of MCP-1 and percentage of donors that responded (*gray bars*) to the aggregated mAb (two fold above the unstressed mAb2) is shown. The black dots represent the concentration of MCP-1 secreted by each individual donor. Different aggregate samples are shown horizontally as follows; stir-20h total (*red*), stir-20h supernatant (enriched in nanometer size particles; *light blue*), and stir-20h pellet (enriched in micron sized particles; *purple*); see Figure 4.1. The media and buffer-stressed controls responded far below the threshold, and the LPS positive control responded much more intensely (SI>>2.0) than the aggregated protein samples (data not shown).

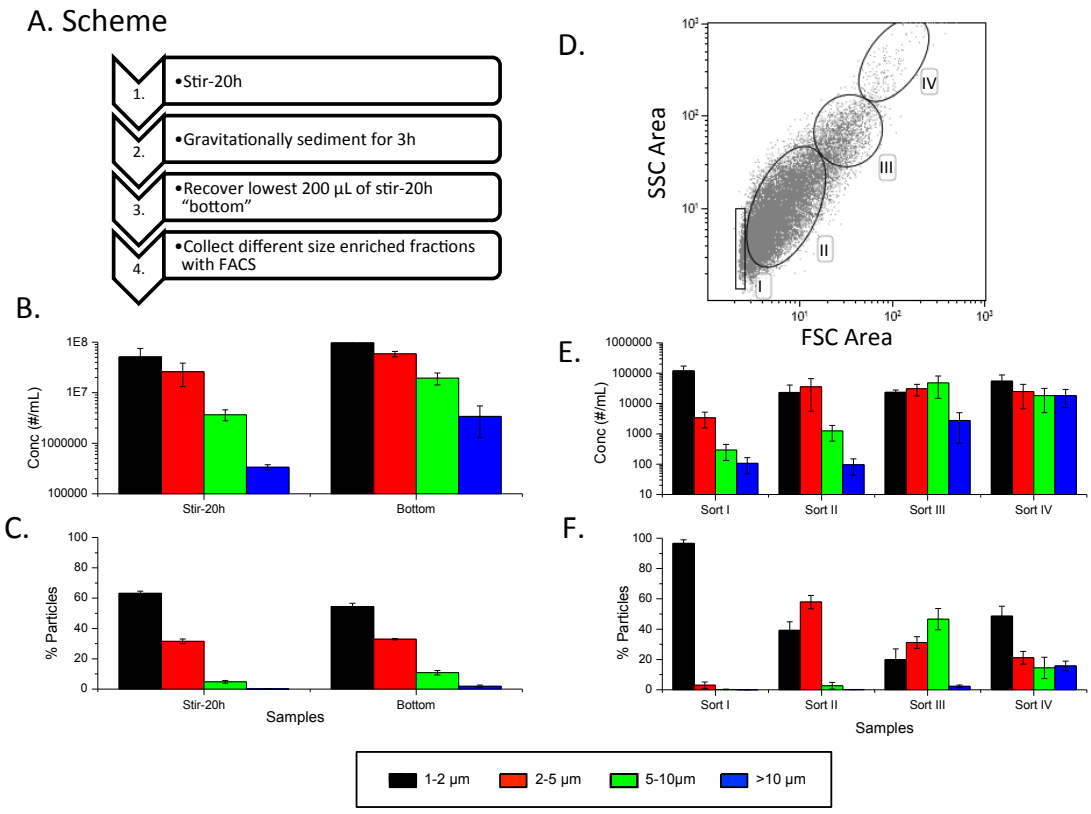

Figure 4.3. Enrichment of different micron sized mAb2 particle populations using FACS separation. (A) Flowchart of experimental steps, (B) subvisible particle counts in stirred sample (stir-20h) and bottom fraction after gravitational settling (bottom sample) as measured by MFI, (C) the percentage of particles in each size bin for these same two samples. (D) Upon FACS sorting the bottom sample, a two dimensional dot plot of response from forward vs side scattering signals (FSC Area vs. SSC Area) is generated with gatings labeled Sort I-IV, (E) Sorts I-IV were analyzed for subvisible particle distribution with MFI, and (F) the percentage of particles in each size bin were determined. The graphs represent the average of three separate experiments (N=3) with the error bars representing one standard deviation.

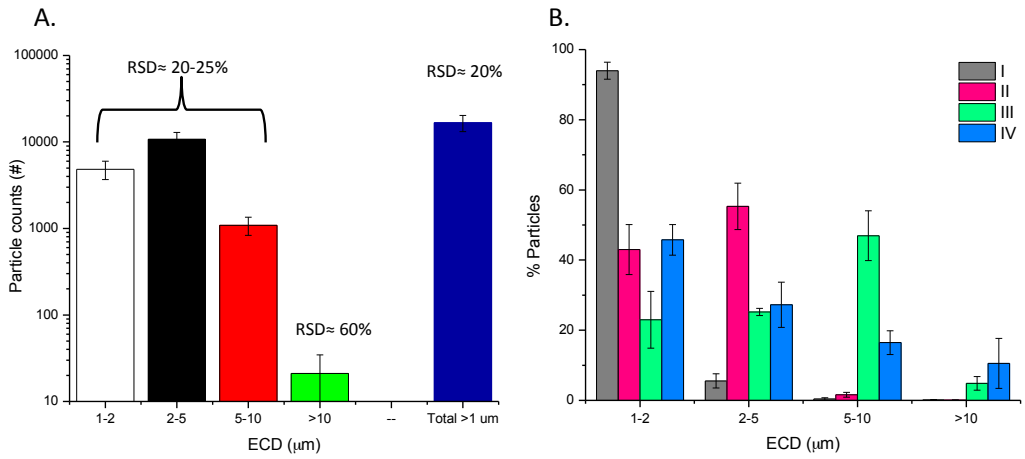

Figure 4.4. Determination of relative standard deviation (% RSD) of MFI particle counting and determination of enrichment factors for FACS separated samples of mAb2 particles. (A) Representative FACS sorted sample of stir-induced aggregated mAb2, obtained as outlined in Figure 4.3 and having undergone two freeze-thaw cycles, was used for repeat MFI testing to determine % RSD as a function of particle size bins (N=9 with the error bars representing one standard deviation), and (B) Enrichment analysis of FACS sorted samples (Sort I, II, III, IV) after undergoing two freeze-thaw cycles. Data are an average of three separate experiments (N=3) with the error bars representing one standard deviation.

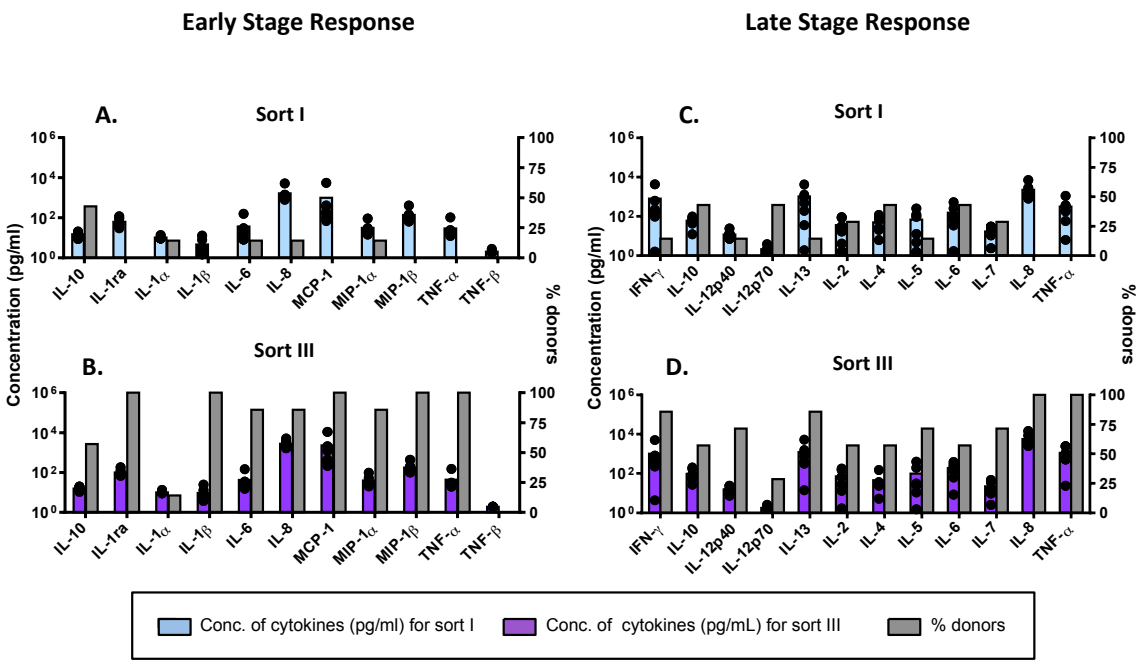

Figure 4.5. Peripheral blood mononuclear cells (PBMC) from 7 human donors were incubated with mAb2 particle samples collected from the FACS separation and analyzed for cytokine release. Sort I (containing enriched 1-2 µm particles) (A, C) and Sort III (containing enriched 5-10 µm particles) (B, D) from FACS separation as well as the relevant controls were tested for the release of cytokines by multiplex cytokine analysis at the early phase (20 h) (A, B) and late phase (7 day) (C, D) at equal volume. The average concentration across donors (N=7, *colored bars*) of the 11 cytokines tested at the early phase (A, B) and 12 cytokines tested at the late phase (C, D) is shown. The percentage of responding donors (*gray bars*) represents the number of the 8 donors tested that responded higher (by magnitude of secreted cytokine) to each sort. The black dots represent the concentration of cytokines secreted by each individual donor. The LPS and PHA positive control responded much more intensely (SI>>2.0) than the aggregated protein samples (data not shown).

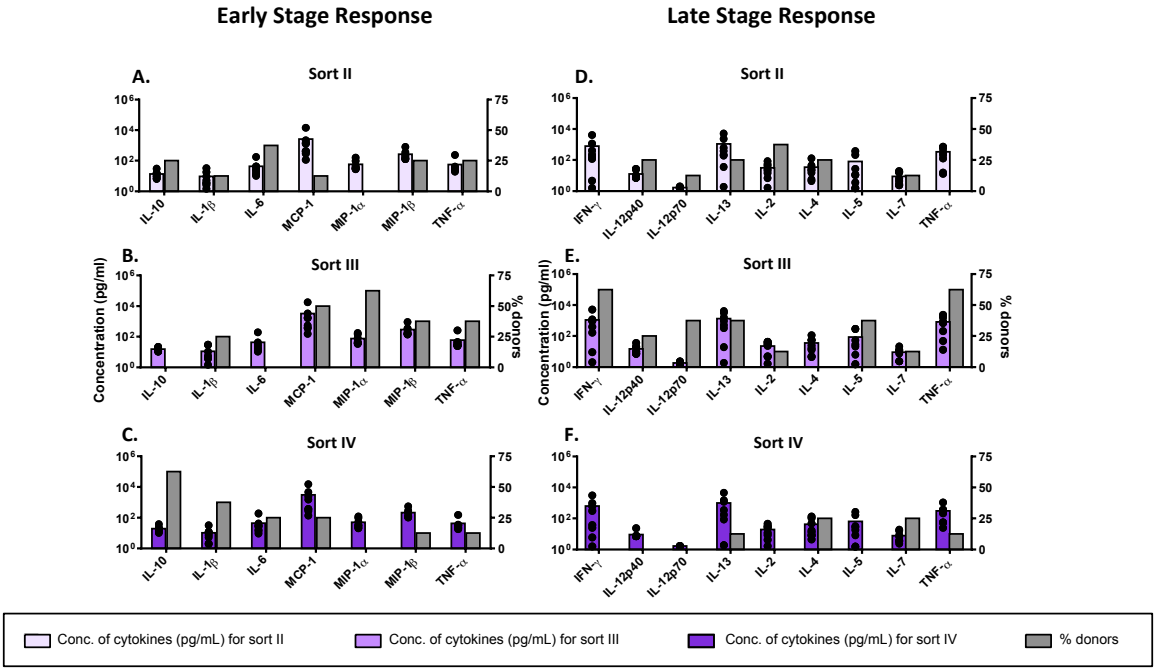

Figure 4.6. Peripheral blood mononuclear cells (PBMC) from 8 human donors were incubated with FACS isolated mAb2 particle samples (containing very little soluble aggregates): Sort II (enriched in 2-5 μm particles) (A, D), Sort III (enriched for 5-10 μm particles) (B, E), and Sort IV (enriched for particles > 10 μm) (C, F) at similar particle numbers and analyzed for their cytokine release. These FACS samples as well as the relevant controls were tested for the release of signature cytokines by multiplex cytokine analysis at the early phase (20h) and late phase (7 days). The average concentration across donors (N=8, *colored bars*) of the 7 cytokines tested at the early phase and 9 cytokines tested at the late phase is shown. The percentage of responding donors (*gray bars*) represents the number of the 8 donors tested that responded higher (by magnitude of secreted cytokines) to each sort. The black dots represent the concentration of cytokines secreted by each individual donor.

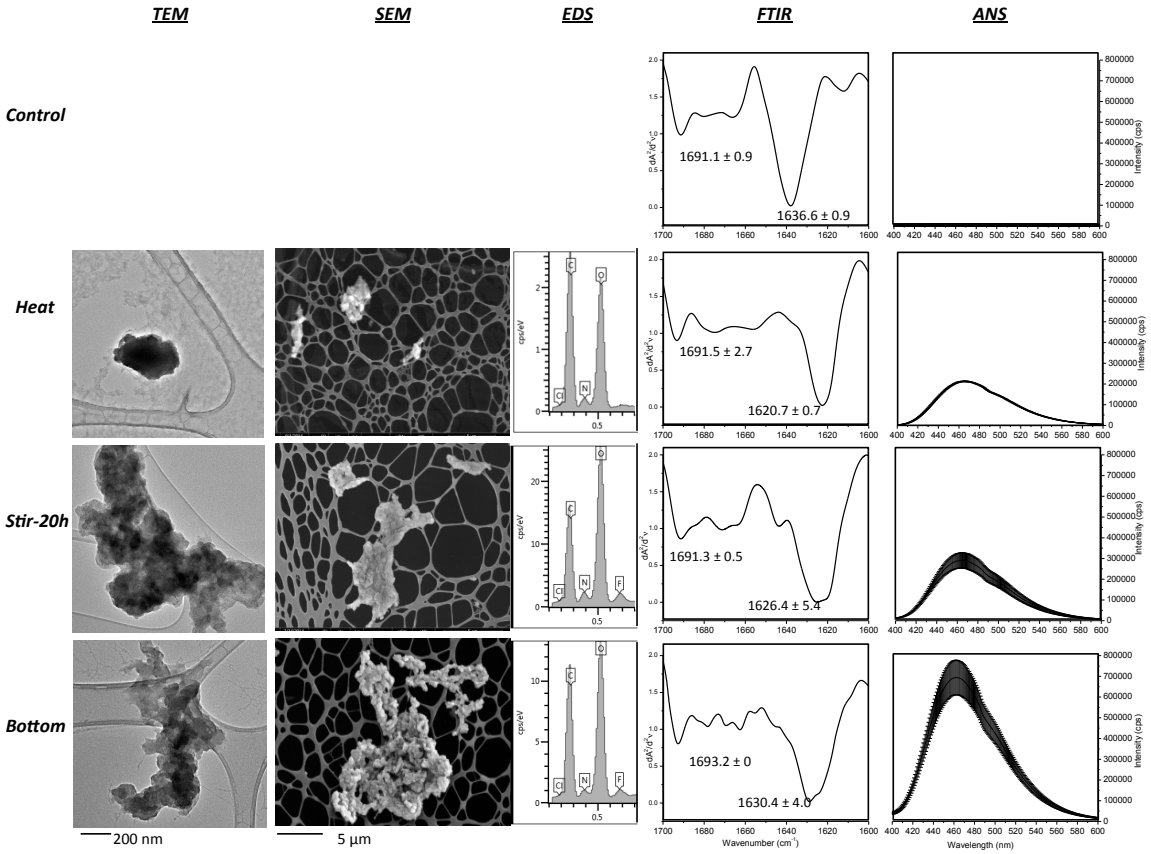

Figure 4.7. Biophysical analysis of mAb2 solutions containing stirring-induced particles that were used as starting material for FACS separation. Control samples (unstressed and heat denatured) and two stirred samples (Stir-20h, Bottom) of mAb2 were characterized for morphology by SEM and TEM, composition by EDS, overall secondary structure by solution FTIR and FTIR microscopy, and surface hydrophobicity by extrinsic fluorescence using 1,8-ANS as indicated in this Figure. Representative TEM and SEM are shown at two resolutions (the unstressed control had virtually no particles so no TEM and SEM images are shown). For FTIR analysis, shifts in two peaks for intramolecular beta sheet content (occurring between 1620 to 1640 cm^{-1} and 1690 to 1700 cm^{-1}) were monitored in the second derivative FTIR spectra. The peak minima are shown for each sample (N=3 with the error bars representing one standard deviation).

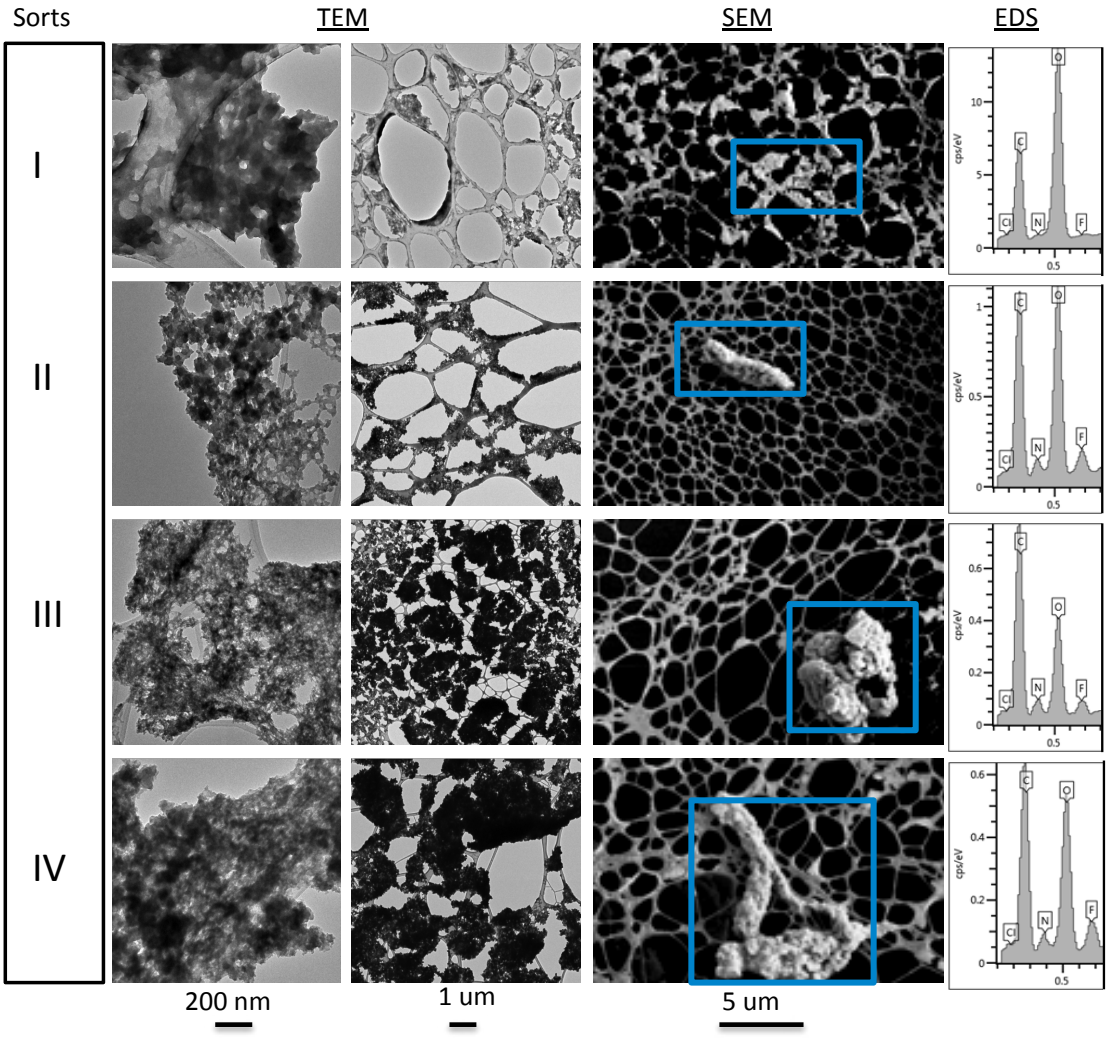

Figure 4.8. Representative TEM (200 nm and 1 µm resolution) and SEM (5 µm resolution) images of mAb2 particles of four different FACS sorted samples (Sort I, II, III, IV). The SEM particle images (representative graphs shown here), selected by the blue boxes, were also analyzed for their elemental composition by EDS as shown in far right column of figure.

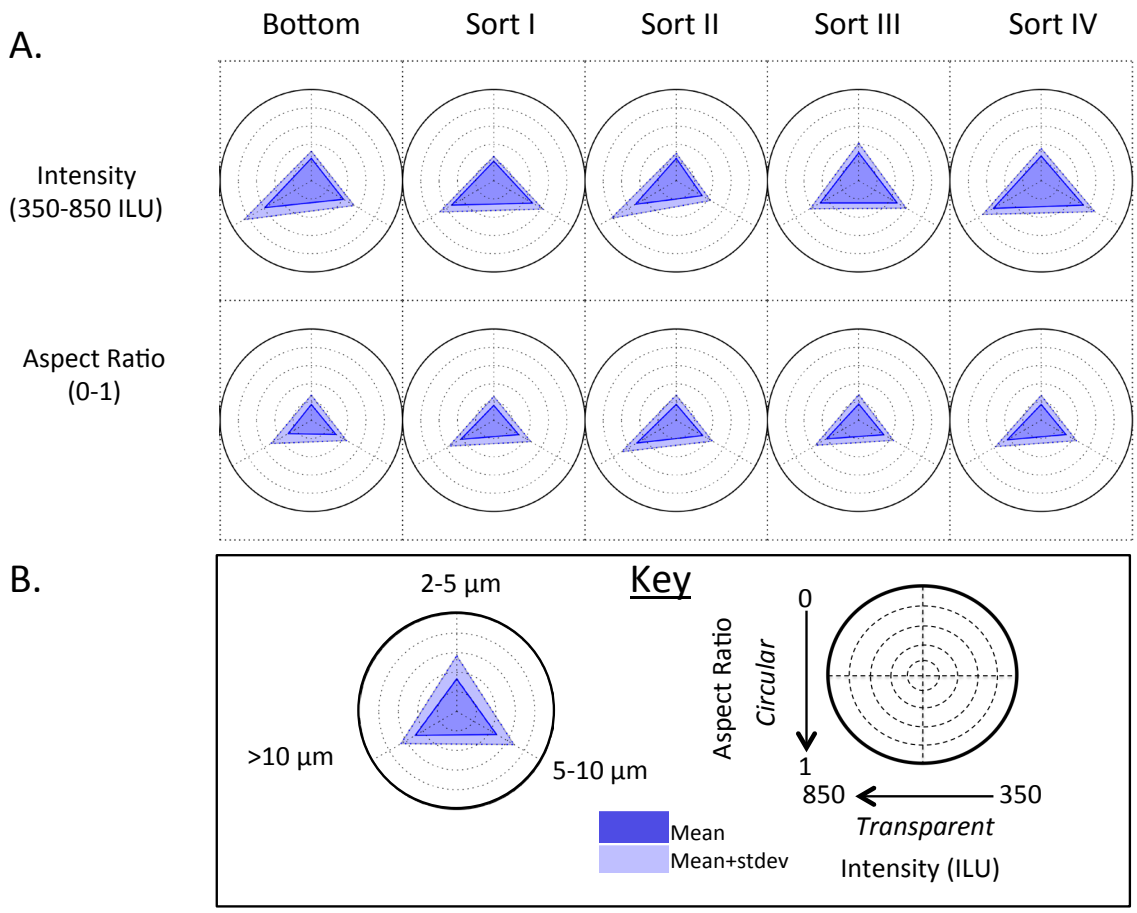

Figure 4.9. Radar plots of MFI morphology data (aspect ratio and intensity; refer to the key in Panel B) for subvisible particles of mAb2 present in the starting material for FACS (bottom sample) and FACS sorted samples (Sorts II-IV, see text) are shown in A. Radar plots show MFI morphology data distributions of the micron sized particles that fall within each of the three size bins shown in the key of Panel B). The data shown are the average of three separate experiments (N = 3) and the error represents one standard deviation.

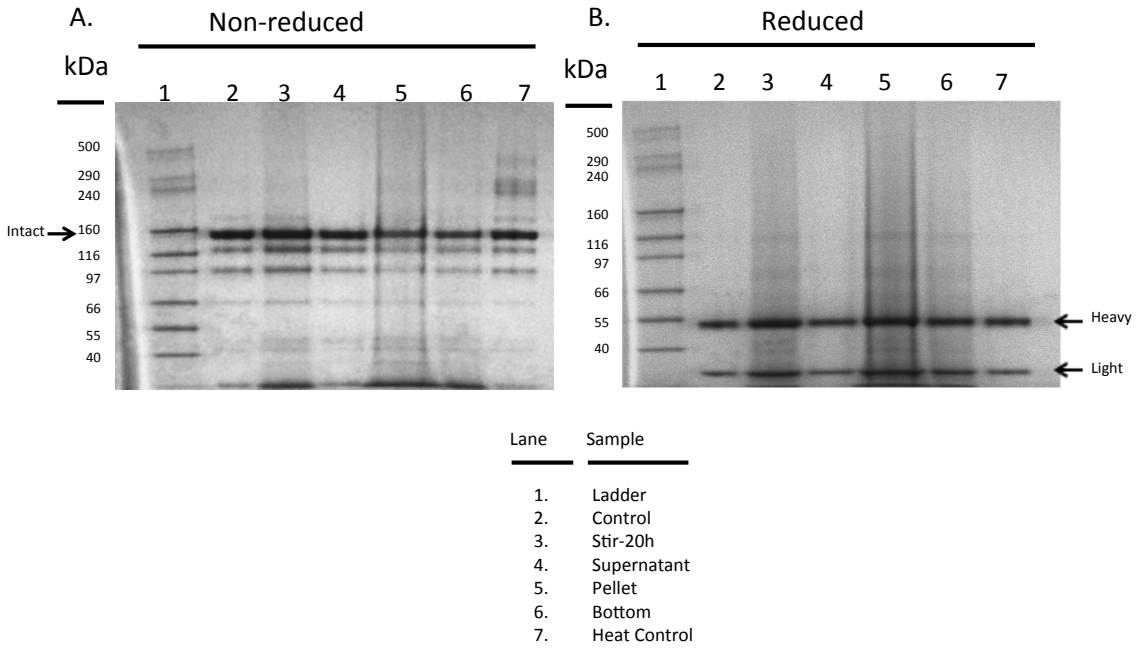

Figure 4.10. **(**A) Nonreduced and (B) reduced SDS-PAGE gels of control mAb2 (unstressed), heat denatured mAb2, and two stirred mAb2 samples (stir-20h, bottom) in A5 buffer. The bottom sample is the starting material for the FACS separation (see text). MW standards are shown with indicated values in kDa. Please note the additional samples in the gel correspond to the supernatant and pellet samples of stirred mAb2 solutions from the slow speed centrifugation approach described in the Methods.

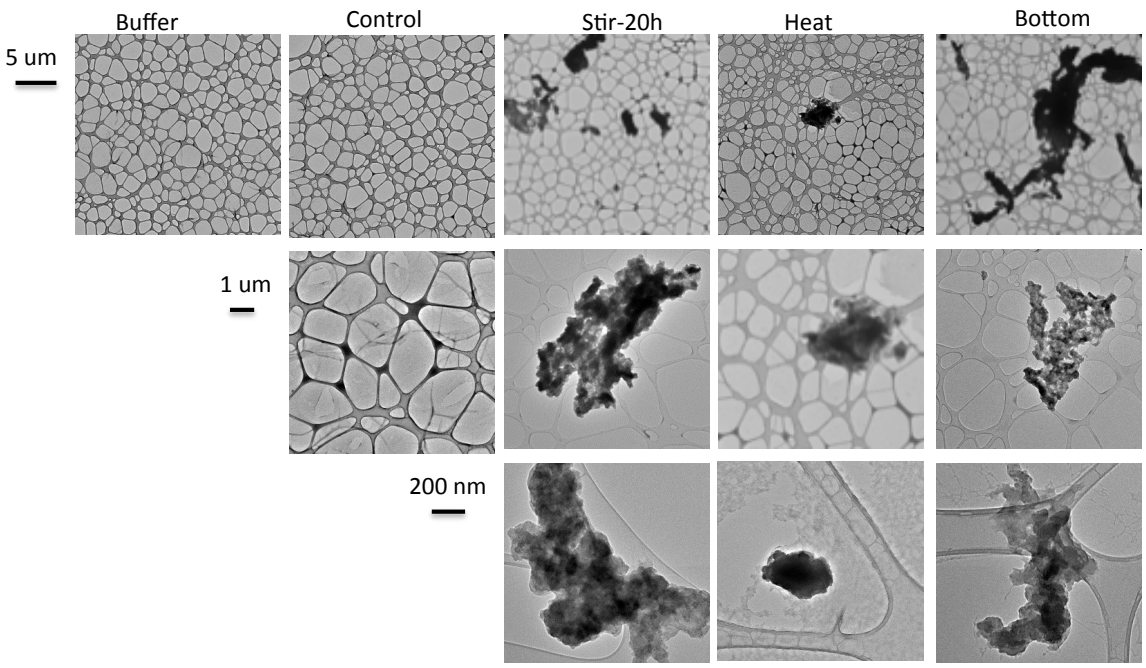

Figure 4.11. Representative TEM images at three size scales of buffer (sodium acetate buffer, pH 5), control mAb2 (unstressed), heat denatured mAb2, and two mAb2 stirred samples (stir-20h, bottom) in A5 buffer. The bottom sample is the starting material for the FACS separation (see text).

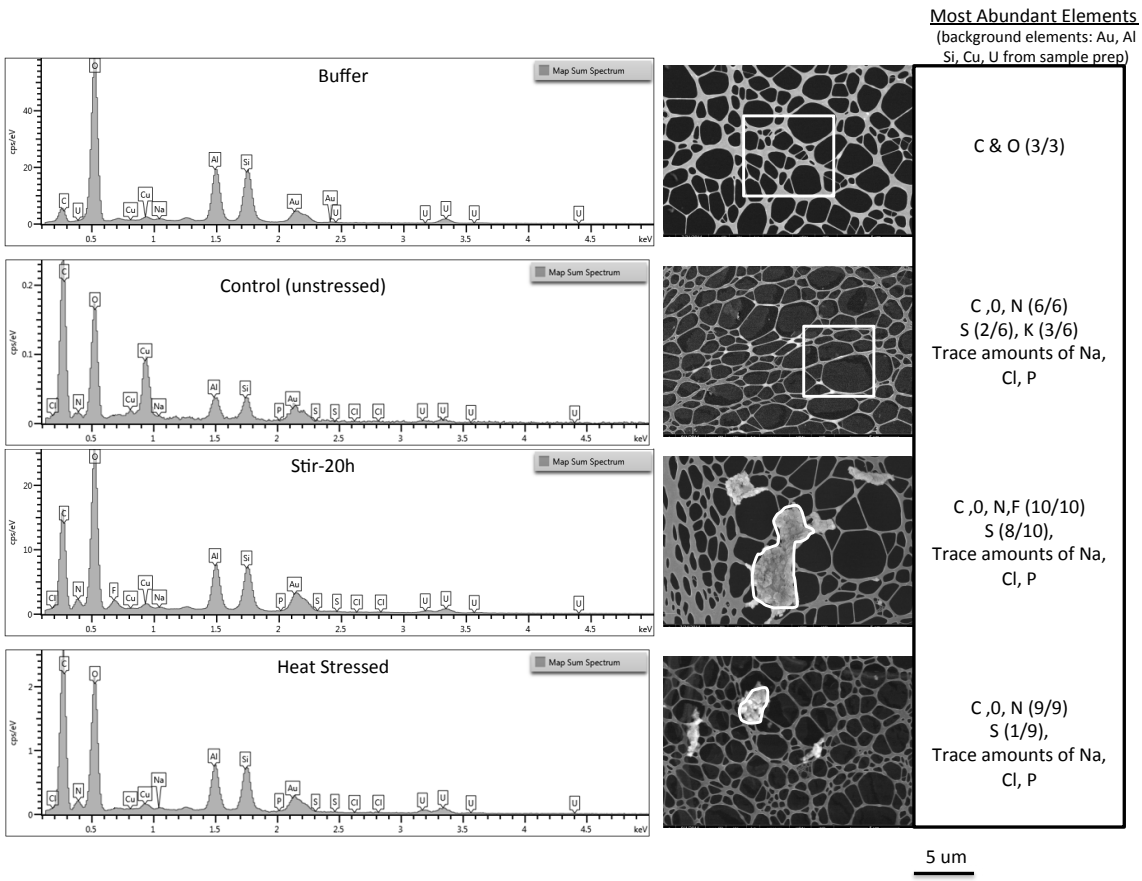

Figure 4.12. Representative EDS spectra and SEM images of buffer (sodium acetate buffer, pH 5), unstressed, heat denatured, and two stirred samples (stir-20h, bottom) of mAb2 in A5 buffer. The bottom sample is the starting material for the FACS separation (see text). Regions in the SEM images (indicated by the white boxes or shapes) were selected for elemental composition determination. Elements in greatest abundance are shown on the right hand side of the figure in ratio form. The numerator depicts the number of times an element is detected in a region while the denominator depicts the total number of regions analyzed. All samples show background levels of carbon and oxygen, uranium, copper, aluminum, silicon, and gold coming from the sample grids, sample studs, and coating required for acquiring proper images.

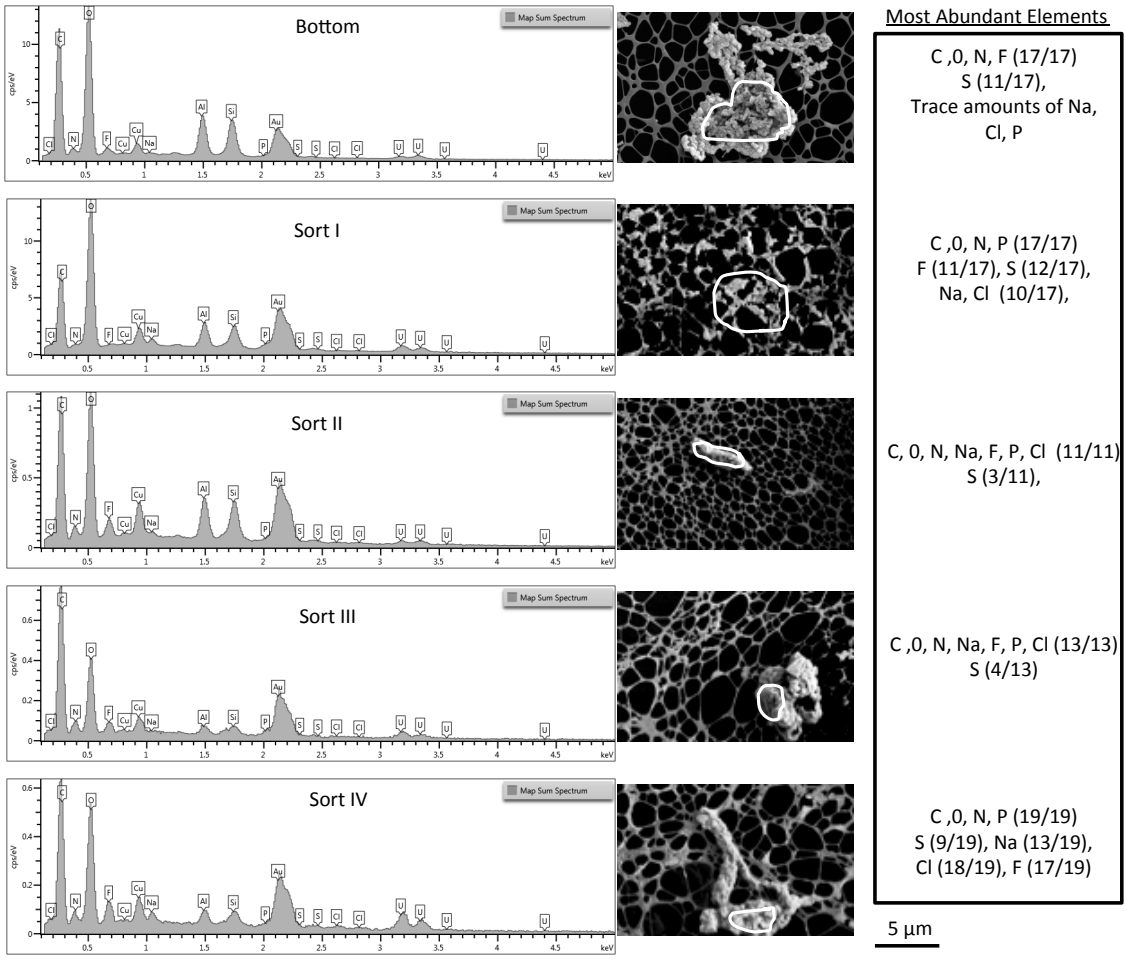

Figure 4.13. Representative EDS spectra and SEM images of bottom and FACS sorted samples (I, II, III, IV) are shown. Regions in the SEM images (indicated by the white shapes) were selected for elemental composition determination. Elements in greatest abundance are shown on the right hand side of the figure in ratio form. The numerator depicts the number of times an element is detected in a region while the denominator depicts the total number of regions analyzed. All samples show background levels of carbon and oxygen, uranium, copper, aluminum, silicon, and gold coming from the sample grids, sample studs, and coating required for acquiring proper images.

4.6 REFERENCES

1. Baker MP, Reynolds HM, Lumicisi B, Bryson CJ 2010. Immunogenicity of protein therapeutics: The key causes, consequences and challenges. Self/nonself 1(4):314-322.
2. Boven K, Knight J, Bader F, Rossert J, Eckardt KU, Casadevall N 2005. Epoetin-associated pure red cell aplasia in patients with chronic kidney disease: solving the mystery. Nephrology, dialysis, transplantation : official publication of the European Dialysis and Transplant Association - European Renal Association 20 Suppl 3:iii33-40.
3. Casadevall N 2005. What is antibody-mediated pure red cell aplasia (PRCA)? Nephrology, dialysis, transplantation : official publication of the European Dialysis and Transplant Association - European Renal Association 20 Suppl 4:iv3-8.
4. Chirino AJ, Ary ML, Marshall SA 2004. Minimizing the immunogenicity of protein therapeutics. Drug discovery today 9(2):82-90.
5. Claman HN 1963. Tolerance to a Protein Antigen in Adult Mice and the Effect of Nonspecific Factors. Journal of immunology 91:833-839.
6. Gamble CN 1966. The role of soluble aggregates in the primary immune response of mice to human gamma globulin. International archives of allergy and applied immunology 30(5):446-455.
7. Goudemand J, Rothschild C, Demiguel V, Vinciguerrat C, Lambert T, Chambost H, Borel-Derlon A, Claeyssens S, Laurian Y, Calvez T, FVIII-LFB, Recombinant FVIII study groups 2006. Influence of the type of factor VIII concentrate on the incidence of factor VIII inhibitors in previously untreated patients with severe hemophilia A. Blood 107(1):46-51.
8. Moore WV, Leppert P 1980. Role of aggregated human growth hormone (hGH) in development of antibodies to hGH. The Journal of clinical endocrinology and metabolism 51(4):691-697.
9. Wang W, Roberts CJ editors. 2010. Aggregation of Therapeutic Proteins. ed., Hoboken, NJ: John Wiley & Sons. p 486.
10. Wang W, Singh SK, Li N, Toler MR, King KR, Nema S 2012. Immunogenicity of protein aggregates--concerns and realities. International journal of pharmaceutics 431(1-2):1-11.
11. Mahler HC, Friess W, Grauschopf U, Kiese S 2009. Protein aggregation: pathways, induction factors and analysis. Journal of pharmaceutical sciences 98(9):2909-2934.
12. Cromwell ME, Hilario E, Jacobson F 2006. Protein aggregation and bioprocessing. The AAPS journal 8(3):E572-579.
13. Joubert MK, Luo Q, Nashed-Samuel Y, Wypych J, Narhi LO 2011. Classification and characterization of therapeutic antibody aggregates. The Journal of biological chemistry 286(28):25118-25133.
14. Luo Q, Joubert MK, Stevenson R, Ketchem RR, Narhi LO, Wypych J 2011. Chemical modifications in therapeutic protein aggregates generated under different stress conditions. The Journal of biological chemistry 286(28):25134-25144.
15. Telikepalli SN, Kumru OS, Kalonia C, Esfandiary R, Joshi SB, Middaugh CR, Volkin DB 2014. Structural characterization of IgG1 mAb aggregates and particles generated under various stress conditions. Journal of pharmaceutical sciences 103(3):796-809.
16. Iwura T, Fukuda J, Yamazaki K, Arisaka F 2014. Conformational stability, reversibility and heat-induced aggregation of alpha-1-acid glycoprotein. Journal of biochemistry.

17. Liu L, Braun LJ, Wang W, Randolph TW, Carpenter JF 2014. Freezing-induced perturbation of tertiary structure of a monoclonal antibody. Journal of pharmaceutical sciences 103(7):1979-1986.
18. Sahin E, Grillo AO, Perkins MD, Roberts CJ 2010. Comparative effects of pH and ionic strength on protein-protein interactions, unfolding, and aggregation for IgG1 antibodies. Journal of pharmaceutical sciences 99(12):4830-4848.
19. Sharma B 2007. Immunogenicity of therapeutic proteins. Part 2: impact of container closures. Biotechnology advances 25(3):318-324.
20. Shire SJ, Shahrokh Z, Liu J 2004. Challenges in the development of high protein concentration formulations. Journal of pharmaceutical sciences 93(6):1390-1402.
21. Wang W 2005. Protein aggregation and its inhibition in biopharmaceutics. International journal of pharmaceutics 289(1-2):1-30.
22. Wiesbauer J, Prassl R, Nidetzky B 2013. Renewal of the air-water interface as a critical system parameter of protein stability: aggregation of the human growth hormone and its prevention by surface-active compounds. Langmuir : the ACS journal of surfaces and colloids 29(49):15240-15250.
23. Schellekens H 2005. Factors influencing the immunogenicity of therapeutic proteins. Nephrology, dialysis, transplantation : official publication of the European Dialysis and Transplant Association - European Renal Association 20 Suppl 6:vi3-9.
24. Ponce R, Abad L, Amaravadi L, Gelzleichter T, Gore E, Green J, Gupta S, Herzyk D, Hurst C, Ivens IA, Kawabata T, Maier C, Mounho B, Rup B, Shankar G, Smith H, Thomas P, Wierda D 2009. Immunogenicity of biologically-derived therapeutics: assessment and interpretation of nonclinical safety studies. Regulatory toxicology and pharmacology : RTP 54(2):164-182.
25. Schellekens H 2002. Immunogenicity of therapeutic proteins: clinical implications and future prospects. Clinical therapeutics 24(11):1720-1740; discussion 1719.
26. Jahn EM, Schneider CK 2009. How to systematically evaluate immunogenicity of therapeutic proteins-regulatory considerations. N Biotechnol 25(5):280-286.
27. Johnson R, Jiskoot W 2012. Models for evaluation of relative immunogenic potential of protein particles in biopharmaceutical protein formulations. Journal of pharmaceutical sciences 101(10):3586-3592.
28. Perry LC, Jones TD, Baker MP 2008. New approaches to prediction of immune responses to therapeutic proteins during preclinical development. Drugs in R&D 9(6):385-396.
29. Koren E, De Groot AS, Jawa V, Beck KD, Boone T, Rivera D, Li L, Mytych D, Koscec M, Weeraratne D, Swanson S, Martin W 2007. Clinical validation of the "in silico" prediction of immunogenicity of a human recombinant therapeutic protein. Clinical immunology 124(1):26-32.
30. Tatarewicz SM, Wei X, Gupta S, Masterman D, Swanson SJ, Moxness MS 2007. Development of a maturing T-cell-mediated immune response in patients with idiopathic Parkinson's disease receiving r-metHuGDNF via continuous intraputaminal infusion. Journal of clinical immunology 27(6):620-627.
31. Wullner D, Zhou L, Bramhall E, Kuck A, Goletz TJ, Swanson S, Chirmule N, Jawa V 2010. Considerations for optimization and validation of an in vitro PBMC derived T cell assay for immunogenicity prediction of biotherapeutics. Clinical immunology 137(1):5-14.

32. Jaber A, Baker M 2007. Assessment of the immunogenicity of different interferon beta-1a formulations using ex vivo T-cell assays. Journal of pharmaceutical and biomedical analysis 43(4):1256-1261.
33. Stickler M, Rochanayon N, Razo OJ, Mucha J, Gebel W, Faravashi N, Chin R, Holmes S, Harding FA 2004. An in vitro human cell-based assay to rank the relative immunogenicity of proteins. Toxicological sciences : an official journal of the Society of Toxicology 77(2):280-289.
34. Brinks V, Jiskoot W, Schellekens H 2011. Immunogenicity of therapeutic proteins: the use of animal models. Pharmaceutical research 28(10):2379-2385.
35. Hermeling S, Aranha L, Damen JM, Slijper M, Schellekens H, Crommelin DJ, Jiskoot W 2005. Structural characterization and immunogenicity in wild-type and immune tolerant mice of degraded recombinant human interferon alpha2b. Pharmaceutical research 22(12):1997-2006.
36. Braun A, Kwee L, Labow MA, Alsenz J 1997. Protein aggregates seem to play a key role among the parameters influencing the antigenicity of interferon alpha (IFN-alpha) in normal and transgenic mice. Pharmaceutical research 14(10):1472-1478.
37. Stewart TA, Hollingshead PG, Pitts SL, Chang R, Martin LE, Oakley H 1989. Transgenic mice as a model to test the immunogenicity of proteins altered by site-specific mutagenesis. Mol Biol Med 6(4):275-281.
38. Whiteley PJ, Lake JP, Selden RF, Kapp JA 1989. Tolerance induced by physiological levels of secreted proteins in transgenic mice expressing human insulin. The Journal of clinical investigation 84(5):1550-1554.
39. Gaitonde P, Balu-Iyer SV 2011. In vitro immunogenicity risk assessment of therapeutic proteins in preclinical setting. Methods in molecular biology 716:267-280.
40. Joubert MK, Hokom M, Eakin C, Zhou L, Deshpande M, Baker MP, Goletz TJ, Kerwin BA, Chirmule N, Narhi LO, Jawa V 2012. Highly aggregated antibody therapeutics can enhance the in vitro innate and late-stage T-cell immune responses. The Journal of biological chemistry 287(30):25266-25279.
41. Narhi LO, Schmit J, Bechtold-Peters K, Sharma D 2012. Classification of protein aggregates. Journal of pharmaceutical sciences 101(2):493-498.
42. Rombach-Riegraf V, Allard C, Angevaare E, Matter A, Ossuli B, Strehl R, Raulf F, Bluemel M, Egodage K, Jeschke M, Koulov AV 2013. Size fractionation of microscopic protein aggregates using a preparative fluorescence-activated cell sorter. Journal of pharmaceutical sciences 102(7):2128-2135.
43. Espargaro A, Sabate R, Ventura S 2012. Thioflavin-S staining coupled to flow cytometry. A screening tool to detect in vivo protein aggregation. Molecular bioSystems 8(11):2839-2844.
44. Mach H, Bhambhani A, Meyer BK, Burek S, Davis H, Blue JT, Evans RK 2011. The use of flow cytometry for the detection of subvisible particles in therapeutic protein formulations. Journal of pharmaceutical sciences 100(5):1671-1678.
45. Nishi H, Mathas R, Furst R, Winter G 2014. Label-free flow cytometry analysis of subvisible aggregates in liquid IgG1 antibody formulations. Journal of pharmaceutical sciences 103(1):90-99.
46. Ludwig DB, Trotter JT, Gabrielson JP, Carpenter JF, Randolph TW 2011. Flow cytometry: a promising technique for the study of silicone oil-induced particulate formation in protein formulations. Analytical biochemistry 410(2):191-199.
47. Bi V, Jawa V, Joubert MK, Kaliyaperumal A, Eakin C, Richmond K, Pan O, Sun J, Hokom M, Goletz TJ, Wypych J, Zhou L, Kerwin BA, Narhi LO, Arora T 2013. Development of

a human antibody tolerant mouse model to assess the immunogenicity risk due to aggregated biotherapeutics. Journal of pharmaceutical sciences 102(10):3545-3555.
48. Shukla AA, Hubbard B, Tressel T, Guhan S, Low D 2007. Downstream processing of monoclonal antibodies--application of platform approaches. Journal of chromatography B, Analytical technologies in the biomedical and life sciences 848(1):28-39.
49. Kalonia C, Kumru OS, Kim JH, Middaugh CR, Volkin DB 2013. Radar chart array analysis to visualize effects of formulation variables on IgG1 particle formation as measured by multiple analytical techniques. Journal of pharmaceutical sciences 102(12):4256-4267.
50. Kalonia C, Kumru OS, Prajapati I, Mathaes R, Engert J, Zhou S, Middaugh CR, Volkin DB 2014. Calculating the mass of subvisible protein particles with improved accuracy using micro-flow imaging data. J Pharm Sci In press.
51. Mach H, Middaugh CR 2010. Ultraviolet spectroscopy as a tool in therapeutic protein development. Journal of pharmaceutical sciences 100(4):1214-1227.
52. Kumru OS, Liu J, Ji JA, Cheng W, Wang YJ, Wang T, Joshi SB, Middaugh CR, Volkin DB 2012. Compatibility, physical stability, and characterization of an IgG4 monoclonal antibody after dilution into different intravenous administration bags. Journal of pharmaceutical sciences 101(10):3636-3650.
53. Jiao N. 2014. Personal Communication. ed.
54. Shapiro HM. 2003. Practical Flow Cytometry. ed., New Jersey: Wiley. p 681.
55. Kim JH, Iyer V, Joshi SB, Volkin DB, Middaugh CR 2012. Improved data visualization techniques for analyzing macromolecule structural changes. Protein science : a publication of the Protein Society 21(10):1540-1553.
56. Hermeling S, Schellekens H, Maas C, Gebbink MF, Crommelin DJ, Jiskoot W 2006. Antibody response to aggregated human interferon alpha2b in wild-type and transgenic immune tolerant mice depends on type and level of aggregation. Journal of pharmaceutical sciences 95(5):1084-1096.
57. Johansen P, Senti G, Martinez Gomez JM, Wuthrich B, Bot A, Kundig TM 2005. Heat denaturation, a simple method to improve the immunotherapeutic potential of allergens. European journal of immunology 35(12):3591-3598.
58. Fradkin AH, Carpenter JF, Randolph TW 2009. Immunogenicity of aggregates of recombinant human growth hormone in mouse models. Journal of pharmaceutical sciences 98(9):3247-3264.
59. Filipe V, Jiskoot W, Basmeleh AH, Halim A, Schellekens H, Brinks V 2012. Immunogenicity of different stressed IgG monoclonal antibody formulations in immune tolerant transgenic mice. mAbs 4(6):740-752.
60. Fradkin AH, Mozziconacci O, Schoneich C, Carpenter JF, Randolph TW 2014. UV photodegradation of murine growth hormone: chemical analysis and immunogenicity consequences. European journal of pharmaceutics and biopharmaceutics : official journal of Arbeitsgemeinschaft fur Pharmazeutische Verfahrenstechnik eV 87(2):395-402.
61. Rombach-Riegraf V, Karle AC, Wolf B, Sorde L, Koepke S, Gottlieb S, Krieg J, Djidja MC, Baban A, Spindeldreher S, Koulov AV, Kiessling A 2014. Aggregation of human recombinant monoclonal antibodies influences the capacity of dendritic cells to stimulate adaptive T-cell responses in vitro. PloS one 9(1):e86322.
62. Van Beers MM, Gilli F, Schellekens H, Randolph TW, Jiskoot W 2012. Immunogenicity of recombinant human interferon beta interacting with particles of glass, metal, and polystyrene. Journal of pharmaceutical sciences 101(1):187-199.

63. van Beers MM, Sauerborn M, Gilli F, Brinks V, Schellekens H, Jiskoot W 2011. Oxidized and aggregated recombinant human interferon beta is immunogenic in human interferon beta transgenic mice. Pharmaceutical research 28(10):2393-2402.
64. Fradkin AH, Carpenter JF, Randolph TW 2011. Glass particles as an adjuvant: a model for adverse immunogenicity of therapeutic proteins. Journal of pharmaceutical sciences 100(11):4953-4964.
65. Seong SY, Matzinger P 2004. Hydrophobicity: an ancient damage-associated molecular pattern that initiates innate immune responses. Nature reviews Immunology 4(6):469-478.

CHAPTER 5: Summary, Conclusions, and Future Directions

5.1 SUMMARY AND CONCLUSIONS

The impact of protein aggregate and particle formation in biotherapeutics has been discussed extensively in literature. Their presence can potentially impact the safety, pharmacodynamics, and efficacy of protein biologics upon patient administration. The United States Pharmacopeia (USP) and European Pharmacopeia (EP) have some guidelines for assessing protein subvisible particles[1]. For example, <USP 788> has defined limits for subvisible particulates greater than 10 and 25 μm based on light obscuration measurements.[1,2] These guidelines, however, were not established to monitor inherent, product related particles, but rather the presence of process related extrinsic particles because of their possibility of obstructing capillaries. No general guidelines exist for protein, product related subvisible particles or smaller aggregates and specifications are usually set on a case-by-case basis, especially since different analytical technologies may be required. For example, limits on the number of protein aggregates in the 0.2 to 10 μm size range have not been generally specified, even though they have been suspected of producing increased immunogenicity risk.[3,4]

As detailed in many studies, [5-8] aggregate size may not be the only factor that may impact immunogenicity. In addition to size, aggregates can be classified in terms of morphology, reversibility, and the nature of the protein within the aggregates including covalent linking and higher order structure.[9] Therefore it is important that in addition to sizing and counting, physicochemical characterization of aggregates is performed as well. This rationale is the general theme of studies performed in Chapter 2.

Characterization of aggregates is the first step to better understanding their clinical impacts. Regulatory agencies strongly suggest that protein therapeutics be subjected to various accelerated stress conditions and the resulting aggregates be monitored and assessed, often

requiring the use of a variety of methods. Stress conditions typically encountered by a protein drug throughout various stages of manufacturing and shipping include thermal stresses, mechanical stresses, and freeze-thaw, among others. In Chapter 2, we investigated the aggregation behavior of an IgG1 mAb as it is subjected to four different environmental stresses, with and without NaCl. The resulting aggregates and particles were analyzed by a variety of sizing and counting techniques. The stresses used were shaking, stirring, freeze-thaw, and thermal stresses. The aggregates generated in the presence of NaCl were extensively characterized in terms of morphology, covalent-crosslinking, and the structure of the protein within protein particles. Depending on the stress, very different types of aggregates formed, resulting from structural changes, colloidal interactions or a combination of the two. Comparisons with other, similar studies in the literature suggested that both the solution conditions and the nature of the protein itself also determine the type of aggregates generated. In some instances, it was shown that the type of stress greatly impacts the types of aggregates formed. This chapter was a case study that underscores the importance of characterizing the types of protein aggregates that result from different types of environmental stresses. The importance of analytical methodology development cannot be emphasized enough as it can lead to more accurate characterization of protein aggregates across a large size range and can serve as the foundation for a better understanding of potential clinical consequences as a result of these aggregates.

Shaking experiments have often been used to mimic shipping and transportation stresses. There are an abundance of studies looking at the impact of this stress on solution-based protein formulations, but very few publications, if any, looking at the impact of this stress on lyophilized protein therapeutic dosage forms. Previous studies have often focused primarily on stresses

encountered during the lyophilization process (e.g., freezing and dehydration) or during subsequent storage stresses on the physical stability of a lyophilized antibody formulation. In Chapter 3, we investigated the effect of shaking stresses on the stability of a lyophilized IgG1 protein formulation. Conditions were setup such that they mimic the environment that a therapeutic protein may encounter during worst-case shipping excursions. It was determined that, compared to the unstressed sample, the shake stressed lyophilized sample, upon reconstitution, showed a greater number of subvisible particles and increased turbidity. These subvisible particles contained protein that showed only minor changes in overall secondary structure content. In conjunction with this stress, we also investigated the effect of moisture content, reconstitution type, diluent addition rate, and subsequent storage stability at elevated temperatures. The effect of moisture content did not show notable differences in aggregation. The effect of subsequent storage duration, temperature, and cake breakage was assessed and it was shown that increasing storage duration, cake breakage, and temperature all led to higher particle counts and higher turbidity upon reconstitution. The effect of reconstitution medium was assessed and some differences in particle formation were seen, especially when solutions containing NaCl or a combination of NaCl and Tween 80 were added, thus emphasizing the importance of choosing the proper reconstitution medium to obtain lower subvisible particle counts. This study stresses that in addition to considering lyophilization cycle and other formulation development practices to ensure the stability of a lyophilized therapeutic, other precautions, especially those that can prevent excessive shaking stress on the protein (i.e., better packaging), should also be considered, and employed, if needed.

Chapter 4 was focused not only on characterization of protein aggregates and particles as described in Chapter 2, but further examined the biological impact of a certain subpopulations of

aggregates. An IgG2 mAb in solution was stressed by stirring, as shown in previous reports, to study the impact of particle size in an *in vitro* immune response using human peripheral blood mononuclear cells (PBMC). [6,10] Prior to this *in-vitro* assay, however, it was necessary to first separate the highly aggregated stirred mAb sample into size-enriched fractions. This was done most successfully using a combination of gravitational sedimentation and fluorescence activated cell sorting (FACS) to obtain four size-enriched samples. The size-enriched samples were placed in the *in-vitro* assay and the cytokine response they induced in the PBMC was monitored. Concurrently, the stir stressed mAb samples were characterized for morphology, structural integrity, composition, and covalent crosslinking of the particles both before and after FACS separation. Samples size-enriched in the 5-10 μm population showed a higher response than the other size-enriched samples in the *in vitro* cell assay, in terms of responding donors, but only marginally in terms of levels of cytokines released. This was probably due to the dilute nature of the samples resulting from the FACS separation step itself. Additionally, these stir induced particles contained protein with some structural alterations compared to the unstressed and heat stressed mAb control samples. The aggregates appeared non-covalently linked with elevated levels of surface hydrophobicity compared to the same controls. Interestingly, elemental fluorine was present in the stir-induced samples, probably arising from the Teflon stir-bars used for stirring. The element was not present in the controls or buffers. The potential advantages and disadvantages associated with this FACS separation technique and with the PBMC *in vitro* assay were discussed as well as methods for further improvement. Overall, obtaining size-enriched protein particle samples was a challenge due to the narrow size range of particles that formed for this particular stress. In addition, the intrinsic properties of the particles (i.e., their stickiness and fragility) and limitations imposed by the FACS instrument and by the *in vitro* assay were other

challenges that were encountered during these studies. The key focus of this study is that the size of protein particles may indeed play a large role in the observed immune responses, but how large of a factor and whether size plays a synergistic role with other aspects such as type of aggregates (ex: oxidized, structurally perturbed, reversible, etc.) is not yet fully understood.

The abundance of literature present concerning protein aggregation is partly due to the fact that many properties of this phenomenon are not fully understood and factors that can instigate it sometimes cannot easily be predicted. Nevertheless, the source of aggregation is not the same for all proteins and their clinical implications in humans is not thoroughly understood. The studies, presented in this thesis, use 3 different IgG monoclonal antibodies, one of the largest class of protein drugs, to understand various aspects of protein aggregation and their potential biological implications. While we have gained a better understanding of the physical stability of these three IgG mAbs under the conditions tested, how well the results correlate with other similar proteins (containing different sequences, structure, and interactions with the environment) is not clear. These studies further provide evidence of the complexities associated with protein aggregation. A greater understanding of this process can be achieved by analyzing numerous similar case studies, making comparisons, and formulating predictions based on previous work. Currently, there is no panacea available to prevent aggregation of all biotherapeutics. This work underscores the importance of comprehensive aggregation characterization using a broad range of analytical instrumentation after subjecting the protein therapeutic to appropriate and relevant accelerated stability conditions to develop formulations that can minimize aggregate formation.

5.2 FUTURE WORK

As mentioned earlier, an improved understanding of protein aggregation behavior of three different IgG mAbs has been gained by the studies presented in this Ph.D. thesis. Further work, however, related to better characterization of protein particles and analysis with the *in vitro* PBMC assay can enhance our current understanding of the stability and the *in vitro* biological responses of the relevant IgG mAbs.

From an analytical point of view, one major challenge faced, not only in this work, but in nearly all work that requires characterization of protein aggregates is that largely spherical, non-protein standards, such as polystyrene beads, are often used for calibration of many analytical instruments. These standards have neither the shape, density, nor refractive index (especially important for light scattering experiments) sufficiently similar to that of proteinaceous particles for accurate characterization work. Furthermore, what complicates this matter further is that protein aggregates themselves are not uniform so the challenges in making more protein-like standards that are representative of all aggregates are very difficult to resolve. Developing and using more appropriate protein-like standards would provide more accurate sizing and counting of protein aggregates and particles by allowing for improved calibration of the analytical instruments.

FACS, as shown in Chapter 4, was a useful technique for obtaining size-enriched samples of micron-sized particles. However, FACS greatly diluted the aggregates in the sample leading to low subvisible particle counts, which may have led to the low PBMC responses. To get a higher PBMC response, it is necessary to scale-up the FACS purification procedure (i.e., preparative FACS) and/or increase the particle concentration while retaining the size enrichment. It will be important to implement a method to increase the concentration of particles using this technique or another to get a more robust response from PBMC from the *in-vitro* assay. In

addition to separating particles based on size, FACS can be a valuable tool for separating and characterizing other aspects of protein aggregates. The size range of FACS can be extended from roughly 0.5 μm to about 40 μm, depending on the nozzle used for the FACS instrument. FACS can be used to separate protein particles by their surface hydrophobicity with the use of a dye, assuming the dye doesn't alter the conformation of the protein. Overall, FACS is an underutilized tool, which has only recently been gaining in importance, to study protein aggregation. Its ability to monitor individual fluorescent signals of subvisible particles makes it a unique and potentially powerful technique. It is a method that should be included among others in the tool kit for characterizing protein subvisible particles and its capabilities should be further explored.

From a clinical point of view, it is known that the best way to determine the immunogenicity potential of a human mAb based biotherapeutic is by conducting clinical studies incorporating sufficient numbers of diverse human patients. However, for practical and ethical reasons, this type of clinical study is not always possible. A more feasible thing to do is to use a combination of *in-silico*, *in-vitro* studies. For example, by using human peripheral blood mononuclear cells, and *in-vivo* studies using transgenic mice or non-human primates, one could better understand the potential of different types of protein aggregates to elicit formation of anti-drug antibodies (ADA). In our study, performing the PBMC *in-vitro* assay using a larger, more genetically diverse MHC population, which is more representative of the world population, would be of interest. This could provide a better representation of the cytokine response of the aggregates in the general human population. For the biological assay results described in Chapter 4, the PBMCs were isolated from randomly chosen 7-8 human donors at Amgen, whose MHC types were not characterized.

Finally, performing shipping experiments as described in Chapter 3 using other lyophilized mAbs in different formulations might allow us to more fully elucidate the mechanism of subvisible particle formation. It was seen in Chapter 3 that increases in turbidity and subvisible particles were observed upon subjecting a lyophilized IgG1 mAb to shipping like stress and reconstitution. Expanding these studies to a wider range of other lyophilized mAbs should permit us to better establish a more general trend, which will allow the mechanism of mAb particle formation upon shaking stress to be more fully elucidated.

Performing all of these future study plans should help scientists obtain more accurate and precise sizing and counting data for protein aggregates and particles, free from many experimental assumptions. In addition, new analytical approaches such as incorporating the revised FACS method to characterize and isolate protein particles and modifying the PBMC *in-vitro* assay to incorporate the genetic heterogeneity of donors, will aid us to better characterize the physical and biological properties of protein aggregates and improve our understanding of their immune potential.

5.3 REFERENCES

1. United States Pharmacopeial (USP): 2011. <788> Particulate Matter in Injections; Revision Bulletin
2. European Pharmacopoeia (Ph.Eur.): 2005. 5th Edition (official on Jan 2005). Particulate Contamination: Subvisible Particles. (reference 01/2005: 20919)
3. Carpenter JF, Randolph TW, Jiskoot W, Crommelin DJ, Middaugh CR, Winter G, Fan YX, Kirshner S, Verthelyi D, Kozlowski S, Clouse KA, Swann PG, Rosenberg A, Cherney B 2009. Overlooking subvisible particles in therapeutic protein products: gaps that may compromise product quality. Journal of pharmaceutical sciences 98(4):1201-1205.
4. Singh SK, Afonina N, Awwad M, Bechtold-Peters K, Blue JT, Chou D, Cromwell M, Krause HJ, Mahler HC, Meyer BK, Narhi L, Nesta DP, Spitznagel T 2010. An industry perspective on the monitoring of subvisible particles as a quality attribute for protein therapeutics. Journal of pharmaceutical sciences 99(8):3302-3321.
5. Bi V, Jawa V, Joubert MK, Kaliyaperumal A, Eakin C, Richmond K, Pan O, Sun J, Hokom M, Goletz TJ, Wypych J, Zhou L, Kerwin BA, Narhi LO, Arora T 2013. Development of a human antibody tolerant mouse model to assess the immunogenicity risk due to aggregated biotherapeutics. Journal of pharmaceutical sciences 102(10):3545-3555.
6. Joubert MK, Hokom M, Eakin C, Zhou L, Deshpande M, Baker MP, Goletz TJ, Kerwin BA, Chirmule N, Narhi LO, Jawa V 2012. Highly aggregated antibody therapeutics can enhance the in vitro innate and late-stage T-cell immune responses. The Journal of biological chemistry 287(30):25266-25279.
7. Filipe V, Jiskoot W, Basmeleh AH, Halim A, Schellekens H, Brinks V 2012. Immunogenicity of different stressed IgG monoclonal antibody formulations in immune tolerant transgenic mice. mAbs 4(6):740-752.
8. Freitag AJ, Shomali M, Michalakis S, Biel M, Siedler M, Kaymakcalan Z, Carpenter JF, Randolph TW, Winter G, Engert J 2014. Investigation of the Immunogenicity of Different Types of Aggregates of a Murine Monoclonal Antibody in Mice. Pharmaceutical research.
9. Narhi LO, Schmit J, Bechtold-Peters K, Sharma D 2012. Classification of protein aggregates. Journal of pharmaceutical sciences 101(2):493-498.
10. Joubert MK, Luo Q, Nashed-Samuel Y, Wypych J, Narhi LO 2011. Classification and characterization of therapeutic antibody aggregates. The Journal of biological chemistry 286(28):25118-25133.